ENGINEERING
LIBRARY
JUL 1 1949

THE QUARTERLY JOURNAL OF MECHANICS AND APPLIED MATHEMATICS

VOLUME II PART 2
JUNE 1949

OXFORD
AT THE CLARENDON PRESS
1949

Price 12*s.* 6*d. net*

PRINTED IN GREAT BRITAIN BY CHARLES BATEY AT THE UNIVERSITY PRESS, OXFORD

THE QUARTERLY JOURNAL OF MECHANICS AND APPLIED MATHEMATICS

Editorial Board

S. GOLDSTEIN
R. V. SOUTHWELL
G. I. TAYLOR
G. TEMPLE

together with

A. C. AITKEN
H. JEFFREYS
S. CHAPMAN
J. E. LENNARD-JONES
A. R. COLLAR
N. F. MOTT
T. G. COWLING
W. G. PENNEY
C. G. DARWIN
A. G. PUGSLEY
W. J. DUNCAN
L. ROSENHEAD
A. A. HALL
ALEXANDER THOM
D. R. HARTREE
A. H. WILSON
WILLIS JACKSON
J. R. WOMERSLEY

Executive Editors

G. C. McVITTIE
V. C. A. FERRARO

THE QUARTERLY JOURNAL OF MECHANICS AND APPLIED MATHEMATICS is published at 12*s*. 6*d*. net for a single number with an annual subscription (for four numbers) of 40*s*. post free.

NOTICE TO CONTRIBUTORS

1. *Communication*. Papers should be communicated to one or other of the Executive Editors, by name, at King's College, Strand, London, W.C. 2.

2. *Presentation*. Manuscripts should preferably be typewritten, and each paper should be preceded by a summary not exceeding 300 words in length. References to literature should be given in standard order, *author*, *title of journal*, *volume number*, *date*, *page*. These should be placed at the end of the paper and arranged according to the order of reference in the paper.

3. *Diagrams*. The number of diagrams should be kept to the minimum consistent with clarity. The lines of the figures should be drawn in ink either on draughtsman's paper or on good quality white paper. Each individual line in the figure should bear reducing to one-half of the size of the original, and great care should be exercised to see that the lines are regular in thickness, especially where they meet. Lettering of the figure should be in pencil and should be sufficient to define clearly the lines and curves in it. The writing of formulae or of explanations on the diagram itself should be avoided. All explanations of symbols, etc., should be given in underline. Contributors should indicate on their manuscripts where figures should be inserted.

4. *Tables*. Tables should preferably be arranged so that they can be printed with the columns parallel to the longer edge of the page.

5. *Vector Notation*. All single letters used to denote vectors in the manuscript should be marked by underlining with a wavy line. Scalar and vector products should be denoted by $\underset{\sim}{a} \cdot \underset{\sim}{b}$ and $\underset{\sim}{a} \wedge \underset{\sim}{b}$ respectively.

6. *Offprints*. Authors of papers will be entitled to 25 free offprints.

7. All correspondence other than that dealing with contributions should be addressed to the Publisher:

GEOFFREY CUMBERLEGE
OXFORD UNIVERSITY PRESS
AMEN HOUSE, LONDON, E.C. 4

ICS

CS is
otion

utive

hould
ature
page.
ler of

with
paper
ucing
t the
ould
The
All
indi-

n the

ould
d be

ssed

ON

Ar
force
base
that
or th
lines
some
ordi

Intr
Toli
(i.e.
ing)
with
only.
tion
the r
howe
plane
by co

Forn
We
gover
formu

and t

where
define
magni

[Quar
5092,

ON A FAMILY OF ROTATIONAL SPATIAL GAS FLOWS

By R. PRIM *and* P. NEMÉNYI

(*Naval Ordnance Laboratory, White Oak, Maryland, U.S.A.*)

[Received 18 May 1948]

SUMMARY

An investigation is made of steady flows of an ideal gas in the absence of body forces for which the three velocity components in a cylindrical coordinate system based on a plane isometric net depend on only one isometric coordinate. It is shown that such flows exist only if the basic isometric net consists of logarithmic spirals or their limiting cases (concentric circles, radial straight lines, and parallel straight lines). Several large classes of rotational and spatial gas-flow solutions are obtained, some in explicit forms involving an arbitrary function, and others as solutions to ordinary differential equations involving several arbitrary parameters.

Introduction

TOLLMIEN (**1**) has investigated plane, irrotational, steady flows of an ideal (i.e. thermodynamically perfect, non-viscous, and thermally non-conducting) gas in the absence of body forces for which the velocity components with respect to an orthogonal coordinate net are functions of one coordinate only. In the present paper these conditions are generalized by the addition of a velocity component normal to the basic coordinate net and by the removal of the restriction to irrotational flows. At the same time, however, the conditions are specialized by the consideration only of those plane orthogonal nets which are isometric, that is, which could be obtained by conformal mapping from a Cartesian net.

Formulation of the problem

We employ the formulation by Munk and Prim (**2**) of the basic equations governing steady flow of an ideal gas in absence of body forces. This formulation yields the continuity equation

$$\operatorname{div}[(1-W^2)^{1/(\gamma-1)}\mathbf{W}] = 0 \tag{1}$$

and the integrability condition for the dynamic equation

$$\operatorname{curl}\left[\frac{\mathbf{W}\wedge\operatorname{curl}\mathbf{W}}{1-W^2}\right] = 0, \tag{2}$$

where γ denotes the adiabatic exponent and $\mathbf{W}$ the reduced velocity vector defined in terms of the actual velocity vector $\mathbf{V}$ and the ultimate velocity magnitude a (constant along any individual streamline) by

$$\mathbf{W} = \frac{\mathbf{V}}{a}. \tag{3}$$

For the present investigation, (1) and (2) will be referred to a cylindrical coordinate system based on a plane isometric net. The squared element of arc length in this system is given by

$$ds^2 = g^2(\xi,\eta)(d\xi^2+d\eta^2)+dz^2, \tag{4}$$

where the limitation of the (ξ,η) net to a plane requires that $\log g$ be a harmonic function of ξ and η, that is, that

$$\frac{\partial^2 \log g}{\partial \xi^2}+\frac{\partial^2 \log g}{\partial \eta^2} = \nabla^2 \log g = 0. \tag{5}$$

Reduced velocity fields of the following type will be considered:

$$\mathbf{W} = \boldsymbol{\xi}_1 u(\xi)+\boldsymbol{\eta}_1 v(\xi)+\mathbf{z}_1 q(\xi), \tag{6}$$

where $\boldsymbol{\xi}_1$, $\boldsymbol{\eta}_1$, and $\mathbf{z}_1$ are unit vectors in the ξ, η, and z directions, respectively.

Discussion of the equations

Specialization of (1) and (2) by (4) and (6) yields four equations (in addition to (5)) restricting the functions $g(\xi,\eta)$, $u(\xi)$, $v(\xi)$, and $q(\xi)$:

$$v\frac{\partial}{\partial \eta}(\log g)+u\frac{\partial}{\partial \xi}\log[gu(1-W^2)^{1/(\gamma-1)}] = 0, \tag{7}$$

$$\frac{\partial}{\partial \xi}\left[\frac{u(dq/d\xi)}{g(1-W^2)}\right] = \frac{\partial}{\partial \eta}\left[\frac{u(dq/d\xi)}{g(1-W^2)}\right] = 0, \tag{8}$$

and

$$v\frac{\partial}{\partial \eta}(\log \Omega)+u\frac{\partial}{\partial \xi}\log\frac{u\Omega}{1-W^2} = 0, \tag{9}$$

where

$$\Omega \equiv \frac{dv}{d\xi}+v\frac{\partial}{\partial \xi}(\log g)-u\frac{\partial}{\partial \eta}(\log g).$$

The double equation (8) requires that one or more of the conditions $u = 0$, $dq/d\xi = 0$, or $\partial g/\partial \eta = 0$ be satisfied. When the various possible combinations of these conditions are examined in the light of the restrictions imposed by (5), (7), and (9), four distinct cases emerge. These cases are characterized by the conditions

$$\text{(I)} \qquad u = 0, \qquad \frac{\partial g}{\partial \eta} \neq 0,$$

$$\text{(II)} \qquad u = 0, \qquad \frac{\partial g}{\partial \eta} = 0,$$

$$\text{(III)} \qquad u \neq 0, \qquad \frac{dq}{d\xi} = 0,$$

$$\text{(IV)} \qquad u \neq 0, \qquad \frac{\partial g}{\partial \eta} = 0.$$

(It should be pointed out that, to be physically meaningful, the magnitude of the reduced velocity vector must be between zero and one. Choice of 'arbitrary' functions and constants in the following analysis must always be made consistent with this limitation.)

Case I: $u = 0$, $\partial g/\partial\eta \neq 0$

For $u = 0$, $\partial g/\partial\eta \neq 0$; (7) requires that v be also zero. No restriction is then imposed on $q(\xi)$ or $g(\xi, \eta)$ by (9), and we are left with a unidirectional flow along the z-axis with the velocity magnitude an arbitrary function of ξ where the (ξ, η) net may be any isometric net. This result is relatively trivial, being a special case of the well-known family of flows parallel to the z-axis, with W an arbitrary function of x and y.

Case II: $u = 0$, $\partial g/\partial\eta = 0$

For $u = 0$, $\partial g/\partial\eta = 0$; (7) and (9) impose no limitation on the functions $v(\xi)$ and $q(\xi)$. However, (5) limits the permissible isometric nets to those for which $\log g = A\xi + C$, where A and C are constants. For $A \neq 0$, the lines $\xi =$ constant form a set of concentric circles; for $A = 0$, a set of parallel straight lines.

Thus we have, basically, flows whose streamlines are helices lying on concentric circular cylinders and in which the tangential and axial velocity components are arbitrary functions of the radius. In the limiting case, $A = 0$, the cylindrical surfaces are a family of parallel planes in each of which the velocity vector may be chosen arbitrarily.

Case III: $u \neq 0$, $dq/d\xi = 0$

For this case, the streamlines no longer lie in the surfaces $\xi =$ constant, but the z-component of velocity is a constant, say $q(\xi) = Q$.

If L denotes the function $\dfrac{\partial}{\partial\eta}(\log g)$ it can be shown by differentiation of (5), (7), and (9) with respect to η that the following equations are necessary restrictions of the function:

$$\frac{\partial^2}{\partial\xi\partial\eta}\left(\log\frac{\partial L}{\partial\xi}\right) = \frac{\partial^2}{\partial\eta^2}\left(\log\frac{\partial L}{\partial\xi}\right) = 0, \tag{10}$$

$$\frac{\partial^2}{\partial\xi\partial\eta}\left(\log\frac{\partial L}{\partial\eta}\right) = \frac{\partial^2}{\partial\eta^2}\left(\log\frac{\partial L}{\partial\eta}\right) = 0, \tag{11}$$

$$\frac{\partial^2 L}{\partial\xi^2} + \frac{\partial^2 L}{\partial\eta^2} = 0. \tag{12}$$

This set of necessary conditions, together with (5), leaves the following possibilities for the function $\log g$:

$$\log g = \frac{E}{F^2}e^{F\eta}\cos F(\xi - D) + A\xi + B\eta + C \quad (F \neq 0) \tag{13}$$

or,
$$\log g = \tfrac{1}{2}G(\eta^2-\xi^2)+H\xi\eta+A\xi+B\eta+C. \tag{14}$$

However, these conditions have been obtained by using (7) and (9) only in their differentiated forms and hence represent necessary, but not sufficient, limitations on $\log g$. The undifferentiated forms of (7) and (9) further restrict (13) and (14) to
$$\log g = A\xi+B\eta+C. \tag{15}$$

Hence, the lines ξ = constant of the basic coordinate net form a set of logarithmic spirals or their limiting cases ($A = 0$, radial straight lines; $B = 0$, concentric circles; $A = B = 0$, parallel straight lines).

Under this restriction of $\log g$ and of q, (7) and (9) reduce to a pair of ordinary differential equations restricting $u(\xi)$ and $v(\xi)$, namely,
$$Bv+Au+u\frac{d}{d\xi}\log[u(1-Q^2-u^2-v^2)^{1/(\gamma-1)}] = 0 \tag{16}$$
and
$$\frac{dv}{d\xi} = -A+vBu+\frac{D}{u}(1-Q^2-u^2-v^2). \tag{17}$$

These equations determine a five-parameter family of spatial gas-flow solutions, only very special cases of which were known before. For $D = 0$, $Q = 0$, the reduced velocity field is irrotational and plane, and Tollmien's flows based on a logarithmic spiral coordinate net (including the Bateman-Taylor spiral flows as special cases) are obtained. For $A = 0$, $D = 0$, Poritsky's (**3**) generalization of the irrotational Prandtl–Meyer corner flow is obtained. For $A = 0$, $D \neq 0$, a generalization of the Prandtl–Meyer corner flow to rotational flows is obtained. A detailed study of the latter case in an independent investigation by Prim (**4, 5**) has yielded, among other results, a simple family of explicit solutions for rotational gas flows.

Case IV: $u \neq 0$, $\partial g/\partial\eta = 0$

As in case II, the lines ξ = constant of the basic coordinate net are restricted to families of concentric circles or of parallel straight lines. However, in the present case the streamlines do not lie in the surfaces ξ = constant and the z-component of velocity is not necessarily a constant.

For $A \neq 0$, that is, the surfaces ξ = constant forming a set of concentric circular cylinders, the constant C may be taken as zero without loss of generality, and the radius of the cylinders ξ = constant may be introduced as independent variable by the substitution
$$r = e^{A\xi}. \tag{18}$$

The restriction of the velocity components $u(r)$, $v(r)$, and $q(r)$ by (7), (8),

and (9) can then be satisfied by the introduction of the auxiliary dependent variable $U(r)$ through the definition

$$U(r) \equiv \int\limits_{r_0}^{r} \rho[1-u^2(\rho)-v^2(\rho)-q^2(\rho)]^{\gamma/(\gamma-1)}\, d\rho \tag{19}$$

if the velocity components are given in terms of the function U by

$$u = Ir^{-(\gamma-1)/\gamma}\left(\frac{dU}{dr}\right)^{-1/\gamma}, \tag{20}$$

$$v = \frac{J}{I} r^{-1} U, \tag{21}$$

and

$$q = \frac{K}{I} U + L \tag{22}$$

(capital letters represent arbitrary constants). Compatibility of the equations (19) and (20)–(22) requires that U be a solution of the ordinary differential equation

$$r^{-(\gamma-1)/\gamma}\left(\frac{dU}{dr}\right)^{(\gamma-1)/\gamma} + I^2 r^{-2(\gamma-1)/\gamma}\left(\frac{dU}{dr}\right)^{-2/\gamma} + \frac{J^2}{I^2} r^{-2} U^2 + \left(\frac{K}{I} U + L\right)^2 = 1. \tag{23}$$

Equations (20)–(23) determine a five-parameter family of rotational spatial gas flows. A common property of these flows is a helicoidal symmetry—any streamline of a given flow can be brought into coincidence with any other by a translation along the z-axis and a rotation about it. It should be added that by going back directly to the formulae (7, 8, 9) we can reduce the problem to a differential equation of the form $du/dr = \phi(r, u)$, but the function ϕ is rather complicated.

For $A = 0$, the surfaces $\xi =$ constant form a family of parallel planes parallel to the z-axis. Without loss of generality we may refer our flows to a Cartesian coordinate system by taking $\xi = x$ and $\eta = y$. Again it is convenient to handle the limitations imposed on the functions $u(x)$, $v(x)$, and $q(x)$ by (7) and (9) through the introduction of a new dependent variable by the definition

$$V(x) \equiv \int\limits_{x_0}^{x} [1-u^2(s)-v^2(s)-q^2(s)]^{\gamma/(\gamma-1)}\, ds. \tag{24}$$

The velocity components are then given in terms of V by

$$u = M\left(\frac{dV}{dx}\right)^{-1/\gamma}, \tag{25}$$

$$v = \frac{N}{M}V, \tag{26}$$

and

$$q = \frac{P}{M}V+R. \tag{27}$$

Compatibility of (24) and (25)–(27) then requires V to be a solution of the ordinary differential equation

$$\left(\frac{dV}{dx}\right)^{(\gamma-1)/\gamma}+M^2\left(\frac{dV}{dx}\right)^{-2/\gamma}+\frac{N^2}{M^2}V^2+\left(\frac{P}{M}V+R\right)^2 = 1. \tag{28}$$

In this particular case it is possible, alternatively, to obtain u in terms of a quadrature, if we go back directly to equations (7), (8), and (9). Under the present assumptions these equations take on the form

$$u = A_1(1-W^2)^{-1/(\gamma-1)}, \tag{7'}$$

$$uq' = C_1(1-W^2), \tag{8'}$$

$$uv' = B_1(1-W^2). \tag{9'}$$

From (8′) and (9′) it follows that

$$q = \frac{C_1}{B_1}v+D_1.$$

Combining this with (7′) we obtain v in terms of u:

$$v = -\frac{C_1 D_1}{B_1\{1+(C_1^2/B_1^2)\}} \pm \left[\frac{C_1^2 D_1^2 B_1^2}{(C_1^2+B_1^2)^2}+\frac{B_1^2(1-D_1^2-u^2-A_1^{\gamma-1}u^{-(\gamma-1)})}{B_1^2+C_1^2}\right]^{\frac{1}{2}}.$$

From (9′) we obtain now:

$$u\frac{dv}{du}u' = B_1 A_1^{\gamma-1}u^{-(\gamma-1)},$$

and hence

$$u' \equiv \frac{du}{dx} = \frac{B_1 A_1^{\gamma-1}u^{-\gamma}}{dv/du},$$

therefore

$$x = B_1^{-1}A_1^{1-\gamma}\int u^{\gamma}\frac{dv}{du}\,du.$$

Integration by parts yields finally the relation

$$B_1 A_1^{\gamma-1}x = u^{\gamma}v+\frac{C_1 D_1 B_1 u^{3\gamma-2}}{(2\gamma-1)(3\gamma-2)(B_1^2+C_1^2)}\pm$$

$$\pm\int u^{2\gamma-1}\left[\frac{C_1^2 D_1^2 B_1^2}{(B_1^2+C_1^2)^2}+\frac{B_1^2(1-D_1^2-u^2-A_1^{\gamma-1}u^{-(\gamma-1)})}{B_1^2+C_1^2}\right]^{\frac{1}{2}}du.$$

Remarks on the results of the investigation

A major result of the above investigation is the manner in which the choice of the basic isometric net is limited by the governing gas dynamic relations. The above analysis establishes the following:

THEOREM. *The only plane isometric nets for which it is possible to find steady flows of an ideal gas in the absence of body forces, such that the velocity components with respect to cylindrical coordinates based on the net are functions of only one isometric coordinate, are families of logarithmic spirals and their limiting cases.*

This result has been established earlier by the present writers in a preliminary publication on this and related questions of gas dynamics (**6**). It should be noted that, as Tollmien's analysis (**1**) has shown, exactly the same isometric nets are admissible as coordinate systems for the special case of irrotational flow.

Apart from the general theorem, and from the previously known flow solutions occurring in cases I and II, the analysis has yielded explicitly or in the forms of solutions to ordinary first-order differential equations several broad families of new gas flow solutions, including truly spatial rotational flows. The detailed study of representative examples of these solutions can be expected to yield valuable insight into the nature of rotational gas flow.

REFERENCES

1. W. Tollmien, 'Zum Übergang von Unterschall- in Überschallströmungen', *Z. f. ang. Math. u. Mech.* **17** (1937), 117–36.
2. M. Munk and R. Prim, 'On the canonical form of the equations of steady motion of a perfect gas,' *Journ. of Applied Phys.* (Oct. 1948).
3. H. Poritsky, *Compressible Flows obtainable from Two-Dimensional Flows through Addition of a Constant Normal Velocity*, Amer. Soc. Mech. Eng., Advance Paper No. 45-A-26 (Nov. 1945).
4. R. Prim, 'On a family of rotational gas flows', *Quart. Applied Math.* (Oct. 1948).
5. —— 'Rotational flow of gas around corners', presented at VIIth Int. Cong. Applied Mech. (London, 1948).
6. P. Neményi and R. Prim: 'Some properties of rotational flow of a perfect gas,' *Proc. Nat. Acad. Sci.* **34** (1948), 119–24.

SUPERSONIC FLOW PAST THIN WINGS
I. GENERAL THEORY

By G. N. WARD

(*Department of Mathematics, The University, Manchester*)

[Received 10 August 1948]

SUMMARY

The linearized potential problem of supersonic flow is solved for nearly plane wings of arbitrary shape of planform and section. The velocity field is divided into its symmetrical and antisymmetrical parts, which are treated separately. The results for the symmetrical part have been given before, by A. E. Puckett, and are only considered briefly. The results for the antisymmetrical part are determined by extending an integral equation method used previously by J. C. Evvard in a more restricted problem. The Kutta–Joukowski condition is applied to the velocity at the trailing edge in order to make the solution determinate. Expressions are given for the potential on the wing, from which the velocities can be obtained. For the smaller aspect ratios, the analysis becomes complicated and only an indication of how the results can be obtained is given. The velocity is singular at the subsonic leading edges and the forces on the wing have to be determined by a limiting process which is illustrated by obtaining expressions for the lift and drag forces. All the results are completely general and no special cases are considered.

1. Introduction

THE problem of determining the supersonic flow of a perfect gas past a thin wing set at a small incidence to an initially uniform stream is solved by assuming that the flow is inviscid and isentropic, and that the perturbation velocities caused by the presence of the wing are so small that their squares and higher powers may be neglected in the equations of motion. The wing surfaces are assumed to be nearly plane, so that wings with a large dihedral angle are excluded. The problem is solved by dividing the velocity field into its symmetrical and antisymmetrical parts and treating each independently; the results are then superposed to give the complete solution for the general case. The symmetrical part corresponds to a wing of small finite thickness set at zero incidence which experiences no lifting force: the solution in this case presents no difficulty and is obtained immediately from the general solution of the equation of motion. The antisymmetrical part corresponds to a wing of infinitesimal thickness and the flow is determined by using an integral equation method following a transformation to characteristic coordinates. It is assumed that the flow over the trailing edge of the wing is smooth in accordance with the hypothesis of Kutta and Joukowski, and a trailing vortex sheet is formed

behind the wing: without this assumption the solution of the anti-symmetrical problem is indeterminate. The velocity components exhibit singularities at the subsonic leading edges and the aerodynamic force and moment on the wing have to be obtained by using a somewhat elaborate limiting process, which is illustrated by the determination of the lift and drag components of the force.

The solution for the symmetrical case has been given previously by Puckett (ref. **1**), and, recently, Evvard (ref. **2**) has solved the problem of obtaining the flow pattern near the wing surface for a restricted class of wing tips with curved subsonic leading edges. The use of the transformation to characteristic coordinates is due to Evvard, and the present treatment extends this idea to solve the completely general problem.

2. Mathematical formulation

Let x, y, z be a right-handed system of Cartesian coordinates such that x is measured in the direction of the undisturbed stream, which has a velocity U and Mach number M relative to the coordinate axes, and such that z is measured vertically upwards. Then, to a linear approximation, the components u, v, w of the perturbation velocity are the components of $U\,\mathrm{grad}\,\phi$, where ϕ satisfies

$$B^2\frac{\partial^2\phi}{\partial x^2}-\frac{\partial^2\phi}{\partial y^2}-\frac{\partial^2\phi}{\partial z^2}=0, \qquad B^2 = M^2-1. \tag{1}$$

The perturbation pressure, p, is given, to the same order of approximation, by the linearized Bernoulli equation

$$p = -\rho U^2\, \partial\phi/\partial x, \tag{2}$$

ρ being the density of the undisturbed stream.

The general solution of eqn. (1) for $z > 0$, say, when the boundary data are specified on $z = 0$, as they will be in our case, can be obtained from Hadamard's solution of the general second-order hyperbolic differential equation (ref. **3**) by using the reflection method (cf. ref. **3**, § 156) and may be written in the alternative forms

$$\phi(x,y,z) = -\frac{1}{\pi}\iint \left\{\frac{\partial\phi(x',y',z')}{\partial z'}\right\}_{z'=+0} \frac{dx'dy'}{\sqrt{\{(x-x')^2-B^2(y-y')^2-B^2z^2\}}} \tag{3}$$

or

$$\phi(x,y,z) = -\frac{1}{\pi}{}^*\!\!\iint \phi(x',y',+0)\frac{\partial}{\partial z}\left[\frac{1}{\sqrt{\{(x-x')^2-B^2(y-y')^2-B^2z^2\}}}\right]dx'dy', \tag{4}$$

where, in both forms, the integration is taken over the area of the plane $z = 0$ for which

$$x' \leqslant x-B\sqrt{\{(y-y')^2+z^2\}} \tag{5}$$

and the star (*) in eqn. (4) denotes that the 'finite part' of the improper integral is taken (cf. ref. **3**). The form of the inequality (5) is an expression of the fact that disturbances are not propagated upstream in supersonic flow.

We restrict ϕ to be continuous except through the wing and the trailing vortex sheet. Sufficient conditions for the validity of eqns. (3) and (4) are that $(\partial\phi/\partial z)_{z=0}$ should be integrable over any finite area of the plane $x = 0$ and should possess discontinuities and singularities on only a finite number of arcs in the plane, and that $\phi(x, y, +0)$ should be continuous and bounded. These conditions are not necessary but are adequate for our purpose.

Consider a wing whose surfaces lie approximately in the plane $z = 0$. Let the vertical projections of the wing and its trailing vortex sheet on the plane $z = 0$ be denoted by S and T respectively, and let the remainder of the plane $z = 0$ be denoted by R. Let l_1, m_1, n_1 and l_2, m_2, n_2 be the direction cosines of the outward normals to the upper and lower wing surfaces respectively, so that l_1, m_1, l_2, m_2 are small and n_1, n_2 are approximately equal to unity.

The boundary condition of zero normal velocity at the upper wing surface is

$$l_1(U+u)+m_1 v+n_1 w = 0. \tag{6}$$

To our degree of approximation, the boundary condition may be applied on the plane $z = 0$, instead of on the actual wing surface, and similarly for conditions on the vortex sheet. Then, by neglecting small quantities of the second and higher orders, the boundary condition (6) becomes

$$\frac{w}{U} = \left(\frac{\partial\phi}{\partial z}\right)_{z=+0} = -l_1, \tag{7}$$

and similarly, for the lower wing surface, the boundary condition is

$$\frac{w}{U} = \left(\frac{\partial\phi}{\partial z}\right)_{z=-0} = l_1, \tag{8}$$

where $z = +0$ and $z = -0$ denote the upper and lower sides of the plane $z = 0$ respectively.

If $\phi = \phi_0+\phi_1$, where ϕ_0 is an even and ϕ_1 an odd function of z, then ϕ_0 is the potential for the symmetrical part of the velocity field and ϕ_1 is the potential for the antisymmetrical part, and the boundary conditions for ϕ_0 and ϕ_1 over the area S are

$$\left(\frac{\partial\phi_0}{\partial z}\right)_{z=+0} = -\left(\frac{\partial\phi_0}{\partial z}\right)_{z=-0} = -\tfrac{1}{2}(l_1+l_2) \tag{9}$$

and

$$\left(\frac{\partial\phi_1}{\partial z}\right)_{z=+0} = \left(\frac{\partial\phi_1}{\partial z}\right)_{z=-0} = -\tfrac{1}{2}(l_1-l_2) \tag{10}$$

respectively.

For the symmetrical problem, $\partial\phi_0/\partial z$ is an odd function of z, and, since the z-component of the velocity must be continuous everywhere except through the wing, we have the following boundary value problem for ϕ_0 satisfying eqn. (1) in the region $z > 0$, say:

$$\left.\begin{array}{l}\text{(i) } \partial\phi_0/\partial z \text{ takes given values on } \mathsf{S} \text{ (from eqn. (9))};\\ \text{(ii) } \partial\phi_0/\partial z = 0 \text{ on } \mathsf{R} \text{ and } \mathsf{T};\\ \text{(iii) } \phi_0 \text{ is continuous everywhere in } z \geqslant +0.\end{array}\right\} \quad (11)$$

The potential ϕ_0 is given everywhere in $z > 0$ by applying eqn. (3), since $\partial\phi_0/\partial z$ is known everywhere on $z = 0$, and this solution satisfying the conditions (11) is known to be unique.

The potential in $z < 0$ is also determined since ϕ_0 is even in z. This is the result given by Puckett (ref. **1**).

For the antisymmetrical problem, $\partial\phi_1/\partial z$ is known only on S. The potential ϕ_1 and $\partial\phi_1/\partial x$ and $\partial\phi_1/\partial y$ are odd in z, and since the pressure must be continuous everywhere except through the wing, we must have $\partial\phi_1/\partial x = 0$ on R and T. Furthermore, ϕ_1 is continuous through R so that $\phi_1 = 0$ on R. In addition it is assumed that the Kutta–Joukowski condition is satisfied at the trailing edge: this condition is that velocity remains finite at the trailing edge. It is shown later that this condition implies that grad ϕ_1 is continuous at subsonic trailing edges, but it may be discontinuous at supersonic trailing edges. Thus the boundary value problem for ϕ_1 satisfying eqn. (3) in $z > 0$, say, is:

$$\left.\begin{array}{l}\text{(i) } \partial\phi_1/\partial z \text{ takes given values on } \mathsf{S} \text{ (from eqn. (10))};\\ \text{(ii) } \partial\phi_1/\partial x = 0 \text{ on } \mathsf{T};\\ \text{(iii) } \phi_1 = 0 \text{ on } \mathsf{R};\\ \text{(iv) } |\mathrm{grad}\,\phi_1| \text{ is finite on the common boundary of } \mathsf{S} \text{ and } \mathsf{T};\\ \text{(v) } \phi_1 \text{ is continuous everywhere in } z \geqslant +0.\end{array}\right\} \quad (12)$$

It is assumed that the solution for ϕ_1 under these conditions is unique. The potential ϕ_1 in $z < 0$ is also determined since ϕ_1 is odd in z.

If the subsonic trailing edge of the wing is not sharp and the Kutta–Joukowski condition cannot be applied, then the solution for ϕ_1 is not unique, and the flow pattern is not determinate on the present assumptions.

It is sufficient to determine the potential ϕ_1 on S, since, from the conditions (12), ϕ_1 is then known on R and T, and is therefore determined everywhere by applying eqn. (4). We shall return to this point later, in § 5.

In order to calculate ϕ_1 on S, we take the special case of eqn. (3) when $z = +0$ to obtain

$$\phi_1(x, y, +0) = -\frac{1}{\pi}\iint \left(\frac{\partial\phi_1}{\partial z'}\right)_{z'=+0} \frac{dx'dy'}{\sqrt{\{(x-x')^2 - B^2(y-y')^2\}}}, \quad (13)$$

where the integration is taken over the area of the plane $z = 0$ for which

$$x' \leqslant x \pm B(y-y'). \tag{14}$$

We transform this integral by putting

$$\alpha = x-By, \qquad \beta = x+By, \tag{15}$$

so that α, β are characteristic coordinates in the plane $z = 0$.

Now

$$\frac{\partial(x,y)}{\partial(\alpha,\beta)} = \frac{1}{2B}, \tag{16}$$

and by putting

$$\frac{1}{2\pi B}\left(\frac{\partial\phi}{\partial z}\right)_{z=+0} = -f(\alpha,\beta) \tag{17}$$

eqn. (13) becomes

$$\phi_1 = \iint \frac{f(\alpha',\beta')\,d\alpha' d\beta'}{\sqrt{\{(\alpha-\alpha')(\beta-\beta')\}}}, \tag{18}$$

the integration being taken over the area for which

$$\alpha' \leqslant \alpha, \qquad \beta' \leqslant \beta. \tag{19}$$

The function $f(\alpha, \beta)$ is not known on R and T, and our procedure is to

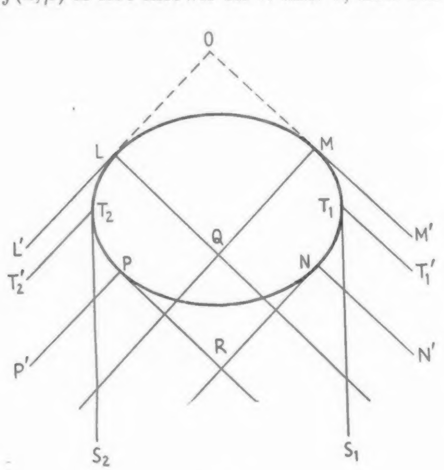

FIG. 1.

set up integral equations to determine it there. In many cases it is not necessary to solve these equations completely in order to determine ϕ_1 on S, as was found by Evvard.

Let C be the boundary of the region S and, in Fig. 1, let L, M, N, P be the points on C at which the tangents LL', MM', NR, PR are characteristic lines for eqn. (1) in the plane $z = 0$, making the Mach angle with the x-axis. LM is then the supersonic leading edge of S. LQ, MQ, NN', PP'

are also characteristic lines. $T_1 S_1$, $T_2 S_2$ are lines parallel to the x-axis, tangent to C at T_1, T_2 and are the boundaries of T, the projection of the vortex sheet.

Let O, the intersection of LL', MM', be the origin of coordinates, and let

$$\left.\begin{array}{l} L \text{ be the point } (\alpha_0, 0), \\ M \text{ be the point } (0, \beta_0), \\ T_1 \text{ be the point } (\alpha_1, \beta_1), \\ T_2 \text{ be the point } (\alpha_2, \beta_2). \end{array}\right\} \tag{20}$$

Let the equation of C be specified as follows:

$$PLM\colon\ \beta = A_1(\alpha); \qquad MNP\colon\ \beta = A_2(\alpha) \tag{21}$$

or

$$LMN\colon\ \alpha = B_1(\beta); \qquad NPL\colon\ \alpha = B_2(\beta) \tag{22}$$

so that A_1, A_2, B_1, B_2 are single-valued functions on the arcs of C for which they are defined, if, for simplicity, we assume that the curvature of C has the same sign everywhere, as depicted in Fig. 1. If this condition is not satisfied, the following analysis may require modification, but this is easily carried out.

The potential in the region LQM of S may be calculated immediately. From condition (12, iii), an application of eqn. (4) shows that ϕ and all its derivatives vanish upstream from the envelope surface of all the downstream characteristic cones having vertices on the supersonic leading edge LM, which we call the leading characteristic surface. Thus

$$(\partial\phi/\partial z)_{z=0} = 0$$

on that part of R which lies upstream from $L'LMM'$, and an application of eqns. (17) and (18) determines ϕ on LQM since $(\partial\phi/\partial z)_{z=+0}$ is known over the relevant part of $z = +0$. More generally, an application of eqn. (3) determines ϕ in the space between the leading characteristic surface and the downstream characteristic cones from L and M.

We now proceed to calculate ϕ_1 over the remainder of S: this is most conveniently done in successive stages.

3. Independent wing-tip flows

We consider first the case when the aspect ratio is sufficiently large for the flows over the two wing tips to be independent, i.e. such that the intersection Q of the characteristic lines LQ, MQ in Fig. 1 lies outside S, and calculate ϕ_1 on that part of S downstream from MQ.

For the wing tip shown in Fig. 2 (which is lettered to correspond with Fig. 1) on S, let

$$f(\alpha, \beta) = \lambda(\alpha, \beta); \tag{23}$$

in the region $M'MT_1S_1$ on R, let

$$f(\alpha, \beta) = \mu(\alpha, \beta), \tag{24}$$

and in the region $N'T_1N$ on **T**, let

$$f(\alpha,\beta) = \mu_s(\alpha,\beta). \tag{25}$$

μ and μ_s are, as yet, unknown functions.

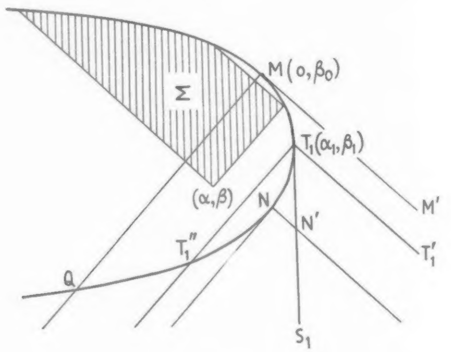

FIG. 2.

For a point (α,β) in the region $M'MT_1T_1'$ (i.e. $\beta > A_2(\alpha)$; $0<\alpha<\alpha_1$) we have from eqn. (18) and condition (12, iii)

$$\phi_1 = \int\limits_0^\alpha \frac{d\alpha'}{\sqrt{(\alpha-\alpha')}}\left\{\int\limits_{A_2(\alpha')}^{\beta} \frac{\mu(\alpha',\beta')\,d\beta'}{\sqrt{(\beta-\beta')}} + \int\limits_{A_1(\alpha')}^{A_2(\alpha')} \frac{\lambda(\alpha',\beta')\,d\beta'}{\sqrt{(\beta-\beta')}}\right\} = 0. \tag{26}$$

This equation is satisfied if

$$\int\limits_{A_2(\alpha)}^{\beta} \frac{\mu(\alpha,\beta')\,d\beta'}{\sqrt{(\beta-\beta')}} + \int\limits_{A_1(\alpha)}^{A_2(\alpha)} \frac{\lambda(\alpha,\beta')\,d\beta'}{\sqrt{(\beta-\beta')}} = 0. \tag{27}$$

This is an integral equation of Abel's type for $\mu(\alpha,\beta)$ (so also, of course, is eqn. (26) for the contents of the brackets) and its solution which we shall require later is (cf. ref. **4**)

$$\mu(\alpha,\beta) = -\frac{1}{\pi\sqrt{\{\beta-A_2(\alpha)\}}}\int\limits_{A_1(\alpha)}^{A_2(\alpha)} \frac{\lambda(\alpha,\beta')\sqrt{\{A_2(\alpha)-\beta'\}}\,d\beta'}{\beta-\beta'}. \tag{28}$$

For a point (α,β) on **S** in the region $T_1''T_1MQ$ (i.e. $B_1(\beta) < \alpha < B_2(\beta)$; $\beta_0 < \beta < \beta_1$), we have from eqn. (18)

$$\phi_1 = \int\limits_{B_1(\beta)}^{\alpha} \frac{d\alpha'}{\sqrt{(\alpha-\alpha')}}\int\limits_{A_1(\alpha')}^{\beta} \frac{\lambda(\alpha',\beta')\,d\beta'}{\sqrt{(\beta-\beta')}} +$$

$$+\int\limits_0^{B_1(\beta)} \frac{d\alpha'}{\sqrt{(\alpha-\alpha')}}\left\{\int\limits_{A_2(\alpha')}^{\beta} \frac{\mu(\alpha',\beta')\,d\beta'}{\sqrt{(\beta-\beta')}} + \int\limits_{A_1(\alpha')}^{A_2(\alpha')} \frac{\lambda(\alpha',\beta')\,d\beta'}{\sqrt{(\beta-\beta')}}\right\}. \tag{29}$$

From eqn. (27) the last term vanishes and we have finally, for points on S in the region under consideration,

$$\phi_1 = \int\limits_{B_1(\beta)}^{\alpha} \frac{d\alpha'}{\sqrt{(\alpha-\alpha')}} \int\limits_{A_1(\alpha)}^{\beta} \frac{\lambda(\alpha',\beta')\,d\beta'}{\sqrt{(\beta-\beta')}} \tag{30}$$

or
$$\phi_1(x,y,+0) = -\frac{1}{\pi}\iint\limits_{\Sigma} \left(\frac{\partial\phi}{\partial z'}\right)_{z'=+0} \frac{dx'dy'}{\sqrt{\{(x-x')^2-B^2(y-y')^2\}}}, \tag{31}$$

the integration in eqns. (30) and (31) being taken over the area Σ, bounded by characteristic lines, shown in Fig. 2. This result is due to Evvard (ref. **2**), who obtained it by essentially the same method.

It remains now to calculate the potential in the region NT_1T_1''.

On T, for $z = +0$, the potential is a function of the coordinate y alone and we can therefore express it as

$$\phi_1 = F_1(\alpha-\beta), \tag{32}$$

F_1 being an unknown function. Since the potential is continuous over $z = +0$, it will be zero on the line T_1S_1 and we have

$$F_1(\alpha_1-\beta_1) = 0, \tag{33}$$

α_1, β_1 being the coordinates of T_1. The line T_1S_1 has the equation

$$\alpha-\beta = \alpha_1-\beta_1 = \gamma_1, \quad \text{say.} \tag{34}$$

For a point on T in the region $N'T_1N$, we can apply the result of eqn. (30) if T is considered to be part of the area for which λ is known, and λ is replaced by μ_s over this area. We have then, on T,

$$\phi_1 = \int\limits_{\beta+\gamma_1}^{\alpha} \frac{d\alpha'}{\sqrt{(\alpha-\alpha')}} \left\{ \int\limits_{A_2(\alpha')}^{\beta} \frac{\mu_s(\alpha',\beta')\,d\beta'}{\sqrt{(\beta-\beta')}} + \int\limits_{A_1(\alpha')}^{A_2(\alpha')} \frac{\lambda(\alpha',\beta')\,d\beta'}{\sqrt{(\beta-\beta')}} \right\} = F_1(\alpha-\beta). \tag{35}$$

This equation is an integral equation of Abel's type for the contents of the brackets, and the solution is

$$\int\limits_{A_2(\alpha)}^{\beta} \frac{\mu_s(\alpha,\beta')\,d\beta'}{\sqrt{(\beta-\beta')}} + \int\limits_{A_1(\alpha)}^{A_2(\alpha)} \frac{\lambda(\alpha,\beta')\,d\beta'}{\sqrt{(\beta-\beta')}} = \frac{1}{\pi} \int\limits_{\beta+\gamma_1}^{\alpha} \frac{F_1'(\alpha'-\beta)\,d\alpha'}{\sqrt{(\alpha-\alpha')}}, \tag{36}$$

where F_1' is the first derivative of F_1; and since $F_1(\gamma_1) = 0$, eqn. (36) is another Abel integral equation for μ_s, and its solution is

$$\mu_s(\alpha,\beta) = -\frac{1}{\pi\sqrt{\{\beta-A_2(\alpha)\}}} \int\limits_{A_1(\alpha)}^{A_2(\alpha)} \frac{\lambda(\alpha,\beta')\sqrt{\{A_2(\alpha)-\beta'\}}\,d\beta'}{\beta-\beta'} +$$

$$+\frac{1}{\pi^2}\frac{\partial}{\partial\beta} \int\limits_{A_2(\alpha)}^{\beta} \frac{d\beta'}{\sqrt{(\beta-\beta')}} \int\limits_{\beta'+\gamma_1}^{\alpha} \frac{F_1'(\alpha'-\beta')\,d\alpha'}{\sqrt{(\alpha-\alpha')}}. \tag{37}$$

The unknown function F_1 has to be determined by the condition that μ_s must be finite at the trailing edge $T_1 N$, where $\beta = A_2(\alpha)$. It will be seen that the second term in eqn. (37) must contain a term which will cancel the singularity at the trailing edge contained in the first term. We need not actually solve for F_1 in order to determine the potential on the wing. Let a function $G_1(\xi)$ be defined by

$$G_1(\xi) = \frac{1}{\pi}\int\limits_{\gamma_1}^{\xi} \frac{F_1'(\xi')\,d\xi'}{\sqrt{(\xi-\xi')}}. \tag{38}$$

Then the second term in eqn. (37) is

$$\frac{1}{\pi}\frac{\partial}{\partial\beta}\int\limits_{A_2(\alpha)}^{\beta} \frac{G_1(\alpha-\beta')\,d\beta'}{\sqrt{(\beta-\beta')}} = \frac{1}{\pi}\left[\frac{G_1\{\alpha-A_2(\alpha)\}}{\sqrt{\{\beta-A_2(\alpha)\}}} - \int\limits_{A_2(\alpha)}^{\beta} \frac{G_1'(\alpha-\beta')\,d\beta'}{\sqrt{(\beta-\beta')}}\right]. \tag{39}$$

As the trailing edge is approached, $\beta \to A_2(\alpha)$ and the first term in the right-hand side of eqn. (39) becomes infinite, while the second term vanishes, as may easily be verified on taking account of the continuity of the function F_1. Thus, by combining equations (37) and (39), if μ_s is to be finite at $\beta = A_2(\alpha)$ we must have

$$G_1\{\alpha-A_2(\alpha)\} = \int\limits_{A_1(\alpha)}^{A_2(\alpha)} \frac{\lambda(\alpha,\beta')\,d\beta'}{\sqrt{\{A_2(\alpha)-\beta'\}}}, \tag{40}$$

whence

$$\mu_s(\alpha,\beta) = \frac{1}{\pi}\sqrt{\{\beta-A_2(\alpha)\}}\int\limits_{A_1(\alpha)}^{A_2(\alpha)} \frac{\lambda(\alpha,\beta')\,d\beta'}{(\beta-\beta')\sqrt{\{A_2(\alpha)-\beta'\}}} - \frac{1}{\pi}\int\limits_{A_2(\alpha)}^{\beta} \frac{G_1'(\alpha-\beta')\,d\beta'}{\sqrt{(\beta-\beta')}}. \tag{41}$$

We now calculate the value of μ_s at the trailing edge. Let

$$J = \sqrt{\{\beta-A_2(\alpha)\}}\int\limits_{A_1(\alpha)}^{A_2(\alpha)} \frac{[\lambda(\alpha,\beta')-\lambda\{\alpha,A_2(\alpha)\}]\,d\beta'}{(\beta-\beta')\sqrt{\{A_2(\alpha)-\beta'\}}}, \tag{42}$$

and let the function λ be such that

$$\lim_{\beta\to A_2(\alpha)} J = 0. \tag{43}$$

Then, since

$$\sqrt{\{\beta-A_2(\alpha)\}}\int\limits_{A_1(\alpha)}^{A_2(\alpha)} \frac{d\beta'}{(\beta-\beta')\sqrt{\{A_2(\alpha)-\beta'\}}} = \pi - 2\tan^{-1}\sqrt{\left\{\frac{\beta-A_2(\alpha)}{A_2(\alpha)-A_1(\alpha)}\right\}}, \tag{44}$$

and from eqns. (41), (42), and (43),

$$\lim_{\beta\to A_2(\alpha)} \mu_s(\alpha,\beta) = \lambda\{\alpha, A_2(\alpha)\}. \tag{45}$$

Equation (43) is certainly true if λ satisfies the conditions

$$\text{(i)}\quad |\lambda(\alpha,\beta)-\lambda\{\alpha,A_2(\alpha)\}| \leqslant K\{A_2(\alpha)-\beta\}^{\delta} \quad \text{for} \quad A_2(\alpha) \geqslant \beta \geqslant k > A_1(\alpha),$$

$$\text{(ii)}\quad \int\limits_{A_1(\alpha)}^{k} |\lambda(\alpha,\beta)-\lambda\{\alpha,A_2(\alpha)\}|\, d\beta \leqslant L, \tag{46}$$

where K, L, δ are positive constants, and these conditions are more general than those usually required in any physical problem.

This shows that $\partial\phi_1/\partial z$ is continuous at the subsonic trailing edge, and hence, from eqns. (13) or (18), ϕ_1, $\partial\phi_1/\partial x$, and $\partial\phi_1/\partial y$ are continuous there. Thus grad ϕ_1 is continuous at the subsonic trailing edge.

The potential at a point (α,β) on S in the region NT_1T_1'' (Fig. 2) is obtained by using eqn. (30), as was done when deriving eqn. (35), and is

$$\phi_1 = \int\limits_{B_1(\beta)}^{\alpha} \frac{d\alpha'}{\sqrt{(\alpha-\alpha')}} \int\limits_{A_1(\alpha')}^{\beta} \frac{\lambda(\alpha',\beta')\,d\beta'}{\sqrt{(\beta-\beta')}} +$$
$$+\int\limits_{\beta+\gamma_1}^{B_1(\beta)} \frac{d\alpha'}{\sqrt{(\alpha-\alpha')}} \left\{ \int\limits_{A_2(\alpha')}^{\beta} \frac{\mu_s(\alpha',\beta')\,d\beta'}{\sqrt{(\beta-\beta')}} + \int\limits_{A_1(\alpha')}^{A_2(\alpha')} \frac{\lambda(\alpha',\beta')\,d\beta'}{\sqrt{(\beta-\beta')}} \right\}. \tag{47}$$

By using the result of eqn. (36) to replace the contents of the brackets in the second term of eqn. (47), and remembering the definition of G_1 (eqn. (38)), we have finally

$$\phi_1 = \int\limits_{B_1(\beta)}^{\alpha} \frac{d\alpha'}{\sqrt{(\alpha-\alpha')}} \int\limits_{A_1(\alpha')}^{\beta} \frac{\lambda(\alpha',\beta')\,d\beta'}{\sqrt{(\beta-\beta')}} + \int\limits_{\beta+\gamma_1}^{B_1(\beta)} \frac{G_1(\alpha'-\beta)\,d\alpha'}{\sqrt{(\alpha-\alpha')}}, \tag{48}$$

where G_1 is given by eqn. (40) in terms of λ. This result may be compared with eqn. (30).

On the subsonic trailing edge T_1N, the first term in eqn. (48) vanishes, and by substituting for G_1 from eqn. (38) and inverting the order of integration, it may be verified that the potential is continuous there. By differentiating eqn. (48) and using eqn. (40) it may also be verified that $\partial\phi_1/\partial x = 0$ on the subsonic trailing edge.

We have now found the potential all over the wing tip on $z = +0$, and the results will be the same but with reversed signs on $z = -0$. The potential on the other wing tip may be written down immediately by using the formal symmetry of the problem with respect to α and β. Thus the potential is known at all points on both sides of the wing and the velocity can be found by differentiation. The calculation of the potential and the velocity for points not on the wing will be considered later.

4. Independent subsonic edges

When the wing-tip flows are not independent in the sense of the last section, an application of the results obtained already enables us to calculate

the potential on the wing for the case when the characteristic lines LQ, MQ intersect on S and intersect C in the supersonic trailing edge PN so that the flows at the subsonic edges are independent. Two possibilities arise: (i) when the downstream characteristic lines from T_1 and T_2 intersect outside S, and (ii) when these lines intersect inside S. We shall consider the latter case for the moment, since the results for the former may be obtained by omitting certain of the terms which arise from the presence of the vortex sheet.

Consider the wing planform shown in Fig. 3 (a).

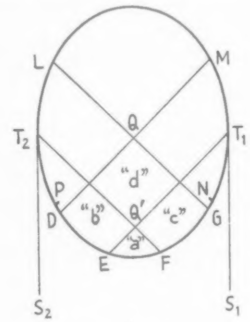

FIG. 3 (a).

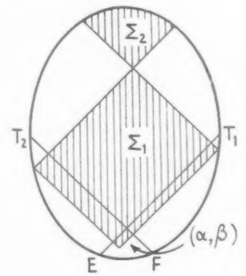

FIG. 3 (b).

From the results of the previous section the potential is known on S except in the region DGQ. We shall calculate first the potential in the region EFQ' denoted by 'a' in Fig. 3 (a). Let the functions ν, ν_s, F_2, G_2 for the left-hand tip correspond to the functions μ, μ_s, F_1, G_1 respectively for the right-hand tip, and let $\gamma_2 = \beta_2 - \alpha_2$ so that the equation of the line $T_2\,S_2$ is $\beta - \alpha = \gamma_2$.

The potential for a point (α,β) in the region EFQ' can be written down immediately from eqn. (48), by substituting ν and ν_s for λ in the appropriate regions, in the form

$$\phi_1 = \int\limits_{B_1(\beta)}^{\alpha} \frac{d\alpha'}{\sqrt{(\alpha-\alpha')}} \left\{ \int\limits_{A_1(\alpha)}^{\beta} \frac{\lambda(\alpha',\beta')\,d\beta'}{\sqrt{(\beta-\beta')}} + \int\limits_{A_1(\alpha')}^{A_1(\alpha)} \frac{\lambda(\alpha',\beta')\,d\beta'}{\sqrt{(\beta-\beta')}} \right\} + \int\limits_{\beta+\gamma_1}^{B_1(\beta)} \frac{G_1(\alpha'-\beta)\,d\alpha'}{\sqrt{(\alpha-\alpha')}} +$$

$$+ \int\limits_{\alpha_2}^{\alpha} \frac{d\alpha'}{\sqrt{(\alpha-\alpha')}} \left\{ \int\limits_{\alpha'+\gamma_2}^{A_1(\alpha')} \frac{\nu_s(\alpha',\beta')\,d\beta'}{\sqrt{(\beta-\beta')}} + \int\limits_{0}^{\alpha'+\gamma_2} \frac{\nu(\alpha',\beta')\,d\beta'}{\sqrt{(\beta-\beta')}} \right\} +$$

$$+ \int\limits_{0}^{\alpha_2} \frac{d\alpha'}{\sqrt{(\alpha-\alpha')}} \int\limits_{0}^{A_1(\alpha')} \frac{\nu(\alpha',\beta')\,d\beta'}{\sqrt{(\beta-\beta')}}. \tag{49}$$

On inverting the order of integration in the second term containing λ and in the terms containing ν and ν_s, and by using the results for the left tip corresponding to eqns. (27) and (36), we can eliminate ν and ν_s to obtain

$$\phi_1 = \int\limits_{B_1(\beta)}^{\alpha} \frac{d\alpha'}{\sqrt{(\alpha-\alpha')}} \int\limits_{A_1(\alpha)}^{\beta} \frac{\lambda(\alpha',\beta')\,d\beta'}{\sqrt{(\beta-\beta')}} - \int\limits_{B_1\{A_1(\alpha)\}}^{B_1(\beta)} \frac{d\alpha'}{\sqrt{(\alpha-\alpha')}} \int\limits_{A_1(\alpha')}^{A_1(\alpha)} \frac{\lambda(\alpha',\beta')\,d\beta'}{\sqrt{(\beta-\beta')}} + \int\limits_{\beta+\gamma_1}^{B_1(\beta)} \frac{G_1(\alpha'-\beta)\,d\alpha'}{\sqrt{(\alpha-\alpha')}} + \int\limits_{\alpha+\gamma_2}^{A_1(\alpha)} \frac{G_2(\beta'-\alpha)\,d\beta'}{\sqrt{(\beta-\beta')}}, \tag{50}$$

where
$$G_2\{\beta-B_2(\beta)\} = \int\limits_{B_1(\beta)}^{B_2(\beta)} \frac{\lambda(\alpha',\beta)\,d\alpha'}{\sqrt{\{B_2(\beta)-\alpha'\}}}. \tag{51}$$

The first two terms of eqn. (50) may be written in the form

$$\iint\limits_{\Sigma_1} \frac{\lambda(\alpha',\beta')\,d\alpha'd\beta'}{\sqrt{\{(\alpha-\alpha')(\beta-\beta')\}}} - \iint\limits_{\Sigma_2} \frac{\lambda(\alpha',\beta')\,d\alpha'd\beta'}{\sqrt{\{(\alpha-\alpha')(\beta-\beta')\}}}, \tag{52}$$

where the areas of integration Σ_1, Σ_2, bounded by characteristic lines, are shown shaded in Fig. 3 (*b*). The area Σ_2 may not exist in some cases of course.

For the region '*b*' in Fig. 3 (*a*) we have to omit the integral containing G_1 in eqn. (50), for region '*c*' we have to omit the integral containing G_2, and for region '*d*' we have to omit both of these integrals. The potential for region '*d*' is given by the expression (52), and this result for such regions was found by Evvard (ref. **2**).

5. The general supersonic wing

When the flows over the subsonic edges are not independent, the calculation of the potential everywhere on the wing is still possible, but the expressions for the potential in those regions not covered by the results of §§ 3, 4 are no longer of simple analytical form, and it would be necessary to have recourse to numerical evaluation in general.

The simplest method of procedure is to determine the function $f(\alpha,\beta)$ of eqn. (17) systematically over the plane $z = +0$ and then to calculate the potential from eqn. (18). A statement of the formulae in full would be very lengthy and is easily reproduced, so only a brief statement of method will be given. We consider first that part of the problem for which $\phi_1 = 0$ on $z = 0$ except on S. On referring back to Fig. 1, the potential in the region $M'MT_1T_1'$ (for a wing of much smaller aspect ratio than is shown) is

$$\phi_1 = \int\limits_{0}^{\alpha} \frac{d\alpha'}{\sqrt{(\alpha-\alpha')}} \left\{ \int\limits_{A_2(\alpha')}^{\beta} \frac{\mu(\alpha',\beta')\,d\beta'}{\sqrt{(\beta-\beta')}} + \int\limits_{A_1(\alpha')}^{A_2(\alpha')} \frac{\lambda(\alpha',\beta')\,d\beta'}{\sqrt{(\beta-\beta')}} + \int\limits_{0}^{A_1(\alpha')} \frac{\nu(\alpha',\beta')\,d\beta'}{\sqrt{(\beta-\beta')}} \right\} = 0, \tag{53}$$

where we have $\nu(\alpha,\beta) = 0$ when $\alpha < \alpha_0$. Similarly for the region $L'LT_2T_2'$ we have

$$\phi_1 = \int\limits_0^\beta \frac{d\beta'}{\sqrt{(\beta-\beta')}}\left\{\int\limits_{B_2(\beta')}^{\alpha} \frac{\nu(\alpha',\beta')\,d\alpha'}{\sqrt{(\alpha-\alpha')}}+\int\limits_{B_1(\beta')}^{B_2(\beta')} \frac{\lambda(\alpha',\beta')\,d\alpha'}{\sqrt{(\alpha-\alpha')}}+\int\limits_0^{B_1(\beta')} \frac{\mu(\alpha',\beta')\,d\alpha'}{\sqrt{(\alpha-\alpha')}}\right\} = 0 \tag{54}$$

and $\mu(\alpha,\beta) = 0$ when $\beta < \beta_0$.

Equations (53) and (54) are satisfied if the contents of the brackets vanish (cf. eqn. (27)), and by solving the two resulting equations, we obtain

$$\mu(\alpha,\beta) = -\frac{1}{\pi\sqrt{\{\beta-A_2(\alpha)\}}}\times$$

$$\times\left[\int\limits_{A_1(\alpha)}^{A_2(\alpha)} \frac{\lambda(\alpha,\beta')\sqrt{\{A_2(\alpha)-\beta'\}}\,d\beta'}{\beta-\beta'}+\int\limits_0^{A_1(\alpha)} \frac{\nu(\alpha,\beta')\sqrt{\{A_2(\alpha)-\beta'\}}\,d\beta'}{\beta-\beta'}\right], \tag{55}$$

$$\nu(\alpha,\beta) = -\frac{1}{\pi\sqrt{\{\alpha-B_2(\beta)\}}}\times$$

$$\times\left[\int\limits_{B_1(\beta)}^{B_2(\beta)} \frac{\lambda(\alpha',\beta)\sqrt{\{B_2(\beta)-\alpha'\}}\,d\alpha'}{\alpha-\alpha'}+\int\limits_0^{B_1(\beta)} \frac{\mu(\alpha',\beta)\sqrt{\{B_2(\beta)-\alpha'\}}\,d\alpha'}{\alpha-\alpha'}\right]. \tag{56}$$

When $0 \leqslant \alpha \leqslant \alpha_0$, $\nu = 0$ and eqn. (55) gives μ in this strip (cf. eqn. (28)); similarly ν is given in $0 \leqslant \beta \leqslant \beta_0$ from eqn. (56). A second application of eqn. (55) then gives μ in the strip $\alpha_0 \leqslant \alpha \leqslant B_2(\beta_0)$ since ν is now known in this strip and so on. Thus μ and ν may be calculated systematically in the regions for which these equations are valid.

An alternative procedure is to substitute the right-hand side of eqn. (56) in the right-hand side of eqn. (55) and vice versa, thus obtaining integral equations for μ and ν, which may be solved by the process of successive substitution. Since μ and ν vanish for $\alpha < 0$ and $\beta < 0$ respectively, the two series of repeated integrals obtained will terminate in general. The series do not terminate, however, if L and M coincide, that is, if the wing is pointed and its leading edges lie inside the Mach cone from its vertex, so that the method of this paper is not ideally suited for a treatment of this case. A solution of eqns. (55) and (56) in closed form would be valuable in this connexion, but the author has not been able to achieve this.

In the regions $T_1'T_1NN'$ and $T_2'T_2PP'$, account must be taken of the effect of the vortex sheet downstream from the trailing edge. The method for doing this is exactly the same in principle as that used already in §§ 3, 4, and μ, ν, μ_s, ν_s may be calculated systematically in the appropriate

regions in the way indicated above by solving a succession of Abel type integral equations.

The potential may then be calculated everywhere on the wing from eqn. (18) and the velocities obtained by differentiation. It must be stated that the above process is likely to be extremely tedious in general.

Once the potential is known all over the wing, the potential may be found everywhere else by a process already given by the author (ref. **5**). The potential in $z > 0$ is given by eqn. (4), the area of integration being those portions of S and T for which the inequality (5) holds, since $\phi_1 = 0$ over R. By integrating eqn. (4) by parts with respect to x', and remembering that ϕ_1 is continuous on $z = +0$ and vanishes on the leading edge, and that $\partial\phi_1/\partial x = 0$ on T, we have

$$\phi_1(x,y,z) = \frac{1}{\pi}\iint \frac{\partial\phi_1(x',y',+0)}{\partial x'}\times$$

$$\times\frac{z(x-x')\,dx'dy'}{[(y-y')^2+z^2]\sqrt{\{(x-x')^2-B^2(y-y')^2-B^2z^2\}}} \tag{57}$$

the integration now being taken over that part of S alone for which the inequality (5) is satisfied. In its general form, this result (57) ranks in importance with eqns. (3) and (4), and is often more convenient than eqn. (4) in applications, since it is no longer necessary to consider 'finite parts'.

6. The aerodynamic forces on the wing

The aerodynamic forces may be calculated by considering the rate of change of momentum through a closed surface enclosing the wing. This surface may be chosen to consist of a cut tubular surface of circular cross-section having a small radius ϵ with the centres of cross-section on C, and two plane surfaces lying very close to the upper and lower sides of S joining the cut edges of the tube. If $\mathbf{n}$ is the outward normal to this surface at any point, then the vector force $\mathbf{F}$ on the wing is given to our order of approximation by

$$\mathbf{F} = -\int \{p\mathbf{n}+\rho U^2[(1-M^2\,\partial\phi/\partial x)\mathbf{i}\,.\,\mathbf{n}+\mathbf{n}\,.\,\nabla\phi]\nabla\phi\}\,dS, \tag{58}$$

where ρ is the density of the undisturbed stream, p is the disturbance pressure given by the approximate Bernoulli equation,

$$p = -\rho U^2\left\{\frac{\partial\phi}{\partial x}-\frac{B^2}{2}\left(\frac{\partial\phi}{\partial x}\right)^2+\frac{1}{2}\left(\frac{\partial\phi}{\partial y}\right)^2+\frac{1}{2}\left(\frac{\partial\phi}{\partial z}\right)^2\right\}, \tag{59}$$

and the integration is taken over the enclosing surface.

If ϕ_0 and ϕ_1 are respectively the symmetrical and antisymmetrical potentials of § 2, then the contribution from the plane surfaces to the

drag force measured in the direction of the undisturbed stream is

$$-2\rho U^2 \iint \left(\frac{\partial\phi_0}{\partial z}\frac{\partial\phi_0}{\partial x}+\frac{\partial\phi_1}{\partial z}\frac{\partial\phi_1}{\partial x}\right)_{z=+0} dxdy \tag{60}$$

on taking account of the symmetry properties of ϕ_0 and ϕ_1, the integration being taken over the upper plane surface.

In order to determine the contribution from the tubular surface, we introduce locally cylindrical coordinates r, θ, s at C: s is distance measured along C, r is distance from C, and θ is measured from the upper side of S, being zero there and taking the value 2π on the lower side. We require the value of the integral over the tubular surfaces as $\epsilon \to 0$. Generally $|\nabla\phi_0|$ is finite everywhere and $|\nabla\phi_1|$ is finite except on the subsonic leading edges, where, from eqns. (55) and (56), it is seen that $\partial\phi_1/\partial z \sim Kr^{-\frac{1}{2}}$ on $\theta = \pi$ and $\partial\phi_1/\partial z \sim$ (constant) on $\theta = 0$ or 2π as $r \to 0$, K being a function of s. If ψ is the inclination of the leading edge to the x-axis, then the contribution from the tubular surface is

$$\lim_{\epsilon\to 0} -\rho U^2 \int\limits_{T_2L, MT_1} ds \times$$

$$\times \int\limits_0^{2\pi} \left[\left\{\frac{\partial\phi_1}{\partial r} - M^2 \sin^2\psi \cos\theta\left(\frac{\partial\phi_1}{\partial r}\cos\theta - \frac{\partial\phi_1}{r\,\partial\theta}\sin\theta\right)\right\}\nabla'\phi_1\right]_{r=\epsilon} \epsilon\, d\theta, \tag{61}$$

where ∇' is the vector gradient operator with respect to x and y, and the integration with respect to s is taken along the subsonic leading edges. All other terms in eqn. (58) vanish in the limit.

The quantity

$$\lim_{\epsilon\to 0} \rho U^2 \int\limits_0^{2\pi} \left[\left\{\frac{\partial\phi_1}{\partial r} - M^2 \sin^2\psi \cos\theta\left(\frac{\partial\phi_1}{\partial r}\cos\theta - \frac{\partial\phi_1}{r\,\partial\theta}\sin\theta\right)\right\}\nabla'\phi_1\right]_{r=\epsilon} \epsilon\, d\theta \tag{62}$$

is the suction force per unit length on the subsonic leading edge analogous to that occurring in subsonic theory, and is directed normally outwards from the wing edge. It is shown in the Appendix that the magnitude of this force per unit length is

$$\frac{\pi\rho U^2 K^2}{\sqrt{(1-M^2\sin^2\psi)}} \equiv \rho U^2 \mathscr{F}. \tag{63}$$

The function K may be obtained from the expressions found for μ and ν. When the flows at the subsonic leading edges are independent, we may use the result for μ given by eqn. (28) at the edge MT_1, and the similar expression for ν at the edge LT_2. Near the edge MT_1, we have

$$\left(\frac{\partial\phi_1}{\partial z}\right)_{z=0} \sim \frac{4B}{\sqrt{\{\beta - A_2(\alpha)\}}} \int\limits_{A_1(\alpha)}^{A_2(\alpha)} \frac{\lambda(\alpha,\beta')\,d\beta'}{\sqrt{\{A_2(\alpha)-\beta'\}}}. \tag{64}$$

If ψ_M is the Mach angle ($\cot\psi_M = B$) we have near C in $z = 0$

$$\beta - A_2(\alpha) = 2r\cos\psi_M \operatorname{cosec}(\psi_M - \psi), \tag{65}$$

whence
$$K = -\frac{4B}{\sqrt{\{2\cos\psi_M \operatorname{cosec}(\psi_M-\psi)\}}} \int\limits_{A_1(\alpha)}^{A_2(\alpha)} \frac{\lambda(\alpha,\beta')\,d\beta'}{\sqrt{\{A_2(\alpha)-\beta'\}}}. \tag{66}$$

By adding the contributions from the plane and tubular surfaces in the limit as $\epsilon \to 0$, we obtain an expression for the drag force on the wing in the form

$$\frac{\text{Drag}}{\frac{1}{2}\rho U^2} = -4\iint\limits_{\mathsf{S}} \left(\frac{\partial\phi_0}{\partial z}\frac{\partial\phi_0}{\partial x} + \frac{\partial\phi_1}{\partial z}\frac{\partial\phi_1}{\partial x}\right)_{z=+0} dxdy - 2\int\limits_{T_2L,MT_1} \mathscr{F}\,dy, \tag{67}$$

the integrations being taken over the upper side of S, and along the subsonic leading edges respectively.

A similar expression may be obtained for the side force on the wing in the direction of the y-axis.

The lifting force in the direction of the z-axis is given to our order of approximation from eqns. (58) and (59) by

$$2\rho U^2 \iint\limits_{\mathsf{S}} \left(\frac{\partial\phi_1}{\partial x}\right)_{z=+0} dxdy. \tag{68}$$

Since $\phi = 0$ on the leading edge, integration with respect to x gives finally

$$\frac{\text{Lift}}{\frac{1}{2}\rho U^2} = 4\int\limits_{T_2PNT_1} (\phi_1)_{z=+0}\,dy, \tag{69}$$

the integration being taken along the trailing edge of S, or, as a result of condition (12, ii), along any line spanning T.

The pitching, rolling, and yawing moments of the aerodynamic forces may be found in a similar manner.

APPENDIX

In order to evaluate the integral of eqn. (62) for the suction force per unit length at the subsonic leading edge, we transform eqn. (1) to a system of locally orthogonal coordinates s, t, z at C, where s is distance measured along C, and t is distance from C such that $t = r\cos\theta$. In a neighbourhood of C, the variation of ϕ_1 with s is small compared with the variation with t and z, and the equation for ϕ_1 is

$$C^4\frac{\partial^2\phi_1}{\partial t^2} + \frac{\partial^2\phi_1}{\partial z^2} = 0, \qquad C^4 = 1 - M^2\sin^2\psi \tag{A.1}$$

approximately.

Let $C^2 t_1 = t$ and define new variables r_1, θ_1 by

$$r_1\cos\theta_1 = t_1, \qquad r_1\sin\theta_1 = z. \tag{A.2}$$

Then a solution of eqn. (A.1) behaving in the required manner ($\partial\phi_1/\partial z \sim Kr^{-\frac{1}{2}}$ when $\theta = \pi$ as $r \to 0$) is

$$\phi_1 = 2Kr_1^{\frac{1}{2}}\cos\tfrac{1}{2}\theta_1 + O(r). \tag{A.3}$$

From eqns. (A. 2) and (A. 3)

$$\frac{\partial\phi_1}{\partial r} = \frac{K}{Cr_1^{\frac{1}{2}}}\cos\tfrac{1}{2}\theta_1\frac{r_1}{r}+O(1), \tag{A. 4}$$

$$\frac{\partial\phi_1}{\partial t} = \frac{K}{C^3 r_1^{\frac{1}{2}}}\cos\tfrac{1}{2}\theta_1+O(1), \tag{A. 5}$$

$$\frac{\partial\theta}{\partial\theta_1} = \frac{C^2\sec^2\theta_1}{C^4+\tan^2\theta_1}, \tag{A. 6}$$

whence the integral of eqn. (62) is

$$\lim_{\epsilon\to 0}\rho U^2\int\limits_0^{2\pi}\left\{\left(\frac{\partial\phi_1}{\partial r}-M^2\sin^2\psi\cos\theta\frac{\partial\phi_1}{\partial t}\right)\frac{\partial\phi_1}{\partial t}\right\}_{r=\epsilon}\epsilon\,d\theta$$

$$= \rho\frac{U^2K^2}{C^2}\int\limits_0^{2\pi}\frac{\cos^2\frac{1}{2}\theta_1\sec^2\theta_1\{1-(C^4-1)\cos\theta_1\}\,d\theta_1}{C^4+\tan^2\theta_1}$$

$$= \frac{\pi\rho U^2K^2}{\sqrt{(1-M^2\sin^2\psi)}}. \tag{A. 7}$$

REFERENCES

1. A. E. PUCKETT, 'Supersonic wave drag of thin airfoils', *Journ. Aero. Sci.* 1946, **13**, No. 9.
2. J. C. EVVARD, *Distribution of Wave Drag and Lift in the Vicinity of Wing Tips at Supersonic Speeds,* National Advisory Committee for Aeronautics (U.S.A.), Technical Note No. 1382 (1947).
3. J. HADAMARD, *Lectures on Cauchy's Problem* (Yale University Press, 1923).
4. E. T. WHITTAKER and G. N. WATSON, *Modern Analysis* (Cambridge University Press, 1940).
5. G. N. WARD, 'A note on the calculation of the down-wash behind a lifting supersonic wing', *The Aeronautical Quarterly,* May, 1949.
6. M. J. LIGHTHILL, 'The drag integral in the linearized theory of compressible flow', *to be published in the Quart. Journ. of Mathematics.*
7. W. D. HAYES, *Linearized Supersonic Flow,* Thesis for Ph.D. at California Inst. of Tech. (1947). North American Aviation Inc. Report No. AL–222.

EDDY DIFFUSION AND EVAPORATION IN FLOW OVER AERODYNAMICALLY SMOOTH AND ROUGH SURFACES: A TREATMENT BASED ON LABORATORY LAWS OF TURBULENT FLOW WITH SPECIAL REFERENCE TO CONDITIONS IN THE LOWER ATMOSPHERE

By K. L. CALDER

(*Chemical Defence Experimental Establishment, Porton, Wiltshire*)

[Received 5 April 1948]

SUMMARY

A theoretical treatment of the problems of eddy diffusion and evaporation is developed, based on the use of well-established laboratory data for the laws of turbulent flow. Expressions which are free from adjustable constants and involve only directly measurable quantities are derived for the two-dimensional diffusion of matter and evaporation of liquid in flow over aerodynamically smooth and rough surfaces. For aerodynamically smooth surfaces the evaporation formulae obtained are identical with those found previously by O. G. Sutton using a different treatment. The latter results, which have been shown to be in good agreement with laboratory experiments, may be derived independently as a special case by a more direct method involving fewer assumptions. The formulae obtained for aerodynamically rough surfaces are in excellent agreement with observational data on the diffusion of smoke in the lower atmosphere under adiabatic conditions, and on the evaporation of liquid from the ground surface.

The treatment may also be applied to the transfer of heat from aerodynamically smooth and rough surfaces provided the temperature differences are not too large.

1. Introduction

THE present paper makes use of a coefficient of turbulent diffusion derived from experimentally established laws for the variation of mean velocity with height in fluid flow over aerodynamically smooth and rough surfaces. Solutions are provided for the problems of the two-dimensional diffusion of matter and evaporation of liquid in turbulent flow over such surfaces, in the absence of buoyancy effects. The work is essentially an extension of the Prandtl (**12, 13**) approach to the turbulence problem, although it does not involve reference to the latter's mixing-length theory. In contrast to an earlier treatment of similar problems by O. G. Sutton (**18 a** and **b**), no use is made of empirical formulations of the Taylor correlation coefficient (**21 b**), and it is shown that Sutton's theoretical expressions for evaporation from smooth liquid surfaces of finite extent, which have been substantiated experimentally, can be deduced as a special case by the

present method. Provided the temperature differences are not too large, the present treatment may also be applied to the transfer of heat from aerodynamically smooth and rough surfaces.

2. Aerodynamic considerations

The existence of two fundamentally different limiting types of turbulent boundary layer flow is now well known from experiments with pipes and flat plates in the laboratory (e.g. Goldstein, **6**). In so-called 'aerodynamically smooth flow' the drag exerted on the fluid by the boundary surface is a function of the Reynolds number only and, except for a region very close to the surface, the distribution of mean velocity is represented to a high degree of accuracy by the logarithmic law

$$\frac{u}{v_*} = \frac{1}{k}\log_e\frac{v_* z}{\nu} + 5{\cdot}5, \tag{1}$$

where u = the velocity at distance z from the pipe wall or plate,
$v_* = \sqrt{(\tau_0/\rho)}$, the so-called 'shearing stress velocity',
τ_0 = shearing stress per unit area of the plate or pipe wall, at the transverse section considered,
ρ = fluid density,
ν = kinematic viscosity of fluid,
$k = 0{\cdot}4$, the so-called von Kármán's constant.

On the other hand, for 'aerodynamically fully rough flow' the drag is independent of the Reynolds number and is proportional to the square of the velocity, while the mean velocity distribution is given by

$$\frac{u}{v^*} = \frac{1}{k}\log_e\frac{z}{z_0}, \tag{2}$$

where k is again von Kármán's constant and z_0 (called the roughness parameter) depends on the size, shape, orientation, and spacing of the roughness elements on the boundary surface. It is evident on physical grounds that equation (2) should involve a 'zero-point displacement' distance, to provide a datum level above which active turbulent exchange first commences and the logarithmic law is valid. Thus modified it becomes

$$\frac{u}{v_*} = \frac{1}{k}\log_e\left(\frac{z-d}{z_0}\right), \tag{3}$$

the zero-point displacement d being of similar magnitude to the depth of the relatively stationary air trapped among the roughness elements of the surface. This formula only applies, of course, when z is greater than (z_0+d).

Whether the flow over a given surface is of the aerodynamically smooth

or fully rough type depends on the Reynolds number, and smooth flow eventually occurs in all cases at sufficiently low values of the latter. Laboratory experiments by Schlichting (**16**) have shown that the criteria for fully rough, transitional, or aerodynamically smooth flow can be expressed in the form

$$\left.\begin{array}{ll} \text{fully rough flow} & \dfrac{v_* z_0}{\nu} > 2{\cdot}5 \\ \text{transitional flow} & 2{\cdot}5 > \dfrac{v_* z_0}{\nu} > 0{\cdot}13 \\ \text{aerodynamically smooth flow} & 0{\cdot}13 > \dfrac{v_* z_0}{\nu} \end{array}\right\}, \tag{4}$$

the roughness parameter z_0 characteristic of the surface being deduced from the velocity profile (3) observed at sufficiently high Reynolds numbers with fully rough flow.

Because of the intractability of certain of the subsequent mathematical developments of the present paper associated with the use of the logarithmic velocity distributions (1) and (3), it is necessary to replace these laws by approximate power laws. For smooth flow one well-known formula of this kind is the Blasius formula (Goldstein, **6**)

$$\frac{u}{v_*} = 8{\cdot}74(v_* z/\nu)^{\frac{1}{7}}, \tag{5}$$

which, except near the boundary surface, is found to agree closely with the more accurate distribution law (1), up to $v_* z/\nu = 700$. For higher values of $v_* z/\nu$, it is found, however, that the $\frac{1}{7}$th power law no longer gives agreement, and that $\frac{1}{8}$th, $\frac{1}{9}$th, $\frac{1}{10}$th, etc., powers have to be taken, giving formulae of the type

$$u/v_* = q(v_* z/\nu)^{\alpha}, \tag{6}$$

where q and α depend on the range of $v_* z/\nu$ within which (6) is to agree approximately with (1). The approximate power law (6) is used in the discussion of aerodynamically smooth flow in the present paper.

A suitable approximation formula for fully rough flow has previously been used by Prandtl and Tollmien (**12**). Comparison with the power-law approximation for smooth flow shows that the appropriate approximation for the velocity distribution (3) of fully rough flow is

$$\frac{u}{v_*} = q'\left(\frac{z-d}{z_0}\right)^{\alpha}, \tag{7}$$

where the values of q' and α will depend on the range of $(z-d)/z_0$ within which (7) is to agree with the more accurate formula (3).

3. Wind-velocity distribution in the lower atmosphere

The preceding discussion is of obvious importance when the flow near the earth's surface is considered. Atmospheric flow under adiabatic conditions may be expected to be comparable with that found in pipe and flat plate flow in the laboratory.

Whether the earth's surface is aerodynamically smooth or rough can be answered in any particular case with a fair degree of certainty. If the surface is smooth, then equation (1) may be expected to be valid. The 'friction velocity' v_* in this equation may be evaluated from the velocity observed at a particular height, and the velocities at other heights may then be computed from the equation and compared with the observed values. This test has been applied by Rossby (**15 b**) to certain wind-velocity observations over the sea, and he concluded that in moderately light winds the sea surface may be aerodynamically smooth.† The test has also been applied by P. A. Sheppard (unpublished) to wind observations obtained by Best (**1**) over very closely cropped grass (a cricket pitch). For wind velocities between 1·5 and 4·0 m.sec.$^{-1}$ and adiabatic conditions, Sheppard found no agreement between equation (1) and the observed wind-velocity distribution. His results are reproduced below in Table 1, the velocities being in arbitrary units.

TABLE 1

z (height above surface, cm.)	2·5	5·0	10	25	50	100	200	506
u (observed) . .	36·4	49·0	63·0	79·2	90·3	100	111·7	122·5
u (calculated) . .	63·4	70·3	77·1	86·1	93·0	(100)	106·7	116·0

Observed wind-velocity distribution under adiabatic conditions over closely cropped grass, compared with theoretical distribution for aerodynamically smooth flow.

Over the height range investigated, the observed velocity gradient is considerably greater than that given by equation (1). The inference is, therefore, that a closely cropped grass surface is rough, even at the relatively low wind velocities considered, and for greater velocities will, of course, remain rough. Any grass surface to be found in practice will therefore be aerodynamically rough according to this test. However, the test does not suffice to show that the flow in the lower atmosphere is normally of the fully rough type, as governed by equation (3), and not of a transitional type. To establish completely the validity of equation (3) as applied to flow in the lower atmosphere it must be verified that the variation of wind with height is of the given logarithmic form and also that the implied

† This conclusion has since been confirmed by Montgomery (**9**) and Sverdrup (**20 a**), from observations of the vertical humidity distribution above the ocean surface.

relation between surface drag and the wind velocity observed at any height, namely

$$\tau_0 = \frac{\rho k^2 u^2}{\{\log_e(z-d)/z_0\}^2}, \tag{8}$$

holds in the atmosphere.

Extensive measurements recently made by E. L. Deacon (unpublished) over various grass-covered surfaces on Salisbury Plain have shown conclusively that the wind-velocity profiles in the lowest decametre of the atmosphere under adiabatic conditions can be represented with great accuracy by a logarithmic law of the form given by equation (3). A brief summary of his results (for adiabatic conditions) is given in Table 2.

TABLE 2

Grass length (cm.)	*Wind velocity at 1 m. (m.sec.$^{-1}$)*	*Average ratio of velocities $u_{2\,\mathrm{m.}}/u_{1\,\mathrm{m.}}$*	*Zero-point displacement d (cm.)*	*Roughness parameter z_0 (cm.)*
60–70	1	1·45	+15	15·9
60–70	2	1·35	+16	8·8
60–70	3	1·32	+21	5·6
60–70	4·5	1·28	+32	3·0
1·5	1–8	1·112	0 approx.	0·20
3·0	1–8	1·140	0 ,,	0·71
4·5	2	1·191	0 ,,	2·65
4·5	4·5	1·170	0 ,,	1·7

Parameters in the logarithmic law (3), related to grass length, from observations by E. L. Deacon on Salisbury Plain.

It is seen that over short-grass surfaces the zero-point displacement d can effectively be taken as zero. Over long-grass surfaces, however, d is definitely positive and becomes more nearly equal to the height of the vegetation as the density of the latter increases. Deacon's observations support this concept that d is an 'aerodynamic length' which is related to a linear dimension of the roughness elements and to the density of their packing.

As to the roughness parameter z_0, Best's (**1**) short-grass observations show no significant change in the velocity gradient, as indicated by the ratio $u_{2\,\mathrm{m.}}/u_{1\,\mathrm{m.}}$, with changes of wind velocity, implying a constant value of z_0, independent of wind velocity. The same is true of Deacon's data for short grass 2–3 cm. long. Deacon's values for grass 4–4·5 cm. long, however, show a tendency for the wind-velocity ratio $u_{2\,\mathrm{m.}}/u_{1\,\mathrm{m.}}$ to decrease with increasing wind velocity, implying a decrease in z_0, while for long grass this effect is accentuated. The explanation of these results is that the deflexion of the long grass blades by the wind results in a 'smoothing' of the surface. Clearly in the case of natural surfaces, with complex

roughness elements which may themselves be distorted by the wind, the only practicable method of estimating the values of the parameters d and z_0 in equation (3) is by observation of the wind velocity at three heights at least.

The verification of equation (8), which is easily done for flow through rough tubes in the laboratory, where τ_0 follows directly from the pressure gradient along the axis of the tube, is not nearly so simple in the atmospheric case, since direct measurements of τ_0 are not available.† Nevertheless, Rossby and Montgomery (**15 a**) have shown that this equation, with a value of z_0 deduced from observations of the wind profile over open grassland, gives values for the surface drag τ_0 in close agreement with those deduced by Taylor (**21 a**) from an analysis of data of pilot balloon ascents over Salisbury Plain.

Knowing the roughness parameter z_0 of any natural surface as obtained from wind-profile observations using equation (3), it is possible by means of the Schlichting criteria (4) to obtain information as to the possibility of flow of the smooth or transitional types.

On calculating $v_* z_0/\nu$ from values of v_* and z_0 obtained using equation (3), for Deacon's short- and long-grass data of Table 2, the following values are obtained, for an assumed wind velocity of 5 m.sec.$^{-1}$ at 2 m. height.

Short grass (1–3 cm. high): $d = 0$ cm., $z_0 = 0{\cdot}5$ cm., $v_* z_0/\nu = 110$

Long grass (60–70 cm. high): $d = 30$ cm., $z_0 = 3{\cdot}0$ cm., $v_* z_0/\nu = 990$

Since the 'friction velocity' v_* is directly proportional to the wind velocity, this shows that only for the short grass, at wind velocities (at 2 m.) less than 0·1 m.sec.$^{-1}$, can any departure from the fully rough régime be expected. Since from measurements of wind profile by Sverdrup (**20 a**) the roughness parameter z_0 even for a smooth snow surface is approximately the same as for a short-grass surface, it may be concluded from the above that, under adiabatic conditions, flow in the lower atmosphere over the land is always of the fully rough type.

4. The eddy diffusivity over smooth and rough surfaces

In the turbulent layer over a smooth or rough surface there must be a region not too far removed from the surface in which the turbulent shearing stress τ, in the mean direction of flow, can be regarded as effectively independent of distance from the surface. Ertel (**5**) has shown that in the atmosphere the turbulent shearing stress is, to a high degree of

† P. A. Sheppard (**17 a**) has measured directly the drag for wind blowing over a very smooth extensive concrete surface, but the flow for this rather artificial case was probably of the aerodynamically smooth or transitional type.

approximation, independent of the height, in the range $1 < z < 30$ m.† The wind direction is also constant within this layer and coincides with the direction of the frictional drag exerted by the wind on the ground surface. Above the layer, wind direction changes with height according to a modified Ekman spiral. Now the vertical component of eddy viscosity $K(z)$ at any height is given (Brunt, **2**) by the relation

$$\tau = \rho K \frac{\partial u}{\partial z}, \tag{9}$$

where ρ is the fluid density and $\partial u/\partial z$ the gradient of velocity normal to the mean flow. It follows that in the region of constant shearing stress the vertical distribution of eddy viscosity can be deduced immediately from the vertical distribution of mean velocity.

Consider first the power-law representations of the velocity profiles given by equation (6) for smooth surface flow and by equation (7) for fully rough flow. With the proper choice of constants to fit the more accurate logarithmic distributions given by (1) and (3) respectively, these equations represent the velocity distributions in the turbulent boundary layers over smooth and rough surfaces to a high degree of accuracy. They will now be applied in the region of constant shearing stress. From equation (6), by rearrangement,

$$\tau_0 = \rho(u/q)^{2/(1+\alpha)}(\nu/z)^{2\alpha/(1+\alpha)}. \tag{10}$$

Similarly, by taking a new origin at distance d above the datum plane of height measurement for the rough surface, equation (7) gives

$$\tau_0 = \rho \frac{u^2}{q'^2}\left(\frac{z_0}{z}\right)^{2\alpha}. \tag{11}$$

Equations (10) and (11) are special cases of a more general form

$$\tau_0 = \epsilon \rho u^{2\beta}(\delta/z)^{2\alpha\beta}, \tag{12}$$

where for smooth flow,

$$\beta = \frac{1}{1+\alpha}, \qquad \delta = \nu, \qquad \epsilon = (1/q)^{2/(1+\alpha)}$$

and for fully rough flow,

$$\beta = 1, \qquad \delta = z_0, \qquad \epsilon = 1/q'^2. \tag{13}$$

This fact enables a uniform mathematical treatment to be adopted for both smooth and rough surfaces. Since in both cases

$$\frac{u}{u_1} = (z/z_1)^{\alpha}, \tag{14}$$

where u_1 is the velocity at a standard height z_1, it is readily verified by

† For other discussions of this subject see Rossby and Montgomery (**15 a**), Calder (**3**), and Sheppard (**17 b**). All assume straight, parallel, steady streamlines.

differentiation and substitution for $\partial u/\partial z$ in equation (9), using equation (12), that

$$\left.\begin{aligned} K(z) &= Mu_1^{2\beta-1}z_1^{\alpha(1-2\beta)}z^{1-\alpha}, \\ \text{where} \qquad M &= (\epsilon/\alpha)\delta^{2\alpha\beta}, \end{aligned}\right\} \tag{15}$$

assuming that in the region of constant shearing stress the shearing stress has the surface value τ_0.

The above procedure may also be applied to the more accurate logarithmic velocity distribution laws as given by equations (1) and (3), and leads to a simple linear variation of K with height,

$$K = v_* kz \tag{16}$$

for both smooth and rough flow. The use of logarithmic velocity distributions, however, leads to insuperable mathematical difficulties in the subsequent treatment of the diffusion problem, as it gives rise to a differential equation (see paragraph 5) containing a transcendental function (u) and an algebraic one (K). This type of equation has not yet yielded to treatment, and consequently the following discussion will be based entirely on the use of power laws for the velocity distributions.

In considering the diffusion of matter, it will be assumed that the diffusion coefficient for turbulent mass transfer (eddy diffusivity) is equal to that for turbulent momentum transfer (eddy viscosity). Thus if χ is the concentration of matter per unit volume (measured in g.cm.$^{-3}$), the vertical flux of matter per unit horizontal area, and per unit time, is given by†

$$F = -K\frac{\partial\chi}{\partial z}, \tag{17}$$

the negative sign indicating that the flux is directed upwards, i.e. in the positive z-direction, when χ decreases with height.

The question now arises as to the validity of the formula (15) for eddy viscosity (or diffusivity) for small values of z. Actually over both smooth and rough surfaces a transitional region must occur close to the surface, in which molecular viscosity and turbulence are of comparable importance. In this region, equation (9) should be replaced by

$$\tau = \rho(K+\nu)\frac{\partial u}{\partial z}, \tag{18}$$

where $\rho K(\partial u/\partial z)$ represents the so-called 'Reynolds apparent shearing stress' and $\rho\nu\,\partial u/\partial z$ is the molecular shearing stress, the latter being

† Strictly speaking the vertical flux is given by $F = -\rho K\dfrac{\partial}{\partial z}\left(\dfrac{\chi}{\rho}\right)$, where χ/ρ is the mass of diffusing substance per unit mass of air. In what follows it will be assumed that the air density is independent of height, so that the flux reduces to the form given in equation (17).

negligibly small compared with the first except near the boundary. Likewise, near a boundary, the flux equation (17) should be replaced by the more accurate equation

$$F = -(K+D)\frac{\partial \chi}{\partial z}, \tag{19}$$

where D is the molecular diffusivity. Montgomery (**9**) has actually applied this equation to the problem of evaporation from an infinitely extended smooth water surface, assuming that the eddy diffusivity K is operative down to the top of the laminar sub-layer, where it vanishes. The application of a similar treatment to rough surface flow is, however, not so straightforward, and in any case the use of an equation of the form of (19) leads to mathematical difficulties in connexion with the main problems of the present paper. Various assumptions have been made by different writers concerning the nature of the turbulent processes very close to a rough surface. Sverdrup (**20 a** and **b**), considering the problem of evaporation from the oceans, assumes that even over a rough surface there is a thin layer of air next to the surface, within which diffusion is molecular, and applies the laws for fully developed rough flow down to the top of this laminar layer. Montgomery (**9**), however, following Millar (**8**), postulates that the velocity distribution for aerodynamically smooth surfaces also applies for a limited distance above a rough surface. Clearly, near a rough surface conditions are likely to be complex, and the validity of these various assumptions is by no means evident. In the following, it will be assumed that the eddy diffusivity, as given by equation (15), is valid down to $z = 0$. The only justification for this procedure is that it leads to a simple mathematical treatment and to results which are in very good agreement with observation.

5. Diffusion of matter from an infinite line source

The problem of the turbulent diffusion of gas or smoke in the lower atmosphere, from a continuously emitting line source of infinite length, situated at ground level and perpendicular to the mean surface wind direction, is one of considerable intrinsic interest. With axes in which Ox is downwind, Oy across-wind, Oz vertically upwards, and the source defined by $(0, -\infty < y < \infty, 0)$ this problem involves the solution of the partial differential equation

$$u\frac{\partial \chi}{\partial x} = \frac{\partial}{\partial z}\left(K(z)\frac{\partial \chi}{\partial z}\right), \tag{20}$$

χ being the concentration of matter in g.cm.$^{-3}$ at the point (x, z), subject to the boundary conditions

(i) $\chi \to 0$ as $x \to \infty$,

(ii) $K\dfrac{\partial\chi}{\partial z} \to 0$ as $z \to 0$, the 'ground' boundary condition of zero vertical flux of matter.

(iii) χ is such that the rate of transfer of matter across unit width of a plane $x = \text{const.}$, i.e. $\int\limits_0^\infty u\chi\,dz$, is constant and equal to Q, the constant rate of emission of the source in g.cm.$^{-1}$ sec.$^{-1}$

(iv) $\chi \to \infty$ at the line of emission ($x = 0 = z$).

This problem was first considered by Roberts (**14**) for the case of constant eddy diffusivity. Subsequently he showed, in an unpublished paper, that the solution of equation (20) subject to the given boundary conditions, and with wind varying as a power of the height $u = Uz^m$, and eddy diffusivity varying as a power of the height $K = \lambda z^n$, was

$$\chi = \frac{QU^{[\{(m+1)/(m-n+2)\}-1]}\exp\{-Uz^{m-n+2}/\lambda(m-n+2)^2x\}}{(m-n+2)^{[\{2(m+1)/(m-n+2)\}-1]}\lambda^{(m+1)/(m-n+2)}\,\Gamma\{(m+1)/(m-n+2)\}x^{\{(m+1)/(m-n+2)\}}} \tag{21}$$

which is valid for $(m-n+2) \geqslant 0$, $\Gamma(\theta)$ being the Gamma-function.

Applying this solution to the particular variations of u and K given by equations (14) and (15) respectively, we obtain†

$$\chi = \frac{Q\exp\{-u_1^{2(1-\beta)}z^{2\alpha+1}/M(2\alpha+1)^2z_1^{2\alpha(1-\beta)}x\}}{(2\alpha+1)^{1/(2\alpha+1)}M^{(\alpha+1)/(2\alpha+1)}\,\Gamma\{(\alpha+1)/(2\alpha+1)\}u_1^{\kappa}z_1^{-\alpha\kappa}x^{(\alpha+1)/(2\alpha+1)}}, \tag{22}$$

where $$\kappa = (2\alpha\beta+2\beta-1)/(2\alpha+1).$$

This general formula, with suitable values for the constants, again applies to both smooth and rough surfaces.

For smooth surfaces, from (15) and (13),

$$M = \frac{1}{\alpha}(1/q)^{2/(1+\alpha)}\nu^{2\alpha/(1+\alpha)}, \tag{23}$$

and (22) reduces to

$$\chi = \frac{Q\exp\{-u_1^{2\alpha/(1+\alpha)}z^{2\alpha+1}/M(2\alpha+1)^2z_1^{2\alpha^2/(1+\alpha)}x\}}{(2\alpha+1)^{1/(2\alpha+1)}M^{(\alpha+1)/(2\alpha+1)}\Gamma\{(\alpha+1)/(2\alpha+1)\}u_1^{1/(2\alpha+1)}z_1^{-\alpha/(2\alpha+1)}x^{(\alpha+1)/(2\alpha+1)}}. \tag{24}$$

Defining the height H of the cloud of diffusing matter as the distance from the surface $z = 0$, to the point at which the concentration has fallen to one-tenth of its surface value, it readily follows from (24) that

$$H = \{2{\cdot}3M(2\alpha+1)^2u_1^{-2\alpha/(1+\alpha)}z_1^{2\alpha^2/(1+\alpha)}x\}^{1/(2\alpha+1)}. \tag{25}$$

† For rough surfaces it should be noted that $z = 0$ is at a distance d above the datum plane of the surface, and the source is assumed to be at this distance, where turbulence first becomes operative.

Similarly for rough surfaces

$$M = z_0^{2\alpha}/\alpha q'^2, \tag{26}$$

and (22) reduces to

$$\chi = \frac{Q\exp\{-z^{2\alpha+1}/M(2\alpha+1)^2x\}}{(2\alpha+1)^{1/(2\alpha+1)}M^{(\alpha+1)/(2\alpha+1)}\Gamma\{(\alpha+1)/(2\alpha+1)\}u_1 z_1^{-\alpha}x^{(\alpha+1)/(2\alpha+1)}}, \tag{27}$$

while the height of the cloud is given by

$$H = \{2{\cdot}3M(2\alpha+1)^2x\}^{1/(2\alpha+1)}. \tag{28}$$

It will be noted that for rough surfaces the vertical distribution of concentration, and consequently the height of the cloud, are independent of the wind velocity, while actual concentrations are inversely proportional to the wind velocity at a standard height. For both smooth and rough surfaces the concentration varies with distance, inversely as a power less than unity of the distance, the actual value of which is determined by the vertical profile of wind velocity, i.e. the value of α in equation (14).

To apply the above formulae it is first necessary to estimate suitable values for the parameters q and α for smooth surfaces, and q', α, and z_0 for rough surfaces. Considering first smooth surface flow, the approximate power law (6) must be so chosen that it closely fits the logarithmic law (1), over the range of $v_* z/\nu$ with which one is concerned in relation to the region of vertical diffusion. The latter proviso is necessary since, owing to the approximate nature of the power-law representation, the index α is a function of the height interval considered, and this means that when using a power-law treatment one must strictly have some *a priori* knowledge of the extent of vertical diffusion for the distance of travel considered. If observations of wind velocity are available at two well-separated heights, which between them include most of the region of vertical diffusion, then a suitable value of α can be obtained immediately, using equation (14). The value of v_* appearing in equation (6) is estimated using the logarithmic law (1), from the velocity observed at one definite height, and hence the value of q can be obtained. If actual velocity measurements are not available at two heights covering the region of vertical diffusion, then values may be extrapolated, using (1), and the same procedure adopted.

Although no observational data are available relating to the diffusion of gas or smoke over aerodynamically smooth surfaces, a rough estimate of the vertical diffusion can be made in any particular case from equation (25), using the values of q and α appropriate to the Blasius formula (5). Thus, to consider an example, we find from (25) that for $z_1 = 200$ cm., $u_1 = 500$ cm.sec.$^{-1}$, $q = 8{\cdot}74$, $\alpha = \frac{1}{7}$, and a distance of travel $x = 100$ m., the height H of the cloud is approximately 200 cm. A more accurate estimate of diffusion can now be made by choosing more appropriate

values for q and α. Thus, assuming in equation (1) that $u(200 \text{ cm.}) = 500$ cm.sec.$^{-1}$, we readily find by trial and error (or, more conveniently, using a graph given by Rossby, **15 a**) that $v_* = 16{\cdot}3$ cm.sec.$^{-1}$ A suitable value for α in equation (14), applying to the velocity profile over the greater part of the layer of diffusion, can be obtained from the ratio, say $u(200 \text{ cm.})/u(10 \text{ cm.})$, the velocity $u(10 \text{ cm.})$ being calculated from equation (1). It is found that $\alpha = 0{\cdot}095$, and equation (6) with the above value of v_* then gives $q = 11{\cdot}9$. Thus, in the example considered, for diffusion to a distance of 100 m. from the source over a smooth surface, the approximate power law which closely represents the velocity distribution over the height of the cloud is

$$\frac{u}{v_*} = 11{\cdot}9\left\{\frac{v_* z}{\nu}\right\}^{0{\cdot}095}. \tag{29}$$

This differs considerably from the Blasius one-seventh power-law formula, given by (5), as is only to be expected, since for the example considered, $v_* z/\nu$ ranges from $1{\cdot}08\times 10^3$ to $2{\cdot}17\times 10^4$ in the layer 10–200 cm., values which are much in excess of the critical value $v_* z/\nu \approx 700$, previously quoted as an upper limit for the Blasius formula. Clearly, for greater distances of travel from the source, the vertical region of diffusion will be greater and the appropriate values of α will be even less. This question will be considered further for the rough surface case. Using the above values for q and α in equation (25) leads to a more accurate estimate, for the height of the cloud at 100 m., of $H = 350$ cm.

Likewise for rough surface flow, if observations of wind velocity are available at two well-separated heights which include the region of vertical diffusion, then a suitable value of α can be obtained immediately using equation (14). The values of v_* and z_0 in equation (7) are estimated using the logarithmic law (3), from the velocities observed at three different heights. Substitution of the values of v_* and α so obtained in (7) then gives q'. If actual velocity measurements are not available over the region of vertical diffusion, then values must be extrapolated from the logarithmic law, and the same procedure adopted. In Table 3 are given values of q' and α so deduced, by extrapolation of the logarithmic law determined from the velocities observed at 200, 300, and 500 cm., over a long-grass surface, up to the greater heights of 1,000, 2,000, 5,000, and 10,000 cm. The velocity at 200 cm. was in all cases used as a lower reference height velocity. Although the extension of the logarithmic law to the extreme heights is probably not completely justified, the values of q' and α deduced are not likely to be in serious error. Table 4 contains similar values as determined from the velocities observed at heights of 200, 300, and 500 cm. over a short-grass surface.

TABLE 3

Height z (cm.)	200	300	500	1,000	2,000	5,000	10,000
	Observed			*Extrapolated*			
Velocity u (cm.sec.$^{-1}$)	500	556	624	715	803	917	1,002
α	—	—	0·220	0·205	0·194	0·179	0·170
q'	—	—	4·14	4·42	4·61	4·91	5·10

Values of q' and α in equation (7), for a long-grass surface, and appropriate to various height ranges ($v_* = 49{\cdot}5$ cm.sec.$^{-1}$, $d = 30$ cm., $z_0 = 3$ cm.).

TABLE 4

Height z (cm.)	200	300	500	1,000	2,000	5,000	10,000
	Observed			*Extrapolated*			
Velocity u (cm.sec.$^{-1}$)	500	531	574	632	690	766	824
α	—	—	0·153	0·146	0·140	0·132	0·128
q'	—	—	6·01	6·28	6·50	6·82	6·97

Values of q' and α in equation (7), for a short-grass surface, and appropriate to various height ranges ($v_* = 33{\cdot}3$ cm.sec.$^{-1}$, $d = 0$ cm., $z_0 = 0{\cdot}5$ cm.).

Observations show that the height of a smoke cloud under adiabatic conditions over downland is about 1,000 cm. at a distance of 100 m. from the source. Thus, in this case, the height range 200–1,000 cm. covers the major portion of the region of vertical diffusion and the appropriate values of q' and α are those given in Table 3 for $z = 1{,}000$ cm. For greater distances of travel it may be assumed as a first approximation that the height of the cloud increases linearly with distance from the source, so that the remaining values of q' and α in the table are roughly appropriate to distances of travel of 200, 500, and 1,000 m. It is seen that the values of q' and α differ considerably for long-grass and short-grass surfaces and, in both cases, α decreases and q' increases as the vertical depth of the layer considered increases. However, for a given type of surface, these variations are not so large as to prohibit the use, in approximate calculations, of mean values over considerable height ranges, so that precise *a priori* knowledge of the region of vertical diffusion is unnecessary.

In Table 5 are given values of the ground-level concentration and the height of the cloud from an infinite line source, calculated by equations (27) and (28) respectively, for travel over both long- and short-grass surfaces. The corresponding theoretical values for an aerodynamically smooth surface are also included.

In agreement with physical expectation, the predicted diffusion over a short-grass surface is considerably less, i.e. greater concentration and

smaller height of cloud, than over the rougher long-grass surface with which is associated a higher degree of turbulence. Bearing in mind, however, that the two cases considered are extreme ones, changes in the rate of diffusion of matter in the lower atmosphere, produced by normal variations of ground-surface roughness, may be expected to be comparatively small and certainly much less than those found to be produced by changes of atmospheric stability.

Unfortunately no observations suitable for testing the theory are available for surfaces of such small roughness as the short-grass surface

TABLE 5

Distance from source (*m.*)	*Rough surfaces (equations* (27) *and* (28))				*Smooth surfaces* (*equations* (24) *and* (25))	
	Long-grass surface $v_* = 49{\cdot}5$ cm.sec.$^{-1}$; $d = 30$ cm.; $z_0 = 3$ cm.		*Short-grass surface* $v_* = 33{\cdot}3$ cm.sec.$^{-1}$; $d = 0$ cm.; $z_0 = 0{\cdot}5$ cm.		$v_* = 16{\cdot}3$ cm.sec.$^{-1}$; $\nu = 0{\cdot}15$ cm.^{2}sec.$^{-1}$;	
100	$q' = 4{\cdot}42$ $\alpha = 0{\cdot}205$	$\chi_s = 3{,}540$ $H = 1{,}050$	$q' = 6{\cdot}28$ $\alpha = 0{\cdot}146$	$\chi_s = 5{,}300$ $H = 810$	$q = 11{\cdot}9$ $\alpha = 0{\cdot}095$	$\chi_s = 14{,}300$ $H = 350$
1,000	$q' = 5{\cdot}10$ $\alpha = 0{\cdot}170$	$\chi_s = 410$ $H = 6{,}800$	— —	— —	— —	— —

Calculated diffusion under adiabatic conditions over various surfaces, from an infinite line source of strength 1 g.cm.$^{-1}$sec.$^{-1}$, in a wind velocity $u(200\text{ cm.}) = 500$ cm.sec.$^{-1}$

(χ_s = ground concentration in mg.m^{-3}; H = height of cloud in cm.)

considered above, since, for the theory to be applicable, a very large area of uniform roughness is required to ensure that turbulence characteristic of this roughness is developed up to considerable heights. A large body of data has, however, been collected at the Chemical Defence Experimental Station, Porton, Wiltshire (Sutton, **18 c**), relating to the diffusion of smoke and gas under adiabatic conditions, from infinite line sources, over downland (grass 20–70 cm. high) on Salisbury Plain. These data cover distances of travel between 100 and 1,000 m. To compare these observational results with the predictions of the present theory as applied to the long-grass case above, it may be noted that, in spite of the actual dependence of the index α on the depth of the layer of diffusion, i.e. the distance of travel, the associated variations in the indices of z and x in equation (27) are quite small, and for distances of travel between 100 and 1,000 m. a close approximation to these indices will be obtained if the mean of the values of α for these distances is adopted ($\alpha = 0{\cdot}187$). In Table 6 are collected the observed and calculated properties of the cloud.

The agreement between theory and observation is very striking, and shows that in the lower atmosphere under adiabatic conditions there is

TABLE 6

Property	*Calculated*	*Observed*
Height of cloud at 100 m. downwind	1,050 cm. Independent of wind velocity	1,010 cm. Independent of wind velocity
Concentration at ground level at 100 m. downwind	3,540 mg.m.$^{-3}$	3,560 mg.m.$^{-3}$†
Variation of concentration with wind velocity	u^{-1}	u^{-1}
Variation of concentration with distance (100–1,000 m.)	$x^{-0.86}$	$x^{-0.9}$
Law of variation of concentration in the vertical	$\exp(-z^{1.37})$	$\exp(-z^{1.2})$ to $\exp(-z^{1.5})$

Observed and calculated properties of the cloud from an infinite line source under adiabatic conditions, over downland on Salisbury Plain.

(Source strength $Q = 1$ g.cm.$^{-1}$sec.$^{-1}$; wind velocity at 2 m. height $= 500$ cm.sec.$^{-1}$)

† The value quoted is the weighted mean of a number of results, and differs slightly from that quoted recently by Sutton (**18 c**).

close similarity between the diffusion of momentum and matter, and the diffusion of matter can be satisfactorily predicted in terms of the vertical profile of wind velocity near the ground.

Returning now to the equation (24) for aerodynamically smooth flow, this is identical in form with that derived by Sutton (**18 c**)—his equation (18)—making use of an empirical formulation of the Taylor (**21 b**) correlation coefficient and mixing length concepts. Sutton has suggested that one reason why this equation predicts a height of cloud at 100 m. of about 2 m., while that observed in the atmosphere is about 10 m., may be that the 'scale' of atmospheric turbulence is different from that arising in pipe flow. In particular, he suggests that in the atmosphere the value of von Kármán's constant k may be considerably greater than the value $k = 0.4$ as determined in the laboratory. The present development makes it clear that this hypothesis is unnecessary, and that the more probable explanation for the non-applicability of equation (24) to the atmosphere is, as alternatively suggested by Sutton (**18 c**), that the earth's surface is not aerodynamically smooth. As shown above, the customary laboratory value of $k = 0.4$ leads to results in excellent agreement with observation if the rough nature of the flow is appreciated. Further light on this important question comes from a consideration of the problem of evaporation.

6. Evaporation from smooth and rough surfaces of finite extent downwind

The problem of evaporation from a permanently saturated or free liquid surface, of finite extent downwind, level with the earth's surface and of such dimensions that it produces no sensible variations of wind structure, was first considered by Sutton (**18 b**) on the basis of his theory of eddy

diffusion. It involves, for the two-dimensional case, the solution of the differential equation of diffusion (20), subject to suitable boundary conditions. To formulate the problem mathematically, Sutton assumed that for an infinite crosswind saturated strip, of length x_0 downwind, and situated at ground level ($z = 0$), the appropriate boundary conditions† were

$$\left.\begin{array}{lll} \text{(i)} & \lim\limits_{z\to 0} \chi(x,z) = \chi_s \text{ (a constant)} & (0 < x \leqslant x_0) \\ \text{(ii)} & \lim\limits_{z\to\infty} \chi(x,z) = 0 & (0 \leqslant x \leqslant x_0) \\ \text{(iii)} & \lim\limits_{x\to 0} \chi(x,z) = 0 & (0 < z) \end{array}\right\}. \tag{30}$$

As will be clear from the later discussion, Sutton's treatment is restricted to aerodynamically smooth surfaces, and for the latter it seems reasonable to assume that, at the evaporating surface, the constant concentration χ_s can be identified with the saturation vapour concentration of the liquid. In the present paper the additional problem of evaporation from aerodynamically rough surfaces will also be considered, such as evaporation from an area of the earth's surface sprinkled with a volatile liquid, and therefore not necessarily saturated. For this case, the appropriate surface boundary condition is not so obvious physically, as the liquid surface will in general be discontinuous, and the area and geometrical disposition of the liquid surface will be determined by the quantity of liquid dispersed, the method of dispersion, and the characteristics of the surface. As a working hypothesis it will be assumed that the concentration of vapour over a rough surface, which is saturated or uniformly sprinkled with evaporating liquid, is constant over a plane at a distance from the datum plane equal to the zero-point displacement d of the velocity profile (3). At this distance turbulence can be regarded as first becoming operative. Thus the boundary conditions (30) will be assumed valid for rough surfaces also, the plane $z = 0$ in this case, however, being at distance d from the datum plane of height reference in (3), and χ_s not necessarily being equal to the saturation vapour concentration corresponding to the temperature of the liquid.

As for the problem of diffusion from an infinite line source of gas or

† Sutton considers the case of dry (or vapour-free) air blowing over an evaporating strip. If the boundary conditions (30) (ii) and (iii) are replaced respectively by

$$\text{(ii)} \quad \lim_{z\to\infty} \chi(x,z) = \chi_0 \quad (0 \leqslant x \leqslant x_0),$$

$$\text{(iii)} \quad \lim_{x\to 0} \chi(x,z) = \chi_0 \quad (0 < z),$$

where χ_0 is the concentration (assumed uniform) in the air stream upwind of the strip, all the subsequently derived equations apply, provided $\chi(x, z)$ is replaced everywhere by $\chi(x,z)-\chi_0$, and χ_s is replaced by $\chi_s-\chi_0$.

smoke, a uniform mathematical method can be employed for both smooth and rough surfaces. Using the general expression (15) for eddy diffusivity, the diffusion equation (20) becomes

$$u_1(z/z_1)^{\alpha}\frac{\partial \chi}{\partial x} = \frac{\partial}{\partial z}\left\{M u_1^{2\beta-1} z_1^{\alpha(1-2\beta)} z^{1-\alpha}\frac{\partial \chi}{\partial z}\right\}. \tag{31}$$

A detailed discussion of this type of equation, subject to various boundary conditions, has been given by W. G. L. Sutton (**19**), regarding the equation as a generalization of the classical equation of heat conduction, and recently by Jaeger (**7**), using the method of the Laplace transformation. In the present paper the method of sources will be used, which leads to a simple integral equation.

Considering the infinite crosswind strip of evaporating surface defined by $z = 0$, $0 < x < x_0$, this may be regarded as an aggregate of elemental, continuous, infinite, crosswind, line sources of vapour. If $Q(x)\,dx$ g.sec.$^{-1}$ is the strength of the line source of width dx at x $(0 < x < x_0)$, then $Q(x)$ is a function of position to be determined by the boundary condition (30) (i). The general formula for the concentration of matter produced by an infinite line source has already been derived in equation (22), which is applicable to both smooth and rough flow, if appropriate values are taken for the parameters, from equations (13). For simplicity (22) will be written in the form

$$\chi = \frac{Q}{Nx^{\sigma}}\exp(-\gamma/x), \tag{32}$$

where

$$\left.\begin{aligned}
&\sigma = \frac{\alpha+1}{2\alpha+1},\\
&\text{and for smooth surfaces, by (24),}\\
&N = (2\alpha+1)^{1/(2\alpha+1)} M^{(\alpha+1)/(2\alpha+1)}\Gamma\left(\frac{\alpha+1}{2\alpha+1}\right) u_1^{1/(2\alpha+1)} z_1^{-\alpha/(2\alpha+1)},\\
&\gamma = \frac{u_1^{2\alpha/(1+\alpha)} z^{2\alpha+1}}{M(2\alpha+1)^2 z_1^{2\alpha^2/(1+\alpha)}},\\
&\text{while for rough surfaces, by (27),}\\
&N = (2\alpha+1)^{1/(2\alpha+1)} M^{(\alpha+1)/(2\alpha+1)}\Gamma\left(\frac{\alpha+1}{2\alpha+1}\right) u_1 z_1^{-\alpha},\\
&\gamma = \frac{z^{2\alpha+1}}{M(2\alpha+1)^2}.
\end{aligned}\right\} \tag{33}$$

The boundary condition (30) (i) then gives

$$\int_0^{\theta} \frac{Q(x)\,dx}{N(\theta-x)^{\sigma}} = \chi_s \quad (0 < \theta \leqslant x_0), \tag{34}$$

which is a simple integral equation of the Abel type (Whittaker and Watson, **22**) determining $Q(x)$. Its solution is

$$Q(x) = \frac{\sin\sigma\pi}{\pi}\frac{d}{dx}\int\limits_0^x \frac{N\chi_s\,d\theta}{(x-\theta)^{1-\sigma}}$$

$$= N\chi_s\frac{\sin\sigma\pi}{\pi}x^{\sigma-1}. \tag{35}$$

The total rate of evaporation E per unit width crosswind of the evaporating strip is thus

$$E(x_0) = \int\limits_0^{x_0} Q(x)\,dx = N\chi_s\frac{\sin\sigma\pi}{\sigma\pi}x_0^\sigma, \tag{36}$$

while the vapour concentration at a point *over* the strip is

$$\chi(x,z) = \int\limits_0^x \frac{Q(\theta)}{N(x-\theta)^\sigma}\exp\left\{\frac{-\gamma}{x-\theta}\right\}d\theta$$

$$= \chi_s\frac{\sin\sigma\pi}{\pi}\int\limits_0^x \theta^{\sigma-1}(x-\theta)^{-\sigma}\exp\left\{\frac{-\gamma}{x-\theta}\right\}d\theta \quad (0 < x \leqslant x_0) \tag{37}$$

and at any point *downwind* beyond the strip is

$$\chi(x,z) = \chi_s\frac{\sin\sigma\pi}{\pi}\int\limits_0^{x_0} \theta^{\sigma-1}(x-\theta)\exp\left\{\frac{-\gamma}{x-\theta}\right\}d\theta \quad (x > x_0). \tag{38}$$

Clearly these expressions for $\chi(x,z)$ also satisfy the boundary conditions (30) (ii) and (iii). They have also been obtained by W. G. L. Sutton (**19**) directly by solving equation (31), subject to the given boundary conditions.

The expression (37) may be further simplified to give an Incomplete Gamma-function, since the integral is a degenerate case of the confluent hypergeometric function. Thus writing $\theta/(x-\theta) = v$ and $\rho = \gamma/x$, in the integral, I say, of equation (37), then

$$d\theta/(x-\theta) = dv/(1+v),$$

and

$$I = \int\limits_0^\infty v^{\sigma-1}e^{-\rho(1+v)}\frac{dv}{1+v}.$$

Hence

$$\frac{dI}{d\rho} = -\int\limits_0^\infty v^{\sigma-1}e^{-\rho(1+v)}\,dv$$

$$= -\rho^{-\sigma}e^{-\rho}\int\limits_0^\infty s^{\sigma-1}e^{-s}\,ds \quad (s = \rho v)$$

$$= -\Gamma(\sigma)\rho^{-\sigma}e^{-\rho}.$$

Therefore $I = \Gamma(\sigma)\int\limits_{\rho}^{\infty} t^{-\sigma}e^{-t}\,dt$, since $I = 0$ for $x = 0$, i.e. for $\rho = \infty$, or

$$I = \Gamma(\sigma)[\Gamma(1-\sigma)-\Gamma(\rho, 1-\sigma)],$$

where the second term in the square brackets is the Incomplete Gamma-function, defined by

$$\Gamma(\theta, n) = \int\limits_{0}^{\theta} t^{n-1}e^{-t}\,dt.$$

Hence from (37)

$$\chi(x,z) = \chi_s \frac{\sin\sigma\pi}{\pi}\Gamma(\sigma)[\Gamma(1-\sigma)-\Gamma(\gamma/x, 1-\sigma)]$$

$$= \chi_s\left[1-\frac{\sin\sigma\pi}{\pi}\Gamma(\sigma)\Gamma(\gamma/x, 1-\sigma)\right] \quad (0 < x < x_0). \tag{39}$$

While this mathematical reduction is possible for expression (37), the integral occurring in (38) for the concentration downwind of the strip has not so far been reduced to known functions and must be evaluated by numerical integration.

From the above general expressions for E and χ we find, using the relations (33), that for

(i) *Smooth surfaces* (M given by equation (23)):

$$E(x_0) = \left\{\frac{2\alpha+1}{\alpha+1}\right\}\frac{\chi_s}{\pi}\sin\left\{\frac{(\alpha+1)\pi}{(2\alpha+1)}\right\}(2\alpha+1)^{1/(2\alpha+1)}M^{(\alpha+1)/(2\alpha+1)}\Gamma\left(\frac{\alpha+1}{2\alpha+1}\right)\times$$

$$\times u_1^{1/(2\alpha+1)}z_1^{-\alpha/(2\alpha+1)}x_0^{(\alpha+1)/(2\alpha+1)}, \tag{40}$$

$$\chi(x,z) = \chi_s\left[1-\frac{1}{\pi}\sin\left\{\frac{(\alpha+1)\pi}{(2\alpha+1)}\right\}\Gamma\left(\frac{\alpha+1}{2\alpha+1}\right)\Gamma\left\{\frac{u_1^{2\alpha/(1+\alpha)}z^{2\alpha+1}}{M(2\alpha+1)^2z_1^{2\alpha^2/(1+\alpha)}x}, \frac{\alpha}{2\alpha+1}\right\}\right]$$

$$(0 < x \leqslant x_0), \tag{41}$$

$$\chi(x,z) = \frac{\chi_s}{\pi}\sin\left\{\frac{(\alpha+1)\pi}{(2\alpha+1)}\right\}\int\limits_{0}^{x_0}\theta^{-\alpha/(2\alpha+1)}(x-\theta)^{-(\alpha+1)/(2\alpha+1)}\times$$

$$\times\exp\left\{\frac{-u_1^{2\alpha/(1+\alpha)}z^{2\alpha+1}}{M(2\alpha+1)^2z_1^{2\alpha^2/(1+\alpha)}(x-\theta)}\right\}d\theta \quad (x > x_0). \tag{42}$$

(ii) *Rough surfaces* (M given by equation (26)):

$$E(x_0) = \left(\frac{2\alpha+1}{\alpha+1}\right)\frac{\chi_s}{\pi}\sin\left\{\frac{(\alpha+1)\pi}{(2\alpha+1)}\right\}(2\alpha+1)^{1/(2\alpha+1)}M^{(\alpha+1)/(2\alpha+1)}\times$$

$$\times\Gamma\left(\frac{\alpha+1}{2\alpha+1}\right)u_1 z_1^{-\alpha}x_0^{(\alpha+1)/(2\alpha+1)}, \tag{43}$$

$$\chi(x,z) = \chi_s\left[1-\frac{1}{\pi}\sin\left\{\frac{(\alpha+1)\pi}{(2\alpha+1)}\right\}\Gamma\left(\frac{\alpha+1}{2\alpha+1}\right)\Gamma\left\{\frac{z^{2\alpha+1}}{M(2\alpha+1)^2x},\frac{\alpha}{2\alpha+1}\right\}\right]$$
$$(0 < x \leqslant x_0), \quad (44)$$

$$\chi(x,z) = \frac{\chi_s}{\pi}\sin\left\{\frac{(\alpha+1)\pi}{(2\alpha+1)}\right\}\int\limits_0^{x_0}\theta^{-\alpha/(2\alpha+1)}(x-\theta)^{-(\alpha+1)/(2\alpha+1)}\times$$
$$\times\exp\left\{\frac{-z^{2\alpha+1}}{M(2\alpha+1)^2(x-\theta)}\right\}d\theta \quad (x > x_0). \quad (45)$$

For computational purposes equations (41) and (44) are most conveniently re-expressed in terms of Karl Pearson's function $I(X,p)$,† values of which have been tabulated (Pearson, **11**). Thus in place of (44) we have

$$\frac{\chi}{\chi_s} = 1-I\left\{\frac{z^{2\alpha+1}}{M(2\alpha+1)^2x},\frac{-(\alpha+1)}{(2\alpha+1)}\right\}. \quad (46)$$

Since the integrands of (42) and (45) are infinite at $\theta = 0$, the numerical integrations must be carried out in two parts. Thus in the subsequent calculation of the vapour distribution downwind of a rough evaporating strip, the integral in (45) was evaluated for $0 < \theta < x_0/10$, i.e. with θ negligibly small compared with x, so that it becomes approximately

$$x^{-(\alpha+1)/(2\alpha+1)}\exp\left\{\frac{-z^{2\alpha+1}}{M(2\alpha+1)^2x}\right\}\int\limits_0^{x_0/10}\theta^{-\alpha/(2\alpha+1)}\,d\theta$$

and the interval $x_0/10 < \theta < x_0$ was treated numerically.

The expressions (41) and (44) involve x and z in the combination $z^{2\alpha+1}/x$ only, from which it follows that for given α, the contours of constant χ are parabolas of degree $(2\alpha+1)$, with the surface as axis, and the leading edge of the evaporating strip as vertex. Furthermore, the distribution of χ with z, when z is small is $\chi-\chi_s \propto z^\alpha$, since when ϕ is small, $\Gamma(\phi,p) \approx \dfrac{\phi^p}{p}$. Hence, from (39), when z is small,

$$\chi = \chi_s\left[1-\frac{\sin\sigma\pi}{\pi}\,\frac{\Gamma(\sigma)}{(1-\sigma)}\left(\frac{\gamma}{x}\right)^{1-\sigma}\right]. \quad (47)$$

On eliminating x between this equation and equation (35) one obtains for the local rate of evaporation from an infinitely extended surface

$$Q = N(\chi_s-\chi)\frac{(1-\sigma)}{\Gamma(\sigma)}\,\frac{1}{\gamma^{1-\sigma}}$$

† Pearson tabulates $I(u,p)$, where $u = X/\sqrt{(1+p)}$.

which can otherwise be obtained by integrating the simplified form of diffusion equation, viz.

$$\frac{\partial}{\partial z}\left\{K(z)\frac{\partial \chi}{\partial z}\right\} = 0,$$

which is applicable when the distribution of vapour can be regarded as horizontally homogeneous, i.e. not varying with distance in the mean direction of the wind.

Equation (41), for the vapour concentration above a smooth saturated strip, is identical with that first obtained by O. G. Sutton, in an unpublished paper, by solving the equation of diffusion in relation to his theory of turbulence and subject to the boundary conditions (30). The expression (40), for the total rate of evaporation from a smooth evaporating strip, was first obtained by the present writer, by direct integration from equation (41), using the relations

$$E(x_0) = \int_0^\infty (u\chi)_{x=x_0}\,dz = \int_0^{x_0} \left(\lim_{z\to 0} K(z)\frac{\partial \chi}{\partial z}\right) dx. \tag{48}$$

It has been shown by Pasquill (**10**) to be in very good agreement with the results of wind-tunnel experiments involving a variety of liquids. The present formulation shows, however, that the final expressions may be derived independently as a special case without making use of Sutton's empirical formulation of the Taylor correlation coefficient or of the semi-empirical concepts of the Prandtl mixing-length theory of turbulence.

With a one-seventh power-law velocity distribution, which is valid at low Reynolds numbers (equation (5)), equation (40) gives

$$E(x_0) \propto u_1^{0\cdot 78} x_0^{0\cdot 89},$$

an experimental result which has been quoted previously for smooth surfaces (Brunt, **2**) and which also represents very well the heat transfer by forced convection from a heated smooth plate (Elias, **4**).

Turning now to the case of rough surfaces, equations (44) and (45) show that, in this case, the distribution of vapour concentration is independent of the wind velocity and depends only on the roughness of the surface, which determines the degree of turbulence present. Furthermore, equation (43) gives

$$E(x_0) \propto u_1 x_0^{(\alpha+1)/(2\alpha+1)},$$

so that for rough surfaces the total rate of evaporation should be *directly* proportional to the wind velocity u_1 at the reference height z_1. Since the index of x_0 is of the same form as that for smooth surfaces, and only changes slowly with α, the variation of E with x_0 will be approximately the same as for smooth surfaces.

As far as is known, no laboratory observations at present exist for rates of evaporation from aerodynamically rough surfaces. Field experiments have, however, been carried out at the Chemical Defence Experimental Station, Porton, Wiltshire, to obtain information on the distribution of vapour concentration both over and downwind of rectangular grassland areas (grass length less than 1 inch) sprinkled with aniline under adiabatic conditions, the vapour concentrations being determined chemically. The contaminated areas were of sufficient extent across wind for them to be regarded as of infinite width with respect to the sampling positions used on the centre lines of the areas, subject to prescribed variations in wind direction.

Comparison between theory and experiment cannot be made directly, since the theory gives the concentration $\chi(x,z)$ at any point in terms of χ_s, the ground concentration on the contaminated area, and this is not known. Satisfactory comparison can, however, be made by expressing all concentrations, both theoretical and observed, in terms of the concentration at a particular position.

Tables 7 and 8 give some mean results for concentrations over and downwind, respectively, of contaminated downland areas. The values of α and q' selected in each case are appropriate to the average height of the vapour cloud.

TABLE 7

	Distance from upwind edge								
	10 yds.			20 yds.			30 yds.		
Height	1″	12·1	(10·0)	1″	11·7	(11·0)	1″	12·8	(11·8)
	6″	5·9	(4·7)	9″	5·4	(4·9)	1′	5·5	(4·9)
	1′	3·2	(2·7)	18″	3·0	(2·2)	2′	3·0	(2·4)
	2′	1·0	(1·0)	3′	1·0	(1·0)	4′	1·0	(1·0)

Relative vapour concentrations under adiabatic conditions over an area of short grassland, 30 yds. long, in the mean wind direction and initially contaminated with aniline to a density of 50 g.m.$^{-2}$

(Calculated values from equation (44): observed values in brackets.
$d = 0{\cdot}0$ cm., $z_0 = 0{\cdot}5$ cm., $\alpha = 0{\cdot}25$, $q = 3{\cdot}56$.)

The general agreement between theory and observation can be considered as very satisfactory for field experiments of this type.

From the above analysis of the two-dimensional evaporation problem it may be concluded that the present formulation of the laws of turbulent transfer satisfactorily predicts both evaporation from aerodynamically smooth surfaces in wind-tunnel experiments and also the distribution of concentration from very much larger aerodynamically rough surfaces in an adiabatic atmosphere. Since equation (44) or (45) may be used to

obtain a value for χ_s, from a knowledge of the value of $\chi(x, z)$ at some definite position, it should also be possible to calculate total rates of evaporation from rough surfaces, using equation (43). Wind-tunnel experiments are in progress to test this suggestion.

TABLE 8

	Ht.	*Distance from upwind edge* 10 *yds.*	15 *yds.*	20 *yds.*	25 *yds.*	40 *yds.*
Vertical distribution	1″	1·00 (1·00)	1·00 (1·00)	1·00 (1·00)	1·00 (1·00)	1·00 (1·00)
	8″	0·50 (0·31)	0·91 (0·94)	0·99 (0·99)	1·10 (1·08)	1·08 (1·13)
	24″	0·13 (0·08)	0·43 (0·51)	0·63 (0·69)	0·79 (0·80)	0·89 (1·05)
	66″	0·006 (0·010)	0·05 (0·06)	0·15 (0·11)	0·34 (0·31)	0·45 (0·83)
Horizontal distribution	8″	1·00 (1·00)	0·62 (0·54)	0·46 (0·47)	0·38 (0·35)	0·23 (0·19)

Relative vapour concentrations under adiabatic conditions, downwind of an area of short grassland, 10 yds. long in the mean wind direction, and initially contaminated with aniline to a density of 10 g.m.$^{-2}$

(Calculated values from equation (45); observed values in brackets.
$d = 0{\cdot}0$ cm., $z_0 = 0{\cdot}5$ cm., $\alpha = 0{\cdot}22$, $q' = 4{\cdot}1$.)

The writer is indebted to Professors O. G. Sutton and P. A. Sheppard for encouragement and discussion throughout the entire course of development of the work described in the present paper. His thanks are also due to Mr. E. L. Deacon, of the Meteorological Office, for permission to employ observational results which have not yet been published in full. Finally, acknowledgement is made to the Chief Scientist, Ministry of Supply, for permission to submit this paper for publication.

REFERENCES

1. A. C. Best, *Geophys. Mem.* **65** (1935).
2. D. Brunt, *Physical and Dynamical Meteorology* (Cambridge, 1939).
3. K. L. Calder, *Quart. J. R. Met. Soc.* **65** (1939), 282.
4. F. Elias, *Z. angew. Math. Mech.* No. 6 (Dec. 1929); ibid., No. 1 (Feb. 1929).
5. H. Ertel, *Met. Z.* **50** (1933), 386.
6. S. Goldstein, *Modern Developments in Fluid Dynamics* (Oxford, 1938).
7. J. C. Jaeger, *Quart. Appl. Math.* **3** (1945), 210–17.
8. F. G. Millar, *Canadian Met. Mem.* **1** (1937), No. 2.
9. R. B. Montgomery, *Pap. Phys. Oceanogr. Met., Mass. Inst. Tech.* **7** (1940), 4.
10. F. Pasquill, *Proc. Roy. Soc.* A **182** (1943), 75.
11. K. Pearson, *Tables of the Incomplete Gamma Function* (H.M.S.O., London, 1922).
12. L. Prandtl and W. Tollmien, *Z.f. Geophys.* **1** (1925), 47.
13. L. Prandtl, *Beitr. Phys. frei. Atmos.* (Bjerknes Festschrift), **19** (1932), 188.
14. O. F. T. Roberts, *Proc. Roy. Soc.* A **104** (1923), 640.

15 a. C. G. Rossby and R. B. Montgomery, *Pap. Phys. Oceanogr. Met., Mass. Inst. Tech.* **4** (1935), 3.
15 b. ——— ———, ibid. **4** (1936), 3.
16. H. Schlichting, *Ingenieur. Archiv*, **7** (1936), 1.
17 a. P. A. Sheppard, *Proc. Roy. Soc.* A **188** (1947), 208.
17 b. ——, *Quart. J. R. Met. Soc.* (to be published).
18 a. O. G. Sutton, *Proc. Roy. Soc.* A **135** (1932), 143.
18 b. ——, ibid. A **146** (1934), 701.
18 c. ——, *Quart. J. R. Met. Soc.* **73** (1947), 257.
19. W. G. L. Sutton, *Proc. Roy. Soc.* A **182** (1943), 48.
20 a. H. U. Sverdrup, *Ann. d. Hydrogr.* **64** (1936), 2.
20 b. ——, *J. Marine Research*, **1** (1937), 3.
21 a. G. I. Taylor, *Proc. Roy. Soc.* A **92** (1915), 196.
21 b. ——, *Proc. Lond. Math. Soc.* **20** (1922), 196.
22. E. T. Whittaker and G. N. Watson, *A Course of Modern Analysis* (Cambridge, 1935).

BENDING OF AN ELLIPTIC PLATE WITH A CONFOCAL HOLE

By B. R. SETH (*Hindu College, Delhi*)

[Received 31 August 1948]

SUMMARY

An approximate solution for the bending of a thin elliptic plate with a confocal hole subjected to uniform pressure and clamped at the edges is discussed. The numerical results obtained are compared with those for a complete plate. It is found that the maximum deflexion w_m occurs near the inner boundary. For the plate bounded by ellipses whose semi-axes are (1·6*c*, 1·249*c*) and (1·14*c*, 0·548*c*) it is found that w_m is almost one-fifth the value for the plate complete up to the outer boundary. By making the minor axis of the hole vanishingly small the interesting case of an elliptic plate with a clamped crack can be treated.

Introduction

THE effect of a hole or a group of holes on the distribution of stress in any member or structure under load is of great importance in engineering problems. Of those problems involving forces, isolated or distributed, normal to the plane of the plate, there are a number of well-known solutions for plates of various shapes.† Among recent papers extending our knowledge of particular solutions of these problems are those of Sen (**1**), Stevenson (**2**), and Sengupta (**3**). The finite circular plate with an eccentric hole and bent by a concentrated load at any point has been discussed by Kudriavtzev (**4**). Very recently Southwell (**5**) has used his method of relaxation to get numerical results for a plate with perforations. It will therefore be not without interest to discuss the bending of an elliptic plate with a confocal hole bent by uniform pressure and clamped at the edges. For the complete elliptic plate the solution is due to Bryan (**6**). As he did not solve this problem directly by using elliptic coordinates (and as we shall require some of those results for the sake of comparison with those for a plate with a confocal hole), we first consider the complete plate problem. By making the minor axis of the hole vanishingly small we can discuss the case of an elliptic plate with a clamped crack coincident with the straight line joining the foci.

Complete elliptic plate

The deflexion w of the middle surface satisfies the differential equation

$$\nabla_1^4 w = \left(\frac{\partial^2}{\partial x^2}+\frac{\partial^2}{\partial y^2}\right)^2 w = \frac{p}{D}, \tag{1}$$

p being the uniform pressure and D the flexural rigidity.

† See, for example, Timoshenko, *Plates and Shells*, Chapter VII (1940).

The elliptic coordinates ξ, η are given by

$$x+iy = c\cosh(\xi+i\eta), \tag{2}$$

and a particular solution of (1) is

$$\frac{1}{8}\frac{p}{D}x^2y^2 = \frac{p}{128D}c^4\sinh^2 2\xi\sin^2 2\eta$$
$$= k[-\cosh 4\xi\cos 4\eta+\cosh 4\xi+\cos 4\eta-1], \tag{3}$$

where $k = pc^4/512D$.

The typical solutions of (1) in elliptic coordinates are (7)

$$e^{(\pm n+1)\xi}\begin{cases}\cos\\ \sin\end{cases}(n-1)\eta+e^{(\pm n-1)\xi}\begin{cases}\cos\\ \sin\end{cases}(n+1)\eta \tag{4.1}$$

and $$e^{(\pm n-1)\xi}\begin{cases}\cos\\ \sin\end{cases}(n-1)\eta+e^{(\pm n+1)\xi}\begin{cases}\cos\\ \sin\end{cases}(n+1)\eta. \tag{4.2}$$

In addition we have solutions of the type

$$A\xi+B \quad \text{and} \quad r^2\xi = \tfrac{1}{2}c^2\xi(\cosh 2\xi+\cos 2\eta). \tag{4.3}$$

As w should be even both with respect to ξ and η we see from (2) that

$$\begin{aligned}w = k[-\cosh 4\xi\cos 4\eta+(\cosh 4\xi-\cosh 4\alpha)+\cos 4\eta]+\\ +A_1[\cosh 4\xi\cos 2\eta+\cosh 2\xi\cos 4\eta]+\\ +A_2[\cosh 2\xi-\cosh 2\alpha+\cos 2\eta]+A_3\cosh 2\xi\cos 2\eta+\\ +A_4\cosh 4\xi\cos 4\eta.\end{aligned} \tag{5}$$

The boundary conditions are

$$w = 0, \quad \partial w/\partial\xi = 0, \quad \text{for} \quad \xi = \alpha.$$

These give rise to five equations involving the constants A_i. But it is found that only four are independent. Thus we get a closed solution for this case. We find

$$\begin{aligned}A_1 &= -\frac{4k\cosh 2\alpha}{1+2\cosh^2 2\alpha} = -\frac{4k\cosh 2\alpha}{2+\cosh 4\alpha}; \qquad A_2 = -4k\cosh 2\alpha;\\ A_3 &= \frac{16k\cosh^2 2\alpha}{2+\cosh 4\alpha}; \qquad A_4 = \frac{2k(1+\cosh^2 2\alpha)}{2+\cosh 4\alpha}.\end{aligned} \tag{6}$$

After some simplification (5) reduces to

$$w = \frac{1}{8}\frac{p}{D}\left(1-\frac{x^2}{a^2}-\frac{y^2}{b^2}\right)^2\bigg/\left(\frac{3}{a^4}+\frac{3}{b^4}+\frac{2}{a^2b^2}\right), \tag{7}$$

a, b being the axes of the ellipse. The maximum deflexion w_m is **(6)**

$$w_m = \frac{1}{8}\frac{p}{D}\Big/\left(\frac{3}{a^4}+\frac{3}{b^4}+\frac{2}{a^2b^2}\right)$$

$$= \frac{1}{8}\frac{p}{D}\frac{c^4\cosh^4\alpha\sinh^4\alpha}{3(\cosh^4\alpha+\sinh^4\alpha)+2\cosh^2\alpha\sinh^2\alpha}, \tag{8}$$

which gives
$$(w_m/k) = \cosh 4\alpha - 4 + \frac{9}{2+\cosh 4\alpha}. \tag{8.1}$$

Elliptic plate with a confocal hole

In this case we can write with the help of (4)

$$\begin{aligned} w = {} & k(\cosh 4\xi+\cos 4\eta)+A_0\xi+B_0+ \\ & +[A_1\sinh 2(\xi-\beta)+A_2\sinh 2(\xi-\alpha)-(A_1\sinh 2\beta+A_2\sinh 2\alpha)\cos 2\eta]+ \\ & +A_3\xi(\cosh 2\xi+\cos 2\eta)+[A_4\cosh 2(\xi-\beta)+A_5\cosh 2(\xi-\alpha)]\cos 2\eta+ \\ & +A_6[\cosh(2\xi-\alpha-\beta)\cos 4\eta+\cosh(4\xi-\alpha-\beta)\cos 2\eta]+ \\ & +A_7\cosh(4\xi-2\alpha-2\beta)\cos 4\eta+ \\ & +A_8[\cosh(6\xi-3\alpha-3\beta)\cos 4\eta+\cosh(4\xi-3\alpha-3\beta)\cos 6\eta]+ \\ & +\ldots \\ = {} & [A_0+B_0\xi+A_1\sinh 2(\xi-\beta)+A_2\sinh 2(\xi-\alpha)+ \\ & +A_3\xi\cosh 2\xi+k\cosh 4\xi]+[-(A_1\sinh 2\beta+A_2\sinh 2\alpha)+A_3\xi+ \\ & +A_4\cosh 2(\xi-\beta)+A_5\cosh 2(\xi-\alpha)+A_6\cosh(4\xi-\alpha-\beta)]\cos 2\eta+ \\ & +[A_6\cosh(2\xi-\alpha-\beta)+A_7\cosh(4\xi-2\alpha-2\beta)+ \\ & +A_8\cosh(6\xi-3\alpha-3\beta)+k]\cos 4\eta+ \\ & +\ldots. \end{aligned} \tag{9}$$

The boundary conditions are $w = 0$, $\partial w/\partial\xi = 0$ over $\xi = \alpha$ and $\xi = \beta$. The first term in (9) gives

$$\begin{aligned} A_0+B_0\alpha+A_1\sinh 2(\alpha-\beta)+A_3\alpha\cosh 2\alpha+k\cosh 4\alpha &= 0, \\ A_0+B_0\beta+A_2\sinh 2(\beta-\alpha)+A_3\beta\cosh 2\beta+k\cosh 4\beta &= 0, \\ B_0+2A_1\cosh 2(\alpha-\beta)+2A_2+A_3(2\alpha\sinh 2\alpha+\cosh 2\alpha)+4k\cosh 4\alpha &= 0, \\ B_0+2A_1+2A_2\cosh 2(\beta-\alpha)+A_3(2\beta\sinh 2\beta+\cosh 2\beta)+4k\cosh 4\beta &= 0. \end{aligned} \tag{10}$$

The second term gives

$$\begin{aligned} A_6\cosh(3\alpha-\beta)+A_5+A_4\cosh 2(\alpha-\beta)+A_3\alpha-A_1\sinh 2\beta-A_2\sinh 2\alpha &= 0, \\ A_6\cosh(3\beta-\alpha)+A_5\cosh 2(\beta-\alpha)+A_4+A_3\beta-A_1\sinh 2\beta-A_2\sinh 2\alpha &= 0, \\ 4A_6\sinh(3\alpha-\beta)+2A_4\sinh 2(\alpha-\beta)+A_3 &= 0, \\ 4A_6\sinh(3\beta-\alpha)+2A_5\sinh 2(\beta-\alpha)+A_3 &= 0. \end{aligned} \tag{11}$$

The third term gives

$$A_6\cosh(\alpha-\beta)+A_7\cosh 2(\alpha-\beta)+A_8\cosh 3(\alpha-\beta)+k = 0,$$

$$A_6+4A_7\cosh(\alpha-\beta)+3A_8[3-4\sinh^2(\alpha-\beta)] = 0. \tag{12}$$

Solving (10), (11), and (12) we get

$$A_4+A_5 = 2A_6\frac{2\sinh(\alpha-\beta)\cosh(\alpha+\beta)-(\alpha-\beta)[1+2\cosh 2(\alpha-\beta)]}{(\alpha-\beta)\cosh(\alpha-\beta)-\sinh(\alpha-\beta)}, \tag{13.1}$$

$$A_4-A_5 = 2A_6\frac{\sinh(\alpha+\beta)\cosh(\alpha-\beta)}{(\alpha-\beta)\cosh(\alpha-\beta)-\sinh(\alpha-\beta)}, \tag{13.2}$$

$$A_3 = -4A_6\frac{\sinh^3(\alpha-\beta)\sinh(\alpha+\beta)}{(\alpha-\beta)\cosh(\alpha-\beta)-\sinh(\alpha-\beta)}, \tag{13.3}$$

$$2A_1\sinh 2\beta+2A_2\sinh 2\alpha = A_3-2A_6\cosh(\alpha+\beta)[2+\cosh 2(\alpha-\beta)], \tag{13.4}$$

$$\begin{aligned}&2(A_1+A_2)[\{1+\cosh 2(\alpha-\beta)\}(\alpha-\beta)-\sinh 2(\alpha-\beta)]+\\&\quad+A_3[(\alpha-\beta)(\cosh 2\alpha+\cosh 2\beta)+(\alpha-\beta)(2\alpha\sinh 2\alpha+2\beta\sinh 2\beta)-\\&\qquad\qquad-2\alpha\cosh 2\alpha+2\beta\cosh 2\beta]+\\&\quad+k[4(\alpha-\beta)(\sinh 4\alpha+\sinh 4\beta)-2(\cosh 4\alpha-\cosh 4\beta)] = 0,\end{aligned} \tag{13.5}$$

$$\begin{aligned}&4(A_1-A_2)\sinh^2(\alpha-\beta)+A_3[\cosh 2\alpha+2\alpha\sinh 2\alpha-\cosh 2\beta-2\beta\sinh 2\beta]+\\&\qquad\qquad+4k(\sinh 4\alpha-\sinh 4\beta) = 0.\end{aligned} \tag{13.6}$$

Combining (13) with (12) we get A_1, A_2, A_3, A_4, A_5, A_6, A_7, and A_8. Substituting these values in (10) we find A_0 and B_0.

It is found from the expression for w given by (9) that it is in general quite sufficient to stop at the coefficient of $\cos 4\eta$; if required, further terms can be taken.

To get a numerical idea of the solution we take

$$\alpha = \tfrac{1}{3}\pi = 1{\cdot}04720, \qquad \beta = \tfrac{1}{6}\pi = 0{\cdot}52360,$$

and we find

$$\left.\begin{matrix} A_0 = 2{\cdot}666k, & B_0 = 50{\cdot}371k, & A_1 = -67{\cdot}109k, & A_2 = 22{\cdot}850k,\\ A_3 = -1{\cdot}074k, & A_4 = 0{\cdot}681k, & A_5 = 0{\cdot}330k, & A_6 = 0{\cdot}035k,\\ A_7 = 1{\cdot}795k, & A_8 = -1{\cdot}671k. & & \end{matrix}\right\} \tag{14}$$

The maximum value, w_m, of w occurs on the major axis and its value is given approximately by

$$w_m = 5{\cdot}712k. \tag{15}$$

The following table gives the values of (w/k) for varying values of ξ.

ξ	0·5236	0·6	0·65	0·70	0·75	0·80	0·90	1·0472
w/k	0	5·624	5·712	5·577	5·192	4·542	3·243	0

From (8.1), if the plate has no hole, is bounded by the ellipse $\xi = 0{\cdot}5236$, and is clamped there, we have

$$(w_m/k) = 1{\cdot}880. \tag{16.1}$$

For a clamped elliptic plate bounded by $\xi = 1{\cdot}0472$

$$(w_m/k) = 29{\cdot}259. \tag{16.2}$$

For the plate with a confocal hole we see that the maximum deflexion occurs near the inner boundary. In the present example it is about three times the values given by (16.1), and one-fifth the value given by (16.2).

REFERENCES

1. B. SEN, *Phil. Mag.* 1942, **33**, 294.
2. A. C. STEVENSON, ibid. p. 639.
3. H. M. SENGUPTA, *Bull. Cal. Math. Soc.* 1948, **40**, 17, 53.
4. N. V. KUDRIAVTZEV, *Comp. Rend. Acad. Sci. URSS.* 1946, **53**, 103.
5. R. V. SOUTHWELL, *Proc. Roy. Soc.* A, 1948, **193**, 147.
6. G. H. BRYAN, see A. E. H. Love's *Theory of Elasticity*, 4th ed., p. 484.
7. E. G. COKER and L. N. G. FILON, *Photo-Elasticity*, 1931, pp. 536–7.

PRINCIPLES AND PROGRESS IN THE CONSTRUCTION OF HIGH-SPEED DIGITAL COMPUTERS

By ANDREW D. BOOTH *and* KATHLEEN H. V. BRITTEN
(*Birkbeck College, University of London, and British Rubber Producers' Research Association, Welwyn Garden City, Herts.*)

[Received 5 November 1947; revised 2 July 1948]

SUMMARY

The basic principles underlying the mathematical design of high-speed digital computers are discussed and the necessary components of such machines defined. Scale of notation, the form of the 'memory', the action of the control, and other practical details are considered, and a brief discussion is included of the exact arithmetic functions of which these machines must be capable.

This is followed by a description of current computer projects in America. Aiken's second relay computer at Harvard, the Bell relay machine, E.D.V.A.C., and the Princeton electronic computer are described briefly and an idea given of their state of completion in 1947.

Introduction

It is the purpose of this paper to discuss the basic principles underlying the mathematical design of high-speed digital computers, and to follow this with an account of the progress which has been made, in the U.S.A. and at home, with the actual construction of such instruments.

Digital versus analogue computers

At the outset it is perhaps worth noticing the essential difference between the two possible types of computing machine, *digital* and *analogue*.

An analogue machine is one which performs its functions by finding some mechanical, hydraulic, or electrical mechanism whose action in effect duplicates the mathematical processes required. A single example suffices; suppose that it is required to calculate the function $a\cos\theta$. A simple mechanism for doing this is shown in Fig. 1.

A cross-head OA is capable of rotation about O, a peg B is positioned on OA, so that $OB = a$. BC is a bar rigidly joined perpendicular to CP which is constrained to move in the line $OCPX$. If BC is maintained in contact with the peg B and OA is rotated through the required angle θ, the displacement of P from its position when $\theta = \frac{1}{2}\pi$ is equal to $a\cos\theta$. It is apparent that such a device will have severe limitations in accuracy and, for more complicated systems than that considered, an upper limit of 1 in 1,000 is expensive to realize, whilst 1 in 10,000 is on the extreme border of practicability. To paraphrase a remark of Professor Hartree, each decimal place multiplies the cost by a factor of about 10.

The most ambitious analogue computer constructed to date (and it now seems for all time) is the Bush–Caldwell differential analyser at the Centre of Analysis in the Massachusetts Institute of Technology; this achieves, on favourable occasions, the upper limit of accuracy quoted above and has a tape-feed device which enables a problem to be set into the machine from

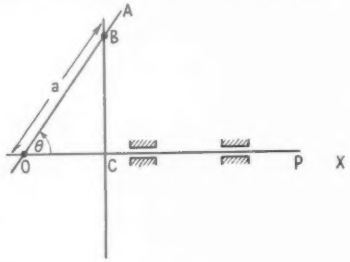

FIG. 1.

a standard commercial electrical typewriter. Electrical gear-boxes eliminate the laborious setting operation required in previous analysers, and the circuits are so arranged that all the integrators receive a fair share of the work of the machine. This feature is important in a machine whose maximum capacity exceeds that normally required on routine problems.

The subject of analogue computers will not be discussed further as the field is well known and is well covered in existing literature (**1**).

A digital computer is defined to be any machine which takes its information in the form of actual numbers (i.e. assemblages of *digits*) and operates with it in this form throughout. It is at once apparent, from this, that only the ordinary operations of arithmetic are possible to such a machine, and that any continuous process must be replaced by a suitable finite difference or other numerical equivalent. The most common example of a digital computer is the ordinary desk Marchant, Monroe, or Brunsviga, and it is perhaps worth observing that such a machine, with a 6×6 decimal multiplication time of around 10 seconds, is faster by a factor of about 25 than a non-expert (i.e. non-professional computer) using pencil and paper methods. At these speeds it is just possible for the human operator to supply the machine with data and instructions at an adequate rate. With an increase in speed by even a factor of 10 this is no longer true and, if the machine is to be hand-controlled, no further improvement in performance is justified.

The control of high-speed computers

These conditions lead naturally to the idea of a machine capable of controlling its own operations and exerting a certain amount of independent

judgement. Before being more explicit it may be well to clear up a point which is often raised in this connexion. If a human operator has to 'programme', i.e. instruct the machine at some stage, does this not impose a fundamental limitation on the speed? The answer is in the negative, since most problems involve a large amount of repetition, and if the machine can exercise a little judgement it is sufficient to detail the process once and then tell the machine to repeat it, either a fixed number of times, or until some criterion is realized. As examples consider three typical problems:

(1) Tabulation of $f(x)$ for $x = 1,\ldots,n$;
(2) Iterative evaluation of $a^{\frac{1}{2}}$;
(3) Multiplication of two matrices $A.B$.

In the first problem the detailed programme for the calculation of $f(x)$ for one value of x would be written down. The next value of x would now be inserted into the scheme and the process repeated. The operation could be terminated by having the machine calculate $y = (x-n)$ at each stage and then using a 'judgement' order of the type:

if $y \geqslant 0$ perform operation sequence A;
but if $y < 0$ perform operation sequence B.

In this example sequence B would be that for calculating $f(x)$, whereas A would signal the end of the calculation, since $(x-n) < 0$ until $x = n$. The process would therefore terminate automatically after the correct number of values of $f(x)$ had been generated.

The word 'programme' as used in this context may require explanation. Before a problem is ready for solution in a computing machine it must first be broken up into processes which the machine is capable of performing. Thus, as mentioned above, when using a digital machine the continuous process of differentiation must be replaced by a finite difference formula. This translating of a problem in terms of the available functions of the machine is generally known as programming.

The second problem, the evaluation of $a^{\frac{1}{2}}$ to a preassigned accuracy, is dealt with in the same fashion although the required number of iterations of the process

$$x_{n+1} = \tfrac{1}{2}(x_n + a/x_n)$$

may not be known *ab initio*. The decision to end the calculation is made by evaluating $(x_{n+1} - x_n)$ at each stage and noticing that it is negative up to a certain point and zero afterwards (to a preassigned number of decimal places). The point at which the two successive approximations become equal is the required termination, and a 'judgement' order is adequate to determine it without human intervention.

The third example, matrix multiplication, is effected by a straightforward triple iteration and the same sort of procedure is adequate.

The scale of notation

So far in this discussion of digital computers 'numbers' and 'digits' have been mentioned without definition, but one of the first problems confronting a designer of machines is the choice of a scale of notation for his numbers. The decimal, or scale of 10, notation, although hallowed by tradition, is by no means mandatory. With present electrical and electronic facilities it is an unfortunate fact that most simple devices favour not decimal but binary scale, and it is pertinent to consider what is in effect the best possible scale. To state the problem in mathematical terms: to record numbers up to a magnitude K, what scale of relationship minimizes the total number of digital positions required? To solve this, let n be the base and m the number of places (decimal or otherwise) required. The minimum value of $D = nm$ subject to the condition $n^m = K$ has to be found. An easy application of the calculus gives the value

$$n = e.$$

The use of this transcendental number as a base is impracticable and 2, 3, or 4 are logically the next best choice. A numerical comparison is interesting; to record numbers up to 10^6 in decimal notation 60 digital positions are required, in binary or quaternary scales 40 digital positions, and in ternary scale 38 positions. The decimal notation is thus inefficient by a factor of about 1·5.

It is, of course, possible to adopt a 'binary decimal' scale, in which decimal digits are represented by their binary equivalents. Thus 8 would appear as (1000), 68 as (0110), (1000) etc. Using this representation, 48 positions would be required to represent numbers up to 10^6 and the scale is therefore inefficient by a factor of 1·2 compared with the binary notation.

The choice between binary and ternary scale is dictated by the fact that the binary representation lends itself to easy application of 'relays' and 'flip-flops' (2)—the electronic equivalent of the relay.

One objection frequently raised against binary scale is the difficulty experienced by humans in the reading of large numbers of ones and zeros. As will be shown later, however, a properly designed machine can take its input in decimal form, convert to binary for its own operations, and then reconvert its output to decimal form.

Another point must be mentioned in this connexion. Binary addition consists of three possible operations ($1+1 = 10$, $1+0 = 1$, $0+0 = 0$), whereas in decimal notation there are fifty-five different operations.

Multiplication is correspondingly more complicated. The engineering problems to be solved in constructing a decimal machine are therefore much more formidable than those encountered when using binary scale. This objection applies equally to the 'binary-decimal' scale.

Serial and parallel operation

The next point which arises in the design of a computer is the form of operation—serial or parallel. In the first type the digits of any number become available one at a time starting from the least significant, whilst, in the latter, all digits are simultaneously available. The decision as to which form of operation is to be used in any particular machine is one which can be made only when the form of the 'memory' of the machine is known, and leads naturally to a discussion of the latter.

General properties of the memory

It was mentioned earlier that human agencies are too slow to control machines which are much faster than those already in use. Some means of ordering the operations of the machine at speeds greatly in excess of neural reaction times is therefore required. This suggests that the machine should have a 'memory', and the characteristics of this will now be considered.

In the past, machines have been built in which the memory consists of two distinct parts, one for orders and the other for numbers. This is, as will be shown, an unsound arrangement, both from the viewpoint of logical arithmetic and from a much more elementary aspect. Two general classes of problem exist: those in which a small number of orders suffice for the handling of a large amount of numerical data, and those in which a large number of orders operate on a few numbers and produce a single number as a solution. If only a finite memory space is available, any idea of dividing it into two independent halves for orders and numbers respectively and exclusively is untenable on these grounds alone, and it will therefore be assumed that both orders and numbers are to be placed in the memory and a selection mechanism provided to pick out the correct material. This leads to the idea of a code.

Basic components of a computer

If orders are to be stored in the same memory as numbers, they must be put into numerical form. This is relatively simple, but requires a careful consideration of the precise set of orders on which the machine is to operate. Before considering this, however, the operating components of the machine must be defined. Fig. 2 gives a general view of the whole.

The main sequence of operations is as follows:

(1) Control extracts order from memory.

(2) Control decodes order and directs memory and arithmetic unit to execute it.

(3) Arithmetic unit emits signal that its operation is complete.

(4) Control locates next order in sequence and extracts it from the memory.

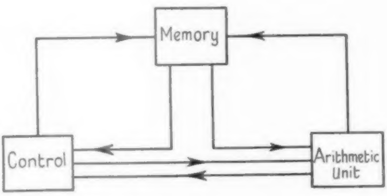

Fig. 2.

Subsidiary sequences allow the control to jump to other orders not in sequence; these shifts may be either conditional or unconditional (*vide infra*).

The exact constitution of an order is of some importance; it is found that a satisfactory make up is:

'Perform operation A using data in memory position B.'

It is not necessary to specify the place of disposal of the result or the memory location of the next order. It will generally be convenient for the latter to be in sequence for the greater part of a calculation so that an automatic advance of the control (via a counter) performs this sequencing operation. For out-of-sequence orders special instructions are needed:

'Control execute order contained in memory position K and then proceed in sequence from *this* order',

which is the *unconditional* transfer referred to above; or

'If $x < 0$ execute order contained in memory position K and then proceed in sequence from *this* order',

which is the *conditional* transfer.

The serial memory

More detailed description of the memory and arithmetic units depends almost entirely upon the details of the former. Serial memories suggested up to the present depend almost universally on the delay-line principle, Fig. 3.

A tube of liquid (usually mercury) has at its ends two quartz crystals Q_1 and Q_2. On applying an electric impulse to Q_1, its piezo-electric property

causes it to emit a mechanical pulse which is propagated down the mercury column as a compression wave. This compression wave affects a second

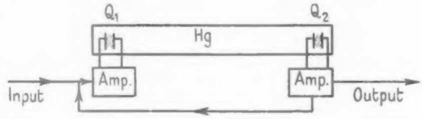

Fig. 3.

quartz crystal Q_2 which this time emits an electrical impulse; this impulse is led back to Q_1 (after suitable amplification and reshaping) and the whole cycle repeats itself.

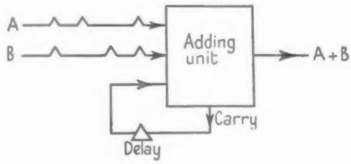

Fig. 4.

The tubes in common use have a delay of about 1 millisecond so that if pulses are applied to Q_1 at megacycle rate, up to 1,000 can be stored in the tube. A binary number now consists of an electrical impulse pattern of the type

The disadvantage of the scheme is of course that, on the average, $\frac{1}{2}$ millisecond will elapse before any given number in the tube becomes available. To perform addition the two numbers are taken from different delay tubes and combined to form the sum, which is recorded in one of the original tubes. The addition of two binary digits may produce a carry; this has to be delayed by a time-interval Δ and fed into the next pair of digits to become available, Δ being the interval between pulses (see Fig. 4).

By a slightly more complicated arrangement, involving the storing of B in a short delay line, multiplication and division can be performed.

Professor F. C. Williams of Manchester has also developed a storage device. He uses a standard cathode-ray tube and stores data as charged areas on the screen, zero and one being represented by dots and dashes. Numbers are read off by scanning the rows of information, and digits are therefore obtained serially. Professor Williams has succeeded in storing 2048 digits in a 12 in. tube and in retaining information for what is effectively an indefinite period with no signs of deterioration.

The parallel operation memory

Of the memories which have been or are being developed for parallel operation machines one of the most promising is the R.C.A. 'Selectron'. In essence this retains data by storage of charge on a dielectric medium. The mode of selection of the particular region for a given digit is interesting. A filament (Fig. 5) emits electrons in the direction of the dielectric medium which is shielded by two parallel grids of mutually perpendicular wires.

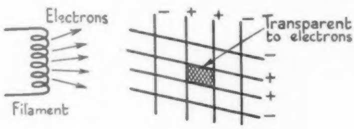

FIG. 5.

Normally the grids are negative with respect to the filament; to select a particular region of the dielectric two adjacent wires in each grid are made positive; the region so defined becomes transparent to electrons, which can thus pass through and affect the dielectric storage medium.

The arithmetic unit for parallel operation

In the parallel operation machine the digits become available at the same time, and different arrangements for addition, multiplication, and division have to be adopted. It is generally agreed that the arithmetic unit must consist of:

(1) An accumulator; that is, a device which will add an incoming number to that already in it and store the result.

(2) A register to store the multiplier in multiplication and the quotient in division.

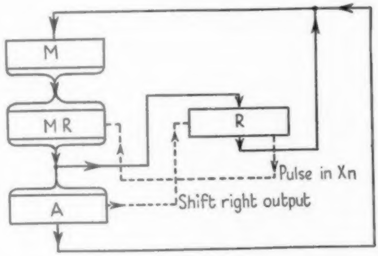

FIG. 6.

In multiplication and division the multiplicand and the divisor are stored in a register associated with the output from the memory. Fig. 6 gives a diagrammatic representation of the kind of arithmetic unit envisaged.

The register and accumulator have facilities which enable numbers contained therein to be shifted to the right or left. Interconnexions, indicated by full lines, are provided between the memory register (*M.R.*), the shifting register (*R*), and the accumulator (*A*) to enable numbers to be transferred from one unit to another. Numbers may also be transferred from the register and accumulator directly to the memory.

The multiplication sequence (positive numbers only) is as follows:

If right-hand digit of the multiplier in the register *R* is unity add *M.R.* into *A* and shift contents of *A* one place to right, the right-hand digit of *A* going to the left-hand digit position of *R* whose contents also shift one place to the right (see dotted lines in Fig. 6). The right-hand digit of *R* is lost and the next digit takes its place as the multiplier for the next cycle.

If the right-hand digit of *R* is zero the contents of *A* and *R* are simply shifted as before but without addition from *M.R.*

The accumulator

It is interesting to examine the mode of operation of the accumulator. Just as in the serial type machine, the adding unit has two inputs together with a carry input from previous stages.

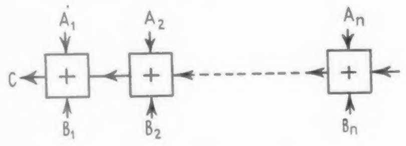

This carry has been a source of speed limitation in many projects, since the speed of operation of the circuit has to be adjusted so that a carry (in the worst possible case) originating at $A_n B_n$ can be propagated through the whole chain of adding units. This limitation is not, however, essential and the following circuit remedies the defect:

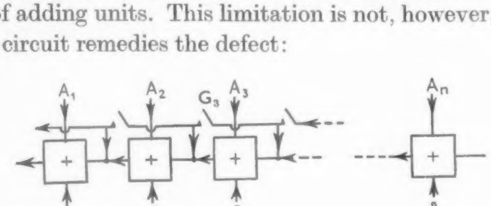

Here, if an incoming carry pulse to any stage (say $A_3 B_3$) is going to produce a carry (i.e. if the result of the $(A_3 B_3)$ addition is 1), the gate G_3 is closed and the incoming pulse by-passes $(A_3 B_3)$ and proceeds unhindered along the chain until it meets a stage which is not going to produce a further carry.

The code

Enough has now been said to make clear the general mode of operation of the machine; it is proposed, however, before describing individual machines, to consider the question of the code in more detail. The following remarks will apply more to the parallel operation type of machine as it seems likely to replace the serial variety as being faster by at least an order of magnitude, and it is significant that Professor von Neumann, who pioneered the serial machine, has forsaken it in favour of a parallel operation type.

If the idea of programming all arithmetic out of the simplest operations is accepted, the list of orders will contain at least:

(1) Left shift.
(2) Right shift.
(3) Control transfer.
(4) Memory to accumulator.
(5) Accumulator to memory.
(6) Control transfer to order at memory location (x).

Out of this simple set all arithmetic operations can be generated, although greater detail will not be given here save to mention, as an example, that the nullity of a number can be sensed and a conditional control transfer generated from this simple set. This is simply done by successively separating (by suitable shifts) the digits, of the numbers whose nullity is required, and substituting into an *order* which sends the control to memory location (x); if the digit being substituted is different from zero, (x) is increased by unity and the order found at location $(x+1)$ forms the start of a new sequence. In practice a more sophisticated code is adopted and as an example that of our own computer A.R.C. is given. The code for a serial type machine may be different in form and for details reference may be made to the report on A.C.E. (**3**).

Although it has been shown how conditional transfer could be generated from logically simple operations, it is a great convenience to have this operation available in the code. It is interesting to consider its best formulation; two possibilities spring to mind:

(1) Transfer if $X < 0$.
(2) Transfer if $X = 0$.

One can be generated from the other, thus using form (1) consideration of $-|X|$ gives (2), whereas given (2) a consideration of $|X|+X$ gives (1). From the engineering point of view (1) is more suited to a machine which represents negative numbers by their complements. The question of the representation of negatives is an important one. In some machines where

magnitudes are restricted to $|X| \leqslant 1$ it turns out that representation by complements is a valuable addition since it allows the use of the number -1.

CODE OF A.R.C.

No.	*Code*	*Symbol*	*Description*
1	0,0000	T_i to M	Fill high-speed memory from input tape.
2	0,0001	T to T_i	Start tape moving to position T_i and proceed with next order.
3	0,0010	${}_nT_i$ to $i+j$ to M_1 to $1+j$	Read material on nth tape between i and $i+j$ into M.
4	0,0011	M_1 to $1+j$ to T_n	Punch material from memory location 1 to $1+j$ on to nth tape.
5	0,0100	C to M	Shift control to order located at $M(x)$.
6	0,0101	Cc to M	If $A \geqslant 0$ shift control as in 5.
7	0,0110	$L(N)$	Shift contents of A and R, N places to left. So that, e.g., $A(0)$—$A(20)$; $R(0)$—$R(20)$ to $A(0)$, $A(2)$—$A(20)$, 0; $R(1)$—$R(20)$, $A(1)$.
8	0,0111	$R(N)$	Shift contents of A, N places to right so that, e.g., $A(0)$, $A(1)$—$A(20)$ to $A(0)$, $A(0)$, $A(1)$—$A(19)$.
9	0,1000	M to cA	
10	0,1001	$\|M\|$ to cA	
11	0,1010	$-M$ to cA	
12	0,1011	$-\|M\|$ to cA	
13	0,1100	M to A	
14	0,1101	$\|M\|$ to A	
15	0,1110	$-M$ to A	
16	0,1111	$-\|M\|$ to A	
17	1,0000	$M.R$ to cA	Clear A. Multiply M by R, place 1st 20 digits and sign in A after adding unity to 21st digit. Leave last 20 digits in R.
18	1,0001	$M.R$ to $cA(N.R.)$	Perform multiplication without rounding off.
19	1,0010	$A \div M$ to cR	Divide A by M, place quotient in R with last digit unity. Leave remainder in A.
20	1,0011	M to cR	
21	1,0100	R to cA	
22	1,0101	R to M	
23	1,0110	A to M	
24	1,0111	A_L to M	Substitute digits 1–8 of A in order located at $M(x)$.
25	1,1000	A to cR	
26	1,1001	E	Signal completion of operation.

Computer projects in America

We shall now give a short survey of current calculating machine projects in America. No description will be given of the E.N.I.A.C., as Hartree has provided this in his book *Calculating Machines* (C.U.P.). In any case, although this machine is of historic interest as the first large electronic calculator to operate successfully, it has been rapidly outmoded by recent developments, and cannot be regarded as typical of modern ideas on automatic computers.

Aiken's relay computers

The A.S.C.C. (Automatic Sequence Controlled Calculator), built by Aiken at Harvard, also falls into this category. This relay controlled computer was completed in 1941 and has operated almost continuously since then to the present day. A very full description of this machine and its operation is given in *A Manual of Operation for the A.S.C.C.* published by Harvard.

Aiken has now completed a second, and larger, edition of this machine. The work of construction and wiring was completed last June (1947), testing was in progress, and the arithmetic unit had just been put into operating order.

The machine consists of the control and four arithmetic units. Input and output is via punched tape and results can be printed directly by the machine. It performs the elementary operations of addition, subtraction, multiplication, and division, and has the discrimination order described above.

Aiken hopes to attain a multiplication time of the order of 1 sec., an improvement by a factor of 5 over the A.S.C.C., and a multiple arithmetic unit has been incorporated with the idea of speeding up the machine. This will, of course, greatly increase the complexity of programming, as in order to use the machine to best advantage all units must be working simultaneously. Indeed, Professor Aiken has mentioned as a major problem the difficulty of programming sufficient work to keep the machines continually busy.

Experience of programming for our own relay machine, A.R.C., has shown, however, that, using the code given above, quite complex problems (e.g. matrix multiplication) can be programmed in about 30 minutes, and it seems reasonable to suppose that most calculations could be dealt with in a matter of hours. It may be concluded from this that an increase in the speed and simplicity of the arithmetic unit is preferable to an increase in size.

The chief reason for the use of binary scale for automatic computers is the lack of a reasonably compact and economical form of decimal memory. An essential difference between Aiken's relay machines and other current projects is that they have only a very small memory and operate in decimal scale. Orders are taken in sequence from punched tape, and all results, intermediate or final, are recorded on tape. This increases the complexity of programming and reduces the speed of the machine, as reading from and recording on tape are comparatively slow operations.

The use of decimal scale, of course, eliminates the necessity for conversions at the beginning and end of every calculation and reduces the number of digits which must be carried, but it has the disadvantage that, from the

engineering point of view, the operations of arithmetic are much more complicated in decimal than in binary scale.

In spite of these defects, however, both relay machines are fine examples of engineering, and Mark I has a most impressive record of continuous performance.

Aiken is also building an electronic computer, but development was not very far advanced last summer (1947). The main outlines of the machine had been decided upon, but the detailed circuits were not then designed. This machine is to have a high-speed memory, consisting of a drum with a number of magnetic tracks, each with its recording and pick-up head. Here again, decimal scale is to be used, decimal numbers being represented by a binary code.

The Bell relay machine

The only other large relay computer in America has been constructed by Bell Telephones, and is now at the Aberdeen Proving Ground, Maryland. This machine is a general purpose calculator, built to the basic plan indicated earlier in this report. It uses modified binary scale, has tape input and output, and uses a code similar to that outlined above. It has been successfully used to solve various differential equations, and for the calculation of a table of the binomial function. The limitations of this machine lie in the size of the high-speed memory—twenty numbers, stored in relay banks—and the experience of those who have used it shows that this restriction in memory size both reduces the effective speed of the machine and increases the complexity of programming.

As is projected for other machines using binary scale, the Bell machine performs its own conversions to and from this scale. It has a certain degree of internal checking in that, when information is transferred from one part of the machine to another, the number of 1's occurring in the number before and after transfer are compared; if these are found to be different, the machine is automatically stopped. This is by no means a complete check, and indeed, no current project has yet found a really satisfactory solution to this problem. It has been proposed to run two identical machines, coupled in parallel, and so arranged that if the results produced at any stage are not identical, the calculation is stopped. This, however, is likely to be costly in practice, and, in any case, is not an absolute check since the comparing mechanism is liable to error.

The E.D.V.A.C.

So far only 'parallel operation' machines have been described. Next comes the only overt project† in America building a serial type computer.

† Eckert and Mauchly's "Univac" is a commercial project and no details are available for publication.

the E.D.V.A.C. (Electronic Discrete Variable Automatic Calculator) at the Moore School of Electrical Engineering, Philadelphia. This is to be an all-purpose, electronic computer using as memory, mercury delay-lines. Its counterparts in England are Wilkes's E.D.S.A.C. at Cambridge and the National Physical Laboratory's A.C.E.

In July (1947) the main body of E.D.V.A.C. was still under construction. A good deal of work has been done on delay-lines, and in particular on the problems arising from corrosion of the tanks by the mercury, and a satisfactory model has been adopted. The designs for the accumulator and control are complete, and a pilot model of the arithmetic unit was operating. This model, 'Shadrac' by name, performs addition, subtraction, multiplication, and division, but no controls were built in and numbers had to be inserted by hand. 'Shadrac' was built for experimental purposes only and has a capacity for twenty digit binary numbers, the delay lines being about 18 in. long. The final machine will work to forty binary digits and on the basis of experience gained with 'Shadrac', it is hoped to achieve a multiplication time of 1 millisecond.

A typical order will consist of four parts:

(1) and (2) Specification of the locations of the two numbers to be operated upon.

(3) Operation (+, — etc.).

(4) Location to which result is to be sent.

Some coded examples are given in a report on E.D.V.A.C. (not published) and these indicate that coding for the machine is a comparatively quick and easy process. Orders and data will be punched on teletype tape, transferred to magnetized wire, and thence to the machine. This rather complicated process is necessary since direct tape input would be far too slow for the machine. The same method is to be adopted for the project next to be described, that of von Neumann at the Institute for Advanced Study, Princeton.

The Princeton electronic computer

This is probably the most ambitious project at present in existence, as it is hoped to attain a multiplication time of less than 100 μ sec. The machine is to be a parallel type electronic computer using binary scale. It differs from all those discussed so far in the size of its memory; this is hoped to be about 4,000, forty digit binary numbers to be stored in the 'selectrons' briefly described above.

The machine will follow the general plan described earlier in this report, and will consist of the memory, accumulator, shifting register, control, and the input and output units.

The input is to be via teletype tape and magnetized wire, and the machine will be provided with a library of these wires containing tabulated functions and codes for routine calculations.

The code is again similar to that described above, and each order will consist of two parts:

(1) The operation to be performed.

(2) The memory location of the number to be operated upon.

Conversions to and from binary scale will be done by the machine, decimal numbers being inserted in binary coded form. The large memory capacity, and simple code, will make the coding of problems for this machine comparatively rapid and easy.

At the end of last summer a shifting register and accumulator were in operation, and the magnetic input and output was complete. The accumulator had an addition time of $2\,\mu$ sec., but it was hoped to improve on this; the control circuits necessary to make multiplication and division possible had not, at that time, been completed.

A great deal of work has been done on the best and most economical medium for the magnetic input and wire has been chosen as providing minimum bulk with good recording capacity. To avoid undue bulk, small gauge wire will be used, and difficulty was experienced at first because the tensions set up when starting and stopping caused breakages. This problem has been solved by mounting two drums on a common shaft and winding the wire from one to the other via the reading and recording heads. The effective radii of these drums will, of course, vary slightly with the amount of wire on them, but the consequent tensions in the wire are eliminated by the use of a differential gear and a small servo-motor.

Another problem which has to be considered in this connexion is that of reading from the wire while accelerating. It is possible to lose digits in this process, and this is to be avoided by having a set of marker pulses between each 'word'. A counting device records the number of digits read out between each marker pulse, and if any are missed, the word is rejected. It is hoped, in the final machine, to record 100 digits to the inch and to run the wire at 50 ft. per sec., giving an input speed of 60,000 digits per sec.

Progress on the memory has, so far, been slow. Originally it was to consist of forty 'selectrons', each containing 4,000 digits. At the end of the summer (1947), however, no working model of the selectron had been produced, and it seems that, when this is available, it may contain, at first, only 256 digits. While this memory is adequate for a relay machine, it will probably be quite insufficient for the much faster electronic computer, and it may be necessary to develop an alternative form of high-speed memory consisting of, for example, magnetized drums.

Forrester, of the Massachusetts Institute of Technology, is engaged on an almost identical project to that of von Neumann. Development is slightly behind that at Princeton, but the only essential difference is in the proposed form of the high-speed memory. Forrester hopes to use some form of electrostatic storage, presumably of the general type suggested by Williams.

Although the United States is comparatively rich in computers and computer projects, it is interesting to note that all are sponsored, in part at any rate, by the Government, and that all, with the exception of the Princeton machine and Forrester's computer, are eventually to be moved to the Aberdeen proving ground or to the U.S. Navy Proving Ground at Dahlgren, Virginia.

REFERENCES

1. Francis Murray, *The Theory of Mathematical Machines.* King's Crown Press, New York.
2. For example, Reich, *The Theory and Application of Electron Tubes*, McGraw-Hill, 1945.
3. *A.C.E. Report*, National Physical Laboratory, 1948.

SUBHARMONICS IN A NON-LINEAR SYSTEM WITH UNSYMMETRICAL RESTORING FORCE

By G. E. H. REUTER

(*Department of Mathematics, The University, Manchester*)

[Received 11 May 1948]

SUMMARY

The behaviour of an oscillatory system which is positively damped but in which the restoring force is unsymmetrical about the equilibrium position is investigated. It is shown that if a periodic external force whose period is approximately half the natural period is applied, the system may oscillate with twice the period of the external force (such oscillations are called subharmonics of order 2). The subharmonics only occur when the amplitude of the external force reaches a certain critical value; if the forcing period is slightly greater than half the natural period, there is a second critical amplitude beyond which the ordinary forced oscillation (with the same period as the external force) becomes unstable. In the range between the two critical amplitudes, therefore, the forced oscillation or the subharmonics may occur (which of them occurs will depend on the initial displacement and velocity of the system), whilst beyond the second critical amplitude only the subharmonics can occur. This gives rise to a 'hysteresis' effect when the amplitude of the external force is increased and then decreased again.

1. Introduction

It is well known that non-linear differential equations of the form

$$\ddot{x}+f(x)\dot{x}+g(x) = f\cos pt$$

(dots denoting derivatives with respect to t) may have periodic solutions whose least period is an integral multiple $2n\pi/p$ of the period $2\pi/p$ of the forcing term (**1**). (Such solutions are called subharmonics of order n.) It has been usual to assume that the restoring force is symmetrical about $x = 0$, i.e. that $g(x)$ is an odd function of x; the simplest equation with an unsymmetrical restoring term is

$$\ddot{x}+k\dot{x}+\omega^2 x(1+\alpha x) = f\cos pt. \tag{1}$$

This equation (with a positive damping term, i.e. $k > 0$) arises in the theory of loud speakers (**2**), and has been investigated both experimentally and theoretically by Pedersen (**3**). As, however, Pedersen's treatment is not rigorous and his results appear to be incorrect, we shall discuss the existence of subharmonics for equation (1) rigorously by Poincaré's method of small parameters (**4**). It will be shown that, when k and α are both small and p is approximately equal to 2ω, equation (1) has under certain

conditions subharmonic solutions of order 2. The stability of these solutions will also be discussed.

I should like to thank Miss M. L. Cartwright for suggesting this investigation to me, and for her advice during its progress.

2. We may arrange, by changing the time scale, that the forcing term in (1) is $f\cos 2t$. In practice, ω would be held fixed and p varied, but since only small variations of p about $p = 2\omega$ will be considered they may be taken into account by varying ω. We assume therefore that $p = 2$, and that ω^2-1, k, and α are all small and of the same order of magnitude. We may then write $k = \lambda\alpha$, $\omega^2 = 1+\mu\alpha$, and $f = 3\nu$, where λ, α, and ν may be assumed to be positive, and λ, μ, and ν will be of order unity. Equation (1) then becomes

$$\ddot{x}+\lambda\alpha\dot{x}+(1+\mu\alpha)x(1+\alpha x) = 3\nu\cos 2t. \tag{2}$$

It will appear that (2) has subharmonics whose amplitude is of order $\alpha^{-\frac{1}{2}}$, and it is therefore convenient to write $\alpha = \epsilon^2$ and $y = \epsilon x$, so that

$$\ddot{y}+\lambda\epsilon^2\dot{y}+(1+\mu\epsilon^2)y(1+\epsilon y) = 3\nu\epsilon\cos 2t, \tag{3}$$

and the subharmonics will now have amplitudes of order unity.

3. We shall now prove that, when λ, μ, and ν are fixed, $\lambda < \nu$, and ϵ is sufficiently small, equation (3) may have subharmonic solutions of order 2 (i.e. periodic solutions of period 2π). These subharmonics will always occur in pairs, since if $y = \phi(t)$ is a solution of (3), so is $y = \phi(t+\pi)$.

When $\epsilon = 0$, the solution of (3) with initial values $y(0) = a$, $\dot{y}(0) = b$ is $y = \phi_0(t) = a\cos t+b\sin t$, and has period 2π. We shall attempt to find solutions of (3), of period 2π, which reduce to such a 'generating solution' when $\epsilon \to 0$.

The solution of (3) with $y(0) = a$, $\dot{y}(0) = b$ is analytic in ϵ for sufficiently small ϵ, and is of the form

$$y = \phi_0(t)+\epsilon\phi_1(t)+\epsilon^2\phi_2(t)+\dots, \tag{4}$$

where the functions $\phi_i(t)$ are analytic in t, a, b, and the series converges uniformly when t, a, b lie in fixed finite intervals and ϵ is sufficiently small (**5**). Substituting from (4) into (3), we find that

$$\left.\begin{aligned}\ddot{\phi}_1+\phi_1 &= 3\nu\cos 2t-\phi_0^2,\\ \phi_1(0) &= \dot{\phi}_1(0) = 0;\end{aligned}\right\} \tag{5}$$

$$\left.\begin{aligned}\ddot{\phi}_2+\phi_2 &= -\lambda\dot{\phi}_0-\mu\phi_0-2\phi_0\phi_1 = \psi, \text{ say},\\ \phi_2(0) &= \dot{\phi}_2(0) = 0.\end{aligned}\right\} \tag{6}$$

From (5) we obtain

$$\begin{aligned}\phi_1(t) = -\tfrac{1}{2}(a^2+b^2)+(\nu+\tfrac{1}{3}a^2+\tfrac{2}{3}b^2)\cos t-\tfrac{2}{3}ab\sin t-&\\ -(\nu-\tfrac{1}{6}a^2+\tfrac{1}{6}b^2)\cos 2t+\tfrac{1}{3}ab\sin 2t,&\end{aligned}$$

and hence we may calculate $\psi(t)$, the right-hand member of (6). We shall only require the values of $\phi_2(2\pi)$ and $\dot{\phi}_2(2\pi)$, and from (6) these are given by

$$\phi_2(2\pi) = -\int\limits_0^{2\pi} \psi(t)\sin t\,dt,$$

$$\dot{\phi}_2(2\pi) = +\int\limits_0^{2\pi} \psi(t)\cos t\,dt.$$

Inserting the value of $\psi(t)$ obtained from (5) and (6) (only terms involving $\cos t$ or $\sin t$ being required) we finally obtain

$$\left.\begin{aligned} \frac{1}{\pi}\phi_2(2\pi) &= -\lambda a+(\mu+\nu)b-\tfrac{5}{6}b(a^2+b^2) = P(a,b), \text{ say,} \\ \frac{1}{\pi}\dot{\phi}_2(2\pi) &= -\lambda b-(\mu-\nu)a+\tfrac{5}{6}a(a^2+b^2) = Q(a,b), \text{ say.} \end{aligned}\right\} \tag{7}$$

Hence, from (4), we find that

$$\left.\begin{aligned} y(2\pi)-y(0) &= \pi\epsilon^2[P(a,b)+\epsilon P_1(a,b)+\ldots], \\ \dot{y}(2\pi)-\dot{y}(0) &= \pi\epsilon^2[Q(a,b)+\epsilon Q_1(a,b)+\ldots], \end{aligned}\right\} \tag{8}$$

where $P(a,b)$, $Q(a,b)$ are given by (7), and $P_1(a,b)$, $Q_1(a,b)$,... are polynomials in a, b (whose values will not be needed further). Our task is now to choose a and b (as functions of ϵ) so that $y(2\pi) = y(0)$ and $\dot{y}(2\pi) = \dot{y}(0)$. To this end, we first choose a_0 and b_0 so that

$$P(a_0, b_0) = Q(a_0, b_0) = 0$$

and then write $a = a_0+\xi$, $b = b_0+\eta$. By Poincaré's expansion theorem (7), $y(2\pi)-y(0)$ and $\dot{y}(2\pi)-\dot{y}(0)$ will then be analytic functions of ξ, η, ϵ which can be expanded in power series convergent when $|\xi|$, $|\eta|$, and ϵ are sufficiently small. These expansions can be obtained by expanding $P(a,b)$, $P_1(a,b)$,..., $Q(a,b)$, $Q_1(a,b)$,... in powers of ξ and η, and inserting these expansions in (8); rearranging in powers of ξ and η, we obtain expansions

$$\left.\begin{aligned} \frac{y(2\pi)-y(0)}{\pi\epsilon^2} &= A(\epsilon)+B(\epsilon)\xi+C(\epsilon)\eta+\ldots = X(\xi,\eta,\epsilon), \text{ say,} \\ \frac{\dot{y}(2\pi)-\dot{y}(0)}{\pi\epsilon^2} &= D(\epsilon)+E(\epsilon)\xi+F(\epsilon)\eta+\ldots = Y(\xi,\eta,\epsilon), \text{ say,} \end{aligned}\right\} \tag{9}$$

where $A(\epsilon)$,..., $F(\epsilon)$ are analytic for sufficiently small ϵ. Using (7) and (8), we find that

$$A(0) = D(0) = 0,$$

$$B(0) = -\lambda-\tfrac{5}{3}a_0 b_0, \qquad C(0) = \mu+\nu-\tfrac{5}{6}a_0^2-\tfrac{5}{2}b_0^2,$$

$$E(0) = -\mu+\nu+\tfrac{5}{2}a_0^2+\tfrac{5}{6}b_0^2, \qquad F(0) = -\lambda+\tfrac{5}{3}a_0 b_0.$$

Hence $$\left[\frac{\partial(X,Y)}{\partial(\xi,\eta)}\right]_{\xi=\eta=\epsilon=0} = \begin{vmatrix} B(0) & C(0) \\ E(0) & F(0) \end{vmatrix} = \Delta, \text{ say,}$$

and so, provided $\Delta \neq 0$, the equations

$$X(\xi,\eta,\epsilon) = Y(\xi,\eta,\epsilon) = 0$$

have, for sufficiently small ϵ, a solution (analytic in ϵ)

$$\xi = \xi(\epsilon), \qquad \eta = \eta(\epsilon),$$

with $\xi(0) = \eta(0) = 0$. The solution of (3) with

$$y(0) = a_0+\xi(\epsilon), \qquad \dot{y}(0) = b_0+\eta(\epsilon)$$

then has period 2π and is of the form $y = y(t,\epsilon)$ (analytic in ϵ), with $y(t,0) = a_0 \cos t + b_0 \sin t$.

4. The equations $$P(a_0,b_0) = Q(a_0,b_0) = 0$$

which determine the possible subharmonics will now be discussed. The solution $a_0 = b_0 = 0$ corresponds to a periodic solution of period π, which will be discussed in § 5. Any other solution must satisfy

$$\left.\begin{aligned} a_0/b_0 &= \{\nu\pm\sqrt{(\nu^2-\lambda^2)}\}/\lambda, \\ a_0^2+b_0^2 &= \tfrac{6}{5}\{\mu\mp\sqrt{(\nu^2-\lambda^2)}\}. \end{aligned}\right\} \tag{10}$$

These equations have solutions (other than $a_0 = b_0 = 0$) if and only if $\lambda \leqslant \nu$ and $\mu > -\sqrt{(\nu^2-\lambda^2)}$. If $-\sqrt{(\nu^2-\lambda^2)} < \mu \leqslant \sqrt{(\nu^2-\lambda^2)}$ there are two solutions, with the lower sign in (10), and if $\mu > \sqrt{(\nu^2-\lambda^2)}$ there are four solutions, with both signs in (10). Each sign in (10) yields a pair of solutions, (a_0, b_0) and $(-a_0, -b_0)$, corresponding to a pair of subharmonics with phase difference π.

With the values of a_0 and b_0 given by (10), it is found that

$$\Delta = 4\sqrt{(\lambda^2-\nu^2)}\{\sqrt{(\nu^2-\lambda^2)}\mp\mu\}.$$

Since the upper sign occurs only if $\mu > \sqrt{(\nu^2-\lambda^2)}$, and the lower sign only if $\mu > -\sqrt{(\lambda^2-\nu^2)}$, $\Delta \neq 0$ with either sign provided $\lambda < \nu$, and this finally establishes the existence of subharmonics for equation (3).

Equation (9) also determines the stability properties of the subharmonics. If a subharmonic has initial values $y(0) = a$, $\dot{y}(0) = b$, then the solution with initial values $a+\xi$ and $b+\eta$ has $y(2\pi) = a+\xi'$, $\dot{y}(2\pi) = b+\eta'$, where from (9)

$$\xi' = [1+\pi\epsilon^2 B(0)]\xi+\pi\epsilon^2 C(0)\eta+\ldots,$$

$$\eta' = \pi\epsilon^2 E(0)\xi+[1+\pi\epsilon^2 F(0)]\eta+\ldots,$$

the terms omitted involving second and higher powers of ξ and η or third

and higher powers of ϵ. The stability of the subharmonic therefore depends (**7**) on the characteristic roots ρ of the matrix

$$\begin{pmatrix} 1+\pi\epsilon^2 B(0) & \pi\epsilon^2 C(0) \\ \pi\epsilon^2 E(0) & 1+\pi\epsilon^2 F(0) \end{pmatrix};$$

these roots are $\rho = 1+\pi\epsilon^2\{-\lambda\pm\sqrt{(\lambda^2-\Delta)}\}$ (using the values of $B(0),..., F(0)$ found in § 3).

There are three cases to discuss:

(*a*) The periodic solution ($a_0 = b_0 = 0$) has $\Delta = \lambda^2+\mu^2-\nu^2$,

$$\rho = 1+\pi\epsilon^2\{-\lambda\pm\sqrt{(\nu^2-\mu^2)}\}.$$

If $\lambda \geqslant \nu$ or if $\lambda < \nu$ and $|\mu| > \sqrt{(\nu^2-\lambda^2)}$ both roots have modulus less than 1 and the solution is completely stable; if $\lambda < \nu$ and $|\mu| < \sqrt{(\nu^2-\lambda^2)}$ both roots are real, one being less than 1 and one greater than 1, so that the solution is 'directly unstable' (of 'col' type).

(*b*) $\lambda < \nu$, $\mu > -\sqrt{(\nu^2-\lambda^2)}$, lower sign in (10). Both roots have modulus less than 1 and the solution is completely stable.

(*c*) $\lambda < \nu$, $\mu > \sqrt{(\nu^2-\lambda^2)}$, upper sign in (10). Both roots are real, one less than 1 and one greater than 1; the solution is directly unstable.

5. It was stated in § 4 that the solution $a_0 = b_0 = 0$ of

$$P(a_0, b_0) = Q(a_0, b_0) = 0$$

corresponds to a periodic solution of period π of equation (3); the amplitude of this solution will be of order $\alpha^{\frac{1}{2}}$. To prove these statements, a method similar to that of § 3 may be used, working with equation (2) and expanding in powers of α. It is easily shown that the periodic solution exists for small α, and is of the form

$$x = x(t,\alpha) \quad \text{(analytic in } \alpha)$$

with $x(t,0) = -\nu\cos 2t$. We shall omit a detailed proof.

6. We shall now summarize the results of §§ 3 and 4, applied to equation (2):

$$\ddot{x}+k\dot{x}+\omega^2 x(1+\alpha x) = 3\nu\cos 2t.$$

The results are valid when $\alpha < \alpha_0$, where α_0 depends on k/α, $(\omega^2-1)/\alpha$, and ν; in practice this will mean that α, k, and ω^2-1 must be small and of the same order of magnitude and that ν must not be too large.

(*a*) There is always a periodic solution of the form

$$x = -\nu\cos 2t+O(\alpha);$$

this solution is completely stable unless $k < \nu\alpha$ and $|\omega^2-1| < (\nu^2\alpha^2-k^2)^{\frac{1}{2}}$, when it is directly unstable.

(*b*) There are subharmonics if $k < \nu\alpha$ and $\omega^2 > 1-\sqrt{(\nu^2\alpha^2-k^2)}$. There

are two or four subharmonics, occurring in pairs with phase-difference π, according as $|\omega^2-1| < (\nu^2\alpha^2-k^2)^{\frac{1}{2}}$ or $\omega^2 > 1+\sqrt{(\nu^2\alpha^2-k^2)}$ respectively.

(c) When $k < \nu\alpha$ and $|\omega^2-1| < \sqrt{(\nu^2\alpha^2-k^2)}$ the two subharmonics are completely stable, and are of the form

$$x = p\cos(t-\theta)+A\cos t+B\sin t-$$
$$-\tfrac{1}{2}\alpha p^2-\nu\cos 2t-\tfrac{1}{6}\alpha p^2\cos(2t+2\theta)+O(\alpha^{\frac{1}{2}}), \tag{11}$$

with

$$p^2 = \frac{6}{5\alpha^2}\{\omega^2-1+\sqrt{(\nu^2\alpha^2-k^2)}\} \quad \text{and} \quad \tan\theta = \frac{\nu\alpha+\sqrt{(\nu^2\alpha^2-k^2)}}{k}$$

(giving two possible values of θ differing by π). The coefficients A and B are $O(1)$ but cannot be determined from our calculations; they are, however, usually of smaller order than p, which is of order $\alpha^{-\frac{1}{2}}$ unless ω^2 is very near to $1-\sqrt{(\nu^2\alpha^2-k^2)}$.

(d) When $k < \nu\alpha$ and $\omega^2 > 1+\sqrt{(\nu^2\alpha^2-k^2)}$, the stable pair of subharmonics is still present, but there is also a directly unstable pair, again given by (11) but with

$$p^2 = \frac{6}{5\alpha^2}\{\omega^2-1-\sqrt{(\nu^2\alpha^2-k^2)}\} \quad \text{and} \quad \tan\theta = \frac{\nu\alpha-\sqrt{(\nu^2\alpha^2-k^2)}}{k}.$$

7. It is of some interest to examine how the solutions vary as the amplitude or the frequency of the forcing term is varied.

(1) Varying amplitude (k, α, ω fixed; ν varied):

(a) As ν increases from 0 to k/α, there is a stable periodic solution of amplitude approximately ν, and there are no subharmonics.

(b) If $\omega > 1$, two pairs of subharmonics appear when ν reaches k/α—a stable pair with amplitude approximately

$$\sqrt{\tfrac{6}{5}}\,\alpha^{-1}[\omega^2-1+\sqrt{(\nu^2\alpha^2-k^2)}]^{\frac{1}{2}},$$

and an unstable pair with amplitude approximately

$$\sqrt{\tfrac{6}{5}}\,\alpha^{-1}[\omega^2-1-\sqrt{(\nu^2\alpha^2-k^2)}]^{\frac{1}{2}};$$

the periodic solution remains stable.

When ν reaches $\alpha^{-1}\sqrt{\{k^2+(\omega^2-1)^2\}}$, the unstable pair of subharmonics disappears, the stable pair remains, and the periodic solution becomes unstable.

(c) If $\omega < 1$, no subharmonics appear until ν reaches $\alpha^{-1}\sqrt{\{k^2+(\omega^2-1)^2\}}$; a stable pair of subharmonics, with amplitude approximately

$$\sqrt{\tfrac{6}{5}}\,\alpha^{-1}[\omega^2-1+\sqrt{(\nu^2\alpha^2-k^2)}]^{\frac{1}{2}},$$

then appears and the periodic solution becomes unstable.

It will also be seen, from (11), that the subharmonics are approximately

sinusoidal when they first appear, but that when ν is increased they become unsymmetrical about $x = 0$ and also contain a marked second harmonic.

(2) Varying frequency (k, α, ν fixed; ω varied):

(*a*) If $k \geqslant \nu\alpha$, there is a stable periodic solution and there are no subharmonics.

(*b*) If $k < \nu\alpha$, there are three different ranges of ω to consider. If $\omega^2 < 1-\sqrt{(\nu^2\alpha^2-k^2)}$, there is a stable periodic solution and there are no subharmonics. If $|\omega^2-1| < \sqrt{(\nu^2\alpha^2-k^2)}$ the periodic solution is unstable

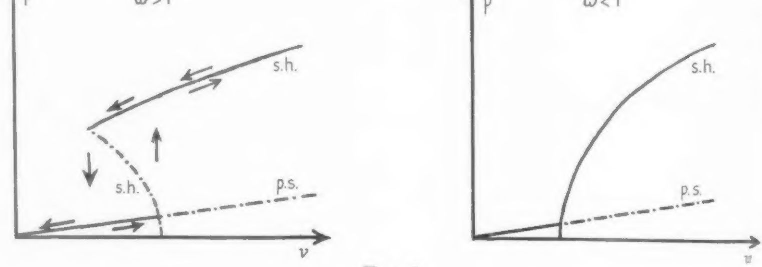

FIG. 1.

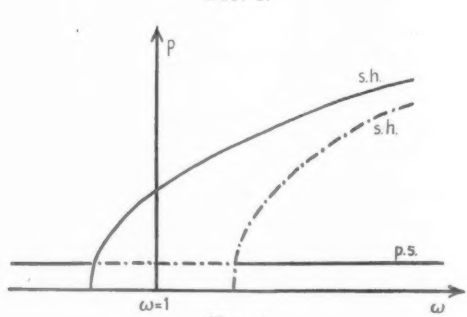

FIG. 2.

and there is a stable pair of subharmonics with approximate amplitude $\sqrt{\tfrac{6}{5}}\,\alpha^{-1}[\omega^2-1+\sqrt{(\nu^2\alpha^2-k^2)}]^{\frac{1}{2}}$ (but this approximation is invalid when ω^2 is very near to $1-\sqrt{(\nu^2\alpha^2-k^2)}$). If $\omega^2 > 1+\sqrt{(\nu^2\alpha^2-k^2)}$ there is a stable periodic solution, a stable pair of subharmonics as before, and an unstable pair, with approximate amplitude $\sqrt{\tfrac{6}{5}}\,\alpha^{-1}[\omega^2-1-\sqrt{(\nu^2\alpha^2-k^2)}]^{\frac{1}{2}}$ when ω^2 is not too near $1+\sqrt{(\nu^2\alpha^2-k^2)}$.

Curves of amplitude p plotted against ν (with ω constant) or ω (with ν constant) are sketched in Figs. 1 and 2, unstable solutions being indicated by dotted lines.† (It should be noted that these curves are only accurate

† In Figs. 1 and 2 *s.h.* stands for *subharmonic* and *p.s.* for *periodic solution.*

when $p \gg 1$.) Fig. 2 shows that there is no definite resonance near $\omega = 1$, but that the amplitude of the subharmonics appears to increase indefinitely as ω is increased (i.e. as the frequency of the forcing term is decreased below twice the natural frequency of the system). It should, however, be borne in mind that our results cease to hold if ω^2-1 becomes too large compared with α, and that then the first approximation to a subharmonic would be a periodic solution of $\ddot{x}+\omega^2x(1+\alpha x) = 0$ rather than of $\ddot{x}+x = 0$.

Inspection of Fig. 1 also reveals the possibility (when $\omega > 1$) of a 'hysteresis' effect if ν is increased and then decreased again. As ν increases, the stable periodic solution will be followed until ν reaches $\alpha^{-1}\sqrt{\{k^2+(\omega^2-1)^2\}}$; the system will then 'jump' to one of the stable subharmonics. If now ν is decreased, this subharmonic will remain until ν reaches k/α, when a jump back to the periodic solution will take place. The process is indicated by arrows in Fig. 1.

A possible objection to using equation (1) for a system with unsymmetrical restoring force is that $\omega^2x(1+\alpha x)$ may cease to represent the restoring force when $|\alpha x|$ becomes comparable with 1, since the actual restoring force probably does not change sign for $\alpha x = -1$. However, for the solutions which we have found $|\alpha x| \ll 1$, and so if necessary the restoring term could be modified when $\alpha x = O(1)$ without affecting the existence of subharmonics.

8. The results of § 3 also show how any solution of equation (3) approaches a subharmonic or periodic solution. For this purpose, we return to equation (8), which shows that the solution with $y(0) = a$, $\dot{y}(0) = b$ has $y(2\pi) = a+\Delta a$, $\dot{y}(2\pi) = b+\Delta b$, where

$$\left.\begin{aligned} \Delta a/\pi\epsilon^2 &= P(a,b)+O(\epsilon), \\ \Delta b/\pi\epsilon^2 &= Q(a,b)+O(\epsilon). \end{aligned}\right\} \tag{12}$$

The behaviour of solutions of (3) as t increases by multiples of 2π is then indicated by the behaviour of points of the (a,b)-plane under iterations of the transformation T: $(a,b) \to (a+\Delta a,\ b+\Delta b)$. Approach to a subharmonic or periodic solution corresponds to approach of (a,b) to a point (a_0,b_0) with $P(a_0,b_0) = Q(a_0,b_0) = 0$, i.e. to a fixed point of the transformation T. By drawing the curves $P(a,b) = 0$ and $Q(a,b) = 0$, the (a,b)-plane can be divided into regions in which $\Delta a \gtrless 0$ and $\Delta b \gtrless 0$, and hence the shape of the 'trajectories' described by points (a,b) under iterations of T can be estimated. Two typical configurations are sketched in Figs. 3 and 4; and signs of Δa and Δb are indicated by symbols like $[-,+]$ (to denote a region in which $\Delta a < 0$ and $\Delta b > 0$).

In Fig. 3 there are two stable fixed points S_1, S_2 of 'focus' type, and one unstable fixed point C of 'col' type. It is known (**8**) that there are two

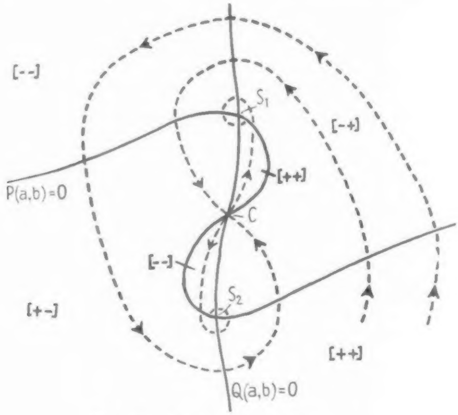

FIG. 3. $|\omega^2-1| < \sqrt{(\nu^2\alpha^2-k^2)}$.

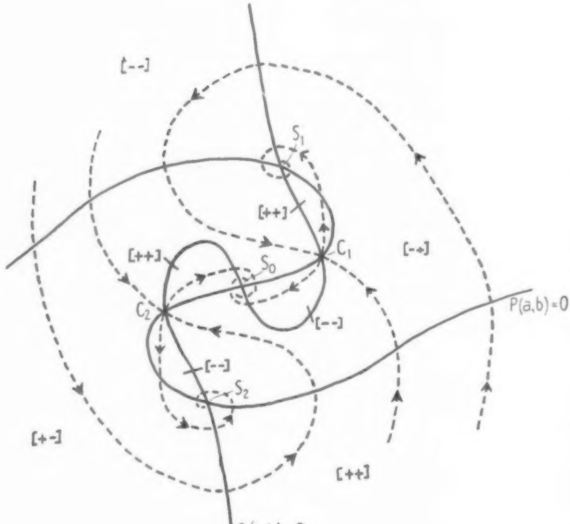

FIG. 4. $\omega^2 > 1+\sqrt{(\nu^2\alpha^2-k^2)}$.

curves invariant under T passing through a fixed point C of 'col' type; points on one of these curves approach C and points on the other recede from C under iterations of T. These curves are indicated by broken lines;

the unstable curve spirals into the two stable fixed points, whilst the stable curve spirals inwards for large values of a^2+b^2 before settling down into a steady approach to C.

In Fig. 4 there are three stable fixed points S_0, S_1, S_2 (S_0 corresponding to the periodic solution) of 'focus' type, and two unstable fixed points C_1, C_2 of 'col' type. In this case, the unstable invariant curve through $C_1(C_2)$ spirals into S_0 and $S_1(S_2)$.

In both cases, points at some distance from the origin spiral inwards until they are attracted towards one of the stable fixed points. Which fixed point is finally reached depends on the initial position of (a, b); the invariant curves through the cols divide any ray through the origin into a sequence of intervals from which points reach $S_1, S_2, S_1,\ldots$ in Fig. 3 and $S_0, S_1, S_0, S_2, S_0, S_1,\ldots$ in Fig. 4. Points near one of the invariant curves will spend some time near one of the cols (first approaching a col and then receding again); the corresponding solution will for a limited time give the impression of settling down to a steady periodic state (periodic solution in Fig. 3, subharmonic in Fig. 4) before settling down to a different final state (subharmonic in Fig. 3, periodic solution or subharmonic in Fig. 4). The parameters in Figs. 3 and 4 have been chosen so that the stable fixed points are all of 'focus' type; for certain ranges of the parameters, it is possible to have fixed points of 'node' type, for which there is a steady 'one-dimensional' approach to the fixed point. The approach of a solution to a subharmonic in the two cases is of a different nature (**9**); for a focus, the approach is like $p(t)\cos[t-\theta(t)]$, where $p(t)$ and $\theta(t)$ oscillate about their final values; for a node, $p(t)$ and $\theta(t)$ tend steadily in one direction towards their final values. From the results of § 4, it follows that the stable subharmonics are of 'node' or 'focus' type according as ω^2 is less than or greater than $1+\dfrac{5k^2-4\nu^2\alpha^2}{4\sqrt{(\nu^2\alpha^2-k^2)}}$ and that the periodic solution (when it is stable) is of 'node' or 'focus' type according as $|\omega^2-1| \leqslant \nu\alpha$ or $|\omega^2-1| > \nu\alpha$.

REFERENCES

1. L. Mandelstam and N. Papalexi, *Zeitschrift für Physik*, **73** (1932), 223–37; M. L. Cartwright and J. E. Littlewood, *Annals of Math.* **48** (1947), 490.
2. N. W. McLachlan, *Theory of Loudspeakers* (Oxford, 1934), 315.
3. F. O. Pedersen, *Journ. Acoust. Soc. America*, **6** (1935), 227–38; 1935, **7**, 64–70.
4. See N. Minorsky, *Introduction to Non-Linear Mechanics* (Ann Arbor, 1946), chap. viii, or Mandelstam and Papalexi, loc. cit. (**1**).
5. S. Lefschetz, *Lectures on Differential Equations* (Princeton, 1946), p. 35 (8.6).
6. —— loc. cit., p. 35 (9.1).
7. N. Levinson, *Annals of Math.* **45** (1944), 723–37.
8. —— loc. cit.
9. M. L. Cartwright, *Journ. Inst. Elect. Eng.* (Pt. III), **95** (1948), 88–96.

A NOTE ON THE NUMERICAL INTEGRATION OF DIFFERENTIAL EQUATIONS

By E. M. WILSON

(*Royal Naval Scientific Service, Admiralty, London, S.W.*1)

[Received 19 February 1948]

THE Taylor-series method for step-by-step integration of a differential equation is well known and used, particularly when high accuracy is needed. However, attention does not seem to have been drawn to the following version of the method, which, though not of universal application, can often be applied to linear equations. For an equation of order m, this form of the method consists in expressing the solution and the first $(m-1)$ derivatives at a point of tabulation as sums of the values of the same functions at the preceding tabular point multiplied by *previously computed* functions of the independent variable.

Consider, first, the linear first-order equation

$$\frac{dy}{dx} = P_1(x)y+Q_1(x). \tag{1}$$

By repeated differentiation of (and substitution from) equation (1), we have

$$\frac{d^r y}{dx^r} = P_r(x)y+Q_r(x), \tag{2}$$

where the successive P's and Q's are given by the recurrence relations

$$\left.\begin{aligned} P_{r+1} &= \frac{dP_r}{dx}+P_1 P_r \\ Q_{r+1} &= \frac{dQ_r}{dx}+Q_1 P_r \end{aligned}\right\}. \tag{3}$$

We may thus write Taylor's series as

$$y(x+w) = \left(1+wP_1+\frac{w^2}{2!}P_2+\ldots\right)y(x)+\left(wQ_1+\frac{w^2}{2!}Q_2+\ldots\right) = \mathbf{P}y(x)+\mathbf{Q}. \tag{4}$$

$\mathbf{P}$ and $\mathbf{Q}$ are functions of x only (for a fixed interval of tabulation), and can be calculated before the integration begins. Their calculation may or may not be easy, but once they have been obtained, the solution of the differential equation can be built up in the most straightforward manner.

Correspondingly, for a second-order equation

$$\frac{d^2y}{dx^2} = P(x)y+Q(x)\frac{dy}{dx}+R(x), \tag{5}$$

we should have two finite difference equations:

$$\left.\begin{aligned} y(x+w) &= \mathbf{P}_1\, y(x)+\mathbf{Q}_1\, y'(x)+\mathbf{R}_1(x) \\ y'(x+w) &= \mathbf{P}_2\, y(x)+\mathbf{Q}_2\, y'(x)+\mathbf{R}_2(x) \end{aligned}\right\}, \tag{6}$$

where dashes denote derivatives; and so on for equations of higher orders.

The number of elementary operations (multiplications and additions) required after the calculation of the functions **P**, **Q**, **R** may be sufficient to make the process uneconomic, unless a large part of the work can be performed mechanically. Until recently, there was no machine suitable for carrying out a continuous series of multiplications and additions, but the new automatic computing machines would seem perfectly suited to the process.

The fact that the accuracy to which **P** and **Q**, etc., must be calculated has to be determined at the outset entails no more difficulty than is normally encountered in deciding how many figures to take initially in y, and this is a decision which depends more upon the degree of stability of the equation to be integrated than upon the particular integration procedure used.

It may happen that calculation of the preliminary functions **P**, **Q**, etc., is simple enough for the process to be useful even without automatic machines. As an example, we take the equation†

$$y'' = y'+\alpha xy, \tag{7}$$

α being a parameter. Here we have

$$y^{(r)} = P_r y+Q_r y', \tag{8}$$

where

$$\left.\begin{aligned} P_{r+1} &= P'_r+\alpha x Q_r \quad \equiv \sum a_{r+1,s}x^s \\ Q_{r+1} &= Q'_r+Q_r+P_r \equiv \sum b_{r+1,s}x^s \end{aligned}\right\} \tag{9}$$

and

$$\left.\begin{aligned} P_0 &= 1 \\ Q_0 &= 0 \end{aligned}\right\} \quad \left.\begin{aligned} P_1 &= 0 \\ Q_1 &= 1 \end{aligned}\right\}.$$

The relations between the coefficients $a_{r,s}$, $b_{r,s}$ in these finite sums appear at once as:

$$\left.\begin{aligned} a_{r+1,s} &= (s+1)a_{r,s+1}+\alpha b_{r,s-1} \\ b_{r+1,s} &= (s+1)b_{r,s+1}+b_{r,s}+a_{r,s} \end{aligned}\right\} \tag{10}$$

† This equation can be reduced to that of the Airy integral, $Y'' = XY$.

from which we can readily construct the following table:

TABLE I

$r \backslash s$	$a_{r,s}$ 0	1	2	3	$b_{r,s}$ 0	1	2	3
0	1				0			
1	0				1			
2	0	α			1	0		
3	α	α			1	α		
4	α	α	α^2		$2\alpha+1$	2α	0	
5	α	$4\alpha^2+\alpha$	$2\alpha^2$		$5\alpha+1$	3α	α^2	
6	$4\alpha^2+\alpha$	$9\alpha^2+\alpha$	$3\alpha^2$	α^3	$9\alpha+1$	$6\alpha^2+4\alpha$	$3\alpha^2$	0
7	$9\alpha^2+\alpha$	$15\alpha^2+\alpha$	$9\alpha^3+4\alpha^2$	$3\alpha^3$	$10\alpha^2+14\alpha+1$	$21\alpha^2+5\alpha$	$6\alpha^2$	α^3

Equations (6) for this case are then

$$\left.\begin{aligned} y(x+w) &= y(x)\{A_0+A_1\,\alpha x+A_2\,\alpha^2x^2+...\}+ \\ &\qquad +y'(x)\{B_0+B_1\,\alpha x+B_2\,\alpha^2x^2+...\} \\ y'(x+w) &= y(x)\{A'_0+A'_1\,\alpha x+A'_2\,\alpha^2x^2+...\}+ \\ &\qquad +y'(x)\{B'_0+B'_1\,\alpha x+B'_2\,\alpha^2x^2+...\} \end{aligned}\right\}, \tag{11}$$

where, w_n being written for $w^n/n!$,

$$\left.\begin{aligned} A_0 &= w_0+\alpha(w_3+w_4+...)+\alpha^2(4w_6+9w_7+...)+... \\ A_1 &= (w_2+w_3+...)+\alpha(4w_5+9w_6+15w_7+...)+... \\ A_2 &= (w_4+2w_5+3w_6+...)+\alpha(9w_7+...)+... \\ A_3 &= (w_6+3w_7+...)+... \\ B_0 &= (w_1+w_2+w_3+...)+\alpha(2w_4+5w_5+9w_6+14w_7+...)+ \\ &\qquad +\alpha^2(10w_7+...)+... \\ B_1 &= (w_3+2w_4+3w_5+...)+\alpha(6w_6+21w_7+...)+... \\ B_2 &= (w_5+3w_6+6w_7+...)+... \\ B_3 &= (w_7+...)+... \end{aligned}\right\}. \tag{12}$$

The expressions for A'_r and B'_r differ from those for A_r and B_r only in having w_{n-1} in place of w_n ($w_{-1} = 0$, $w_0 = 1$).

The multipliers of $y(x)$ and $y'(x)$ are infinite series in x, with coefficients which are infinite series in α, these series again having infinite series in w as coefficients; but, in fact, calculation is easy. Rates of convergence depend upon the choice of w, which may be taken so that $\mathbf{P}_1$, $\mathbf{P}_2$, $\mathbf{Q}_1$, and $\mathbf{Q}_2$ can be treated as polynomials in x of low order, and either built up at interval w from a constant difference, or, perhaps, interpolated from a building-up at a wider interval (when there would be fewer extra figures needed). These preliminary computations could be carried out on, say, a National accounting machine, or Hollerith tabulator, and the straightforward integration of y then performed with the help of any ordinary desk machine.

With an interval w of 0·1, equations (12) become:

$$\left.\begin{aligned}
A_0 &= 1+0{\cdot}00017\ 09181\alpha+0{\cdot}0^8\ 57\alpha^2+\ldots\\
A_1 &= 0{\cdot}00517\ 09181+0{\cdot}0^6\ 3461\alpha+\ldots\\
A_2 &= 0{\cdot}0^5\ 43376+0{\cdot}0^9\ 2\alpha+\ldots\\
A_3 &= 0{\cdot}0^8\ 14+\ldots\\
B_0 &= 0{\cdot}10517\ 09181+0{\cdot}0^5\ 87628\alpha+\ldots\\
B_1 &= 0{\cdot}00017\ 52557+0{\cdot}0^8\ 88\alpha+\ldots\\
B_2 &= 0{\cdot}0^7\ 876+\ldots\\
B_3 &= 0{\cdot}0^{10}+\ldots\\
A_0' &= 0{\cdot}00517\ 09181\alpha+0{\cdot}0^6\ 3461\alpha^2+\ldots\\
A_1' &= 0{\cdot}10517\ 09181+0{\cdot}00001\ 74379\alpha+\ldots\\
A_2' &= 0{\cdot}00017\ 52557+0{\cdot}0^7\ 131\alpha+\ldots\\
A_3' &= 0{\cdot}0^7\ 876+\ldots\\
B_0' &= 1{\cdot}10517\ 09181+0{\cdot}00035\ 49365\alpha+0{\cdot}0^7\ 147\alpha^2+\ldots\\
B_1' &= 0{\cdot}00534\ 61737+0{\cdot}0^6\ 5301\alpha+\ldots\\
B_2' &= 0{\cdot}0^5\ 44251+\ldots\\
B_3' &= 0{\cdot}0^8\ 15+\ldots
\end{aligned}\right\}. \qquad (13)$$

We use this interval of $w = 0{\cdot}1$ to carry out the integration with ten decimals for the case $\alpha = 0{\cdot}1$, from $x = 0$ to $x = 1$, taking the initial values of y and y' to be respectively unity and zero. The results are set out in Table II.

TABLE II

x	$\mathbf{P}_1 = \Sigma A_r\alpha^r x^r$	$\mathbf{Q}_1 = \Sigma B_r\alpha^r x^r$	$\mathbf{P}_2 = \Sigma A_r'\alpha^r x^r$	$\mathbf{Q}_2 = \Sigma B_r'\alpha^r x^r$	$y(x)$	$y'(x)$
0·0	1·00001 70919	0·10517 17944	0·00051 70953	1·10520 64119	1·00000 00000	0·00000 00000
·1	6 88018	35470	156 88394	25 98746	1 70919	51 70953
·2	12 05127	52996	262 06186	31 33382	14 02796	214 03909
·3	17 22244	70522	367 24329	36 68027	48 59255	498 67888
·4	22 39369	7 88048	472 42822	42 02680	118 27293	918 64482
·5	27 56503	8 05574	577 61665	47 37343	237 31507	1488 47558
·6	32 73646	23101	682 80859	52 72014	421 50421	2224 45808
·7	37 90798	40628	788 00404	58 06694	688 35230	3144 88557
·8	43 07958	58155	893 20299	63 41383	1057 31306	4270 35298
0·9	48 25127	75682	998 40545	68 76081	1550 02869	5624 09498
1·0	1·00053 42305	0·10518 93209	0·01103 61141	1·10574 10788	1·02190 61274	0·07232 37315

$$y(x+0{\cdot}1) = y(x)\mathbf{P}_1(x)+y'(x)\mathbf{Q}_1(x)\,; \qquad y'(x+0{\cdot}1) = y(x)\mathbf{P}_2(x)+y'(x)\mathbf{Q}_2(x).$$

We may compare the final values with those of $y(1)$ and $y'(1)$ found by summing the readily obtained ascending series. These are, respectively, 1·02190 61274 and 0·07232 37314.

Many thanks are due to Mr. D. H. Sadler, for helpful comments on the method herein described, and to Mr. B. W. Conolly for assistance with the example.

TABLE OF $\int_0^x I_0(x)\,dx$ FOR $x = 0(0{\cdot}1)20(1)25$

By M. ROTHMAN (*Royal Technical College, Glasgow*)

[Received 15 March 1948; revised 3 September 1948]

THE solution of the problem of a lubricant or viscous fluid flowing through two very close horizontal plates was first given by Michell, whose method is reproduced by Stanton (**1**).

If we consider the plates to be vertical and fixed instead of horizontal we are led, by the same analysis, to the equations:

$$p = \sum p_m, \tag{1}$$

$$p_m = (\omega_m \sin mz)/mx, \tag{2}$$

where p is the pressure at a point of one of the plates and ω_m satisfies the equation

$$\frac{\partial^2 \omega_m}{\partial \zeta^2} + \frac{1}{\zeta}\frac{\partial \omega_m}{\partial \zeta} - \left(1+\frac{1}{\zeta^2}\right)\omega_m + \frac{k}{m^2} = 0, \tag{3}$$

where $\zeta = mx$ and $k = 12\rho g/\pi$, this being a Bessel equation with the added constant k/m^2.

These equations are the same as those derived by Stanton for the horizontal case except for the constant k/m^2, and the solution of equation (3) will therefore have the same complementary function as the corresponding equation of Stanton but a slightly different particular integral, the solution in this case being

$$\omega_m = A_m I_1(\zeta) + B_m K_1(\zeta) - \frac{k}{m^2}\left(\frac{\zeta^2}{3} + \frac{\zeta^4}{5.3^2} + \dots\right), \tag{4}$$

where A_m, B_m, k, and m are constants.

The total pressure on the plates is then given by $P = \iint p\,dxdz$, the integrals being taken over the plates. The evaluation of P necessitates a knowledge of the values of the integrals

$$\int_0^x \frac{I_1(x)}{x}\,dx \quad \text{and} \quad \int_\alpha^x \frac{K_1(x)}{x}\,dx,$$

which may also be written in the forms

$$\int_0^x \frac{I_1(x)}{x}\,dx = \int_0^x I_0(x)\,dx - [I_1(x)]_0^x \tag{5}$$

and
$$\int_{\alpha}^{x} \frac{K_1(x)}{x}\,dx = -\int_{\alpha}^{x} K_0(x)\,dx - [K_1(x)]_{\alpha}^{x}, \tag{6}$$

so that the solution of the problem is dependent on tables of the two integrals
$$\int_0^x I_0(x)\,dx \quad \text{and} \quad \int_0^x K_0(x)\,dx. \tag{7}$$

In the actual solution of the problem it is
$$\sum_1^{\infty} A_m \int_0^{mx} I_0(mx)\,d(mx)$$

that is wanted, and this is convergent; but it may happen, as was the case for a particular experiment, that the integral exceeded the limit of existing tables before its product with the constant A_m was ignorable.

Müller (2) has computed both the integrals (7) to $x = 16$, at which point the latter is sufficiently near to its limiting value to make further computation unnecessary. His computation of the former integral is for the range $x = 0(0{\cdot}1)5{\cdot}2(0{\cdot}2)16$, and as it was found convenient to have a slightly extended form of this table for a particular experiment, the table has been recomputed to $x = 20$, the results being given to 8 significant figures and at intervals of 0·1 up to this value. The values of this integral multiplied by e^{-x} for successive integers is also given up to $x = 25$.

Several formulae are suitable for the computation of this integral.

Firstly:
$$I_0(x) = J_0(ix) = 1 + \frac{x^2}{2^2.1^2} + \frac{x^4}{2^4.1^2.2^2} + \cdots$$

and therefore:
$$\int_0^x I_0(x)\,dx = \frac{2}{1}\left(\frac{x}{2}\right) + \frac{2}{3}\left(\frac{x}{2}\right)^3 + \frac{2}{5(2!)^2}\left(\frac{x}{2}\right)^5 + \frac{2}{7(3!)^2}\left(\frac{x}{2}\right)^7 + \cdots. \tag{8}$$

Secondly, terms in (8) may not be computed individually, but by means of
$$T_{n+1} = \frac{2}{(2n+1)(n!)^2}\left(\frac{x}{2}\right)^{2n+1} = \frac{2n-1}{2n+1}\,\frac{1}{n^2}\left(\frac{x}{2}\right)^2 T_n, \tag{9}$$

where T_n is the nth term in (8).

Thirdly:
$$\int_0^x I_0(x)\,dx = \tfrac{1}{2}\pi x[I_1(x)\{I_0(x) - L_0(x)\} - I_0(x)\{I_1(x) - L_{-1}(x)\}], \tag{10}$$

where $L_0(x)$ and $L_{-1}(x)$ are modified Struve functions.

Fourthly, the asymptotic expansion of (10):

$$\int_0^x I_0(x)\,dx \sim \frac{e^x}{\sqrt{(2\pi x)}}\left[\left(1-\frac{1.3}{1!\,8x}-\frac{1^2.3.5}{2!\,(8x)^2}-\frac{1^2.3^2.5.7}{3!\,(8x)^3}-...\right)\times\right.$$
$$\times\left(1+\frac{1^2}{x^2}+\frac{1^2.3^2}{x^4}+\frac{1^2.3^2.5^2}{x^6}+...\right)+$$
$$\left.+\left(1+\frac{1^2}{1!\,8x}+\frac{1^2.3^2}{2!\,(8x)^2}+\frac{1^2.3^2.5^2}{3!\,(8x)^3}+...\right)\left(\frac{1}{x}+\frac{1^2.3}{x^3}+\frac{1^2.3^2.5}{x^5}+...\right)\right], \tag{11}$$

and fifthly the formula

$$\int_0^x I_0(x)\,dx = 2(I_1-I_3+I_5-I_7+I_9-...). \tag{12}$$

Müller's table was first of all extended to $x = 20$ by formula (8) and was later recomputed from $x = 0$ to $x = 20$ at intervals of $x = 0{\cdot}1$ using formula (12), the results being given to 8 figures. This method depended on a table of $I_n(x)$ which is as yet unpublished, and the author is indebted in this respect to Dr. J. C. P. Miller for kindly lending him the proofs of *B.A. Mathematical Tables, Bessel Functions*, Part II. The results were checked by comparison with the first table as far as possible and also by differencing. The values of the integral for $x = 20(1)25$ were computed using formula (9) and as the differences are rather large in this region, a table of $e^{-x}\int_0^x I_0(x)\,dx$ is given for $x = 15(1)25$. The results have been checked by differencing. The differences δ_m^2 and γ^4, (3) and (4), where

$$\delta_m^2 = \delta^2-0{\cdot}184(\delta^4-\tfrac{1}{5}\delta^6); \qquad \gamma^4 = \delta^4/1000,$$

are given for use with the formula:

$$f_\theta = (1-\theta)f_0+\theta f_1+E_0^2\,\delta_{m0}^2+E_1^2\,\delta_{m1}^2+M_0^4\gamma_0^4+M_1^4\gamma_1^4.$$

I wish to express my thanks to Professor R. O. Street for the interest he has shown and the helpful suggestions he has made in connexion with the computation, and to a referee for suggesting the use of formulae (10)–(12).

REFERENCES

1. T. E. Stanton, *Friction* (Longmans Green & Co., London, 1923), 112.
2. R. Müller, *Zeitschrift für angewandte Mathematik und Mechanik*, **19** (1939), 52–3.
3. *Interpolation and Allied Tables* (H.M.S.O. 1936), 928.
4. J. C. P. Miller, *B.A. Mathematical Tables*, Part Volume B, 'The Airy Integral' (1946), 36.
5. V. R. Bursian and V. Fock, *Travaux Inst. Phys.-Math. Stekloff* (Trudy Fiz.-Mat. Inst. imeni V. A. Steklova), **2** (1), Leningrad, Acad. Sci. U.S.S.R., 1931.

x	$10^n \int_0^x I_0(x)\,dx$	n	δ_m^2	γ^4	x	$10^n \int_0^x I_0(x)\,dx$	n	δ_m^2	γ^4
0·0	0000 0000	8	0	0	5·0	3184 8668	6	24 3145	2
·1	1000 8336		5 0027	0	·1	3469 8150		26 6576	2
·2	2006 6767		10 0423	1	·2	3781 4628		29 2290	3
·3	3022 5761		15 1580	1	·3	4122 3859		32 0521	3
·4	4053 6544		20 3872	2	·4	4495 4119		35 1514	3
0·5	5105 1481	8	25 7699	2	5·5	4903 6452	6	38 5548	3
·6	6182 4474		31 3468	2	·6	5350 4946		42 2913	4
·7	7291 1369		37 1596	3	·7	5839 7028		46 3949	4
·8	8437 0377		43 2536	3	·8	6375 3801		50 9017	4
·9	9626 2523	8	49 6749	4	·9	6962 0406		55 8513	5
1·0	1086 5211	7	5 6472	0	6·0	7604 6420	6	61 2880	5
·1	1216 0721		6 3701	0	·1	8308 6299		67 2603	6
·2	1352 0021		7 1412	1	·2	9079 9863		73 8209	6
·3	1495 0834		7 9672	1	·3	9925 2826	6	81 0282	7
·4	1646 1431		8 8541	1	·4	1085 1738	5	8 8947	1
1·5	1806 0694	7	9 8089	1	6·5	1186 7285	5	9 7649	1
·6	1975 8186		10 8399	1	·6	1298 0639		10 7209	1
·7	2156 4230		11 9539	1	·7	1420 1376		11 7715	1
·8	2348 9985		13 1616	1	·8	1554 0020		12 9265	1
·9	2554 7543		14 4709	1	·9	1700 8138		14 1951	1
2·0	2775 0019	7	15 8939	1	7·0	1861 8439	5	15 5901	1
·1	3011 1663		17 4411	1	·1	2038 4895		17 1230	2
·2	3264 7971		19 1259	2	·2	2232 2861		18 8083	2
·3	3537 5815		20 9612	2	·3	2444 9217		20 6604	2
·4	3831 3577		22 9628	2	·4	2678 2517		22 6974	2
2·5	4148 1303	7	25 1472	2	7·5	2934 3162	5	24 9360	2
·6	4490 0869		27 5314	2	·6	3215 3577		27 3975	2
·7	4859 6156		30 1368	2	·7	3523 8418		30 1041	3
·8	5259 3256		32 9840	3	·8	3862 4796		33 0802	3
·9	5692 0684		36 0965	3	·9	4234 2521		36 3526	3
3·0	6160 9615	7	39 5014	3	8·0	4642 4372	5	39 9511	4
·1	6669 4150		43 2269	4	·1	5090 6395		43 9088	4
·2	7221 1600		47 3036	4	·2	5582 8232		48 2611	4
·3	7820 2797		51 7669	4	·3	6123 3479		53 0476	5
·4	8471 2443		56 6541	5	·4	6717 0083		58 3131	5
3·5	9178 9487	7	62 0070	5	8·5	7369 0784	5	64 1036	6
·6	9948 7541	7	67 8708	6	·6	8085 3587		70 4738	6
·7	1078 6533	6	7 4295	1	·7	8872 2299		77 4804	7
·8	1169 8722		8 1336	1	·8	9736 7106	5	85 1890	8
·9	1269 2370		8 9055	1	·9	1068 6522	4	9 3668	1
4·0	1377 5209	6	9 7511	1	9·0	1173 0158	4	10 2998	1
·1	1495 5710		10 6787	1	·1	1287 6964		11 3260	1
·2	1624 3163		11 6959	1	·2	1413 7220		12 4554	1
·3	1764 7755		12 8109	1	·3	1552 2238		13 6977	1
·4	1918 0655		14 0343	1	·4	1704 4463		15 0651	1
4·5	2085 4116	6	15 3761	1	9·5	1871 7591	4	16 5695	2
·6	2268 1578		16 8482	1	·6	2055 6691		18 2245	2
·7	2467 7785		18 4633	2	·7	2257 8343		20 0465	2
·8	2685 8914		20 2354	2	·8	2480 0796		22 0510	2
·9	2924 2715		22 1804	2	·9	2724 4130		24 2573	2
5·0	3184 8668	6	24 3145	2	10·0	2993 0445	4	26 6854	2

Interpolation formula: $f_\theta = (1-\theta)f_0 + \theta f_1 + E_0^2\,\delta_{m0}^2 + E_1^2\,\delta_{m1}^2 + M_0^4\gamma_0^4 + M_1^4\gamma_1^4$

x	$10^n \int_0^x I_0(x)\,dx$	n	δ^2_m	γ^4	x	$10^n \int_0^x I_0(x)\,dx$	n	δ^2_m	γ^4
10·0	2993 0445	4	26 6854	2	**15·0**	3526 2048	2	32 7813	3
·1	3288 4063		29 3575	3	·1	3882 8031		36 1154	3
·2	3613 1751		32 2989	3	·2	4275 5793		39 7892	4
·3	3970 2972		35 5362	3	·3	4708 2136		43 8373	4
·4	4363 0154		39 0992	4	·4	5184 7612		48 2984	5
10·5	4794 8989	4	43 0218	4	**15·5**	5709 6909	2	53 2146	5
·6	5269 8768		47 3390	4	·6	6287 9274		58 6322	6
·7	5792 2738		52 0917	5	·7	6924 8977		64 6021	6
·8	6366 8507		57 3238	5	·8	7626 5823		71 1820	7
·9	6998 8484		63 0832	6	·9	8399 5723		78 4325	7
11·0	7694 0363	4	69 4243	6	**16·0**	9251 1311	2	86 4242	8
·1	8458 7662		76 4050	7	·1	1018 9264	1	9 5230	1
·2	9300 0308	4	84 0907	8	·2	1122 2793		10 4938	1
·3	1022 5529	3	9 2553	1	·3	1236 1442		11 5634	1
·4	1124 3737		10 1870	1	·4	1361 5926		12 7424	1
11·5	1236 3988	3	11 2126	1	**16·5**	1499 8056	1	14 0422	1
·6	1359 6557		12 3425	1	·6	1652 0851		15 4739	1
·7	1495 2760		13 5859	1	·7	1819 8656		17 0530	2
·8	1644 5054		14 9556	1	·8	2004 7287		18 7926	2
·9	1808 7159		16 4639	2	·9	2208 4172		20 7107	2
12·0	1989 4183	3	18 1243	2	**17·0**	2432 8524	1	22 8244	2
·1	2188 2760		19 9532	2	·1	2680 1518		25 1546	2
·2	2407 1210		21 9675	2	·2	2952 6496		27 7229	3
·3	2647 9709		24 1852	2	·3	3252 9186		30 5537	3
·4	2913 0474		26 6283	2	·4	3583 7947		33 6748	3
12·5	3204 7976	3	29 3181	3	**17·5**	3948 4042	1	37 1143	4
·6	3525 9162		32 2814	3	·6	4350 1929		40 9066	4
·7	3879 3714		35 5446	3	·7	4792 9595		45 0863	4
·8	4268 4321		39 1389	4	·8	5280 8912		49 6947	5
·9	4696 6988		43 0980	4	·9	5818 6042		54 7738	5
13·0	5168 1373	3	47 4583	4	**18·0**	6411 1868	1	60 3736	6
·1	5687 1156		52 2618	5	·1	7064 2485		66 5468	6
·2	6258 4453		57 5522	5	·2	7783 9733		73 3519	7
·3	6887 4261		63 3804	6	·3	8577 1783		80 8543	8
·4	7579 8961		69 8000	7	·4	9451 3790	1	89 1253	8
13·5	8342 2861	3	76 8719	7	**18·5**	1041 4861	0	9 8243	1
·6	9181 6802	2	84 6624	8	·6	1147 6758		10 8297	1
·7	1010 5882	2	9 3244	1	·7	1264 7141		11 9377	1
·8	1112 3489		10 2701	1	·8	1393 7111		13 1598	1
·9	1224 3973		11 3111	1	·9	1535 8909		14 5067	1
14·0	1347 7765	2	12 4593	1	**19·0**	1692 6029	0	15 9923	2
·1	1483 6363		13 7230	1	·1	1865 3351		17 6293	2
·2	1633 2429		15 1161	1	·2	2055 7276		19 4351	2
·3	1797 9916		16 6506	2	·3	2265 5892		21 4255	2
·4	1979 4196		18 3413	2	·4	2496 9139		23 6202	2
14·5	2179 2206	2	20 2042	2	**19·5**	2751 9002	0	26 0400	2
·6	2399 2607		22 2568	2	·6	3032 9722		28 7084	3
·7	2641 5960		24 5182	2	·7	3342 8029		31 6501	3
·8	2908 4919		27 0100	3	·8	3684 3392		34 8937	3
·9	3202 4446		29 7561	3	·9	4060 8305		38 4706	4
15·0	3526 2048	2	32 7813	3	**20·0**	4475 8599	0	42 4142	2

x	$10^9 . e^{-x} \int_0^x I_0(x)\, dx$	δ^2_m	γ^4
15	1078 6742 2	4 4030 8	22
16	1041 0776 6	3 6753 6	16
17	1007 1857 4	3 1072 0	12
18	0976 4224 5	2 6557 8	9
19	0948 3309 8	2 2917 4	7
20	0922 5434 8	1 9943 1	5
21	0898 7597 7	1 7484 8	4
22	0876 7320 0	1 5432 5	3
23	0856 2534 2	1 3703 3	3
24	0837 1499 6	1 2234 7	2
25	0819 2738 6	1 0977 7	2

ON THE HEAVING MOTION OF A CIRCULAR CYLINDER ON THE SURFACE OF A FLUID

By F. URSELL

(*Department of Mathematics, The University, Manchester*)

[Received 20 April 1948]

SUMMARY

We consider the motion of a fluid of infinite depth which arises when a horizontal cylinder of circular cross-section oscillates with small amplitude about a mean position, in which the axis of the cylinder is assumed to lie in the mean surface. It is further assumed that the resulting motion is two-dimensional; this assumption is justified when the cylinder is long compared with a wave-length, or when the fluid is contained between vertical walls at right angles to the axis of the cylinder. Expressions are obtained for the wave motion at a distance from the cylinder, and for the increase in the inertia of the cylinder due to the presence of the fluid.

Introduction

A CYLINDER of circular section is immersed in a fluid with its axis in the free surface. If the cylinder is given a forced simple harmonic motion of small amplitude about its initial position, a surface disturbance is set up in which waves travel away from the cylinder, and a stationary state is rapidly attained. When the cylinder is very long or when the fluid is contained between vertical walls at right angles to the axis of the cylinder, the velocity component parallel to the axis of the cylinder vanishes and the motion is two-dimensional. It is well known that at a distance of a few wave-lengths from the cylinder the motion on each side is described by a single regular wave-train travelling away from the cylinder, and that the wave-amplitude is proportional to the amplitude of oscillation of the cylinder, provided that the latter is sufficiently small compared with the radius of the cylinder, and that the wave-length is not much smaller than the diameter of the cylinder.

In this paper it will be shown how the fluid motion can be calculated when the cylinder is oscillating vertically. The foregoing assumptions will be made, and viscosity and surface tension will be neglected. Then a velocity potential and a conjugate stream function exist, and it will be assumed that terms involving their squares may be neglected. From the potential or the stream function it is easy to deduce the wave-amplitude at a distance from the cylinder and the added mass of the cylinder due to the fluid motion.

Formulation of the problem

Take the origin of rectangular Cartesian coordinates at the mean position of the axis of the cylinder. The x-axis is horizontal and perpendicular to the axis of the cylinder, the y-axis is vertical, y increasing with depth. Define polar coordinates by the equations

$$x = r\sin\theta, \qquad y = r\cos\theta.$$

Since the motion is symmetrical about the y-axis, it is sufficient to consider the quadrant $0 \leqslant \theta \leqslant \frac{1}{2}\pi$. The velocity potential ϕ satisfies

$$\frac{\partial^2\phi}{\partial x^2}+\frac{\partial^2\phi}{\partial y^2} = 0, \tag{A}$$

the stream function ψ satisfies

$$\frac{\partial^2\psi}{\partial x^2}+\frac{\partial^2\psi}{\partial y^2} = 0. \tag{B}$$

On the free surface the pressure is constant, whence to the first order

$$K\phi+\frac{\partial\phi}{\partial y} = 0, \qquad \theta = \tfrac{1}{2}\pi, \qquad r > a, \tag{C}$$

where $K = \sigma^2/g$ and $2\pi/\sigma$ is the period (cf. ref. **1**). Also, by symmetry,

$$\partial\phi/\partial\theta = 0, \qquad \theta = 0. \tag{D}$$

It remains to express the boundary condition on the cylinder. This is that the velocity component normal to the boundary just inside the fluid is equal to the corresponding component of the velocity of the cylinder. Suppose that the ordinate of the axis of the cylinder is

$$y = l\cos(\sigma t+\epsilon).$$

Then at $(a\sin\alpha,\, a\cos\alpha+l\cos(\sigma t+\epsilon))$, the normal velocity is

$$-\frac{1}{a}\frac{\partial\psi}{\partial\alpha} = \frac{dy}{dt}\cos\alpha,$$

$$\psi = -a\frac{dy}{dt}\sin\alpha,$$

and to the first order this condition holds at $(a\sin\alpha,\, a\cos\alpha)$, whence

$$\psi = l\sigma a\sin(\sigma t+\epsilon)\sin\theta \quad \text{on} \quad r = a. \tag{E}$$

It is required to find a velocity potential and a stream function satisfying the boundary conditions (C), (D), and (E), and representing a diverging wave-train at infinity. To this end a series of non-orthogonal harmonic polynomials will be constructed satisfying (C) and (D); these will be superposed to satisfy (E) for values of Ka less than $3\pi/2$ by a numerical process. It is shown that when Ka is less than 1·5, this is permissible, and it will be supposed that the process is permitted in the wider range.

Construction of polynomial set

It is easily verified that the set of stream functions

$$a^{2m}\left[\frac{\sin 2m\theta}{r^{2m}}+\frac{K}{2m-1}\,\frac{\sin(2m-1)\theta}{r^{2m-1}}\right]\begin{matrix}\cos\\ \sin\end{matrix}\,\sigma t \quad (m = 1, 2, 3,\ldots)$$

is such that the conjugate velocity potentials satisfy (C) and (D), while on $r = a$ it takes the values

$$\sin 2m\theta+\frac{Ka}{2m-1}\sin(2m-1)\theta.$$

It is clear on physical grounds that this set is not closed on $r = a$, since the sum of functions of the set tends to zero as r tends to infinity, whereas in fact the stream function for large r must represent a diverging wave-train. It is therefore necessary to add a function satisfying (C) and (D) and representing such a train of waves, e.g. the function describing a source at the origin (cf. ref. **3**)

$$\frac{gb}{\pi\sigma}[\Psi_c(Kr;\theta)\cos\sigma t+\Psi_s(Kr;\theta)\sin\sigma t],$$

where b is the amplitude at infinity and

$$\Psi_c(Kr;\theta) = \pi e^{-Kr\cos\theta}\sin(Kr\sin\theta),$$

$$\Psi_s(Kr;\theta) = \int\limits_0^\infty \frac{e^{-kr\sin\theta}}{K^2+k^2}\{k\sin(kr\cos\theta)+K\cos(kr\cos\theta)\}\,dk- \\ -\pi e^{-Kr\cos\theta}\cos(Kr\sin\theta).$$

The functions of the closed set must be superposed so as to satisfy (E), and since there are no singularities on the cylinder, ψ must be continuous on $r = a$ when $0 \leqslant \theta \leqslant \frac{1}{2}\pi$.

Suppose, then, that the stream function ψ is expressed in the form

$$\frac{\pi\sigma\psi}{gb} = \Psi_c(Kr;\theta)\cos\sigma t+\Psi_s(Kr;\theta)\sin\sigma t+ \\ +\cos\sigma t\sum_1^\infty p_{2m}(Ka)a^{2m}\left[\frac{\sin 2m\theta}{r^{2m}}+\frac{K}{2m-1}\,\frac{\sin(2m-1)\theta}{r^{2m-1}}\right]+ \\ +\sin\sigma t\sum_1^\infty q_{2m}(Ka)a^{2m}\left[\frac{\sin 2m\theta}{r^{2m}}+\frac{K}{2m-1}\,\frac{\sin(2m-1)\theta}{r^{2m-1}}\right],$$

where the coefficients $p_{2m}(Ka)$, $q_{2m}(Ka)$ are assumed to be of order $1/m^2$.

This series converges uniformly outside and on $r = a$. On $r = a$ the function ψ is a multiple of $\sin\theta$, by condition (E), i.e. putting $r = a$,

$$\Psi_c^*(Ka;\theta)\cos\sigma t+\Psi_s^*(Ka;\theta)\sin\sigma t+$$
$$+\cos\sigma t\sum_1^\infty p_{2m}(Ka)\left[\sin 2m\theta+\frac{Ka}{2m-1}\sin(2m-1)\theta\right]+$$
$$+\sin\sigma t\sum_1^\infty q_{2m}(Ka)\left[\sin 2m\theta+\frac{Ka}{2m-1}\sin(2m-1)\theta\right]$$
$$= C(Ka;t)\sin\theta.$$

To determine $C(Ka;t)$, put $\theta = \frac{1}{2}\pi$ (say); then

$$C(Ka;t) = \Psi_c^*(Ka;\tfrac{1}{2}\pi)\cos\sigma t+\Psi_s^*(Ka;\tfrac{1}{2}\pi)\sin\sigma t+$$
$$+\cos\sigma t\sum_1^\infty p_{2m}(Ka)\frac{Ka}{2m-1}\sin\tfrac{1}{2}(2m-1)\pi$$
$$+\sin\sigma t\sum_1^\infty q_{2m}(Ka)\frac{Ka}{2m-1}\sin\tfrac{1}{2}(2m-1)\pi,$$

whence it follows that $p_{2m}(Ka)$, $q_{2m}(Ka)$ are the coefficients in the expansions

$$\Psi_c^*(Ka;\theta)-\Psi_c^*(Ka;\tfrac{1}{2}\pi)\sin\theta = \sum_1^\infty p_{2m}(Ka)f_{2m}(Ka;\theta),$$
$$\Psi_s^*(Ka;\theta)-\Psi_s^*(Ka;\tfrac{1}{2}\pi)\sin\theta = \sum_1^\infty q_{2m}(Ka)f_{2m}(Ka;\theta),$$

where

$$f_{2m}(Ka;\theta) = -\left[\sin 2m\theta+\frac{Ka}{2m-1}\{\sin(2m-1)\theta-\sin\theta\sin\tfrac{1}{2}(2m-1)\pi\}\right].$$

Write

$$\Psi_c^*(Ka;\tfrac{1}{2}\pi)+\sum_1^\infty\frac{(-1)^{m-1}Ka}{2m-1}p_{2m}(Ka) = A(Ka),$$
$$\Psi_s^*(Ka;\tfrac{1}{2}\pi)+\sum_1^\infty\frac{(-1)^{m-1}Ka}{2m-1}q_{2m}(Ka) = B(Ka).$$

Then the stream function on the cylinder is given by

$$\psi = \frac{gb}{\pi\sigma}[A(Ka)\cos\sigma t+B(Ka)\sin\sigma t]\sin\theta,$$

whence by comparison with condition (E) the ratio

$$\frac{\text{wave-amplitude}}{\text{amplitude of forced oscillation}}$$

is

$$\frac{\pi Ka}{\sqrt{(A^2+B^2)}}.$$

Calculation of the coefficients $A(Ka)$ and $B(Ka)$

The coefficients p_{2m}, q_{2m} are the roots of an infinite number of equations in an infinite number of unknowns. For purposes of calculation, the system of equations was replaced by a system involving only a finite number of the polynomials $f_{2m}(Ka;\theta)$. The functions

$$\Psi_c(Ka;\theta)-\Psi_c(Ka;\tfrac{1}{2}\pi)\sin\theta,$$
$$\Psi_s(Ka;\theta)-\Psi_s(Ka;\tfrac{1}{2}\pi)\sin\theta$$

were evaluated at $=0^\circ(10^\circ)90^\circ$ by quadrature, with

$$Ka/\pi=\tfrac{1}{6},\ \tfrac{1}{4},\ \tfrac{1}{2},\ \tfrac{2}{3},\ \tfrac{3}{4},\ 1,\ \tfrac{5}{4},\ \tfrac{3}{2}$$

and the polynomials $f_2(Ka;\theta),\dots,f_{2N}(Ka;\theta)$ were fitted at these values by least squares, the corresponding coefficients being

$$\begin{matrix}p_{2m}\\ q_{2m}\end{matrix}(Ka;N)\quad(m=1,\dots,N).$$

The least squares condition provides a set of N simultaneous linear equations for $p_{2m}(Ka;N)$ and similarly for $q_{2m}(Ka;N)$. The matrix of the equations is symmetrical and the terms on the principal diagonal are larger than any other terms in the same row (except for the first row). The system could therefore be solved conveniently by relaxation methods. Trial calculations were carried out and it was found that an expansion in terms of six polynomials was adequate, giving a close fit at the chosen values of Ka and θ. Table 1 shows various functions of Ka to three significant figures.

TABLE 1

Ka/π	$A(Ka)$	$B(Ka)$	$\sqrt{(A^2+B^2)}$	$\tan^{-1}(B/A)$	$\dfrac{\pi Ka}{\sqrt{(A^2+B^2)}}$	$m(Ka)$
0	0	−1·57	1·57	−90°	0	∞
1/6	1·75	−2·23	2·83	−52°	0·58	0·78
1/4	2·75	−2·06	3·44	−37°	0·72	0·73
1/2	5·64	+0·65	5·68	+7°	0·87	0·83
2/3	6·17	4·39	7·57	35°	0·87	0·91
3/4	5·55	6·62	8·64	50°	0·86	0·94
1	−0·88	12·33	12·4	94°	0·80	1·01
5/4	−12·6	11·2	16·9	138°	0·73	1·06
3/2	−22·0	−1·17	22·0	183°	0·67	1·09

These calculations are based on six polynomials. The values of $\sqrt{(A^2+B^2)}$ and $\tan^{-1}(B/A)$ are given for convenience in interpolation, each of these functions being monotone increasing in the range; in fact the angle varies nearly linearly except near $Ka=0$; when $Ka=0$

$$\frac{d}{d(Ka)}\tan^{-1}(B/A)=2\text{ radians},$$

as can be shown by expanding in a power series in Ka.

Virtual mass due to the fluid

It is well known that when a long cylinder completely immersed in an ideal fluid is moving in any way perpendicular to its axis, the reaction of the fluid may be expressed in the form

$$M'\mathbf{f} \text{ per unit length}$$

where $M' = \pi\rho a^2$ is the mass of fluid displaced by unit length of the cylinder and $\mathbf{f}$ is the acceleration vector (ref. **1**, Art. 68). This expression shows that the motion is unaltered if the fluid is supposed to be removed and a mass M' per unit length is added to the cylinder. The mass M' is called the virtual mass due to the fluid.

When the cylinder is in the free surface, the reaction of the fluid is no longer in phase with the acceleration. There is a component in quadrature which does a positive amount of work in each cycle and is thus simply related to the wave-amplitude. The component in phase with the acceleration does no work: it consists partly of a hydrostatic force which dominates the motion for small values of Ka, and which is easily seen to be

$$\frac{2\rho a^2}{Ka}\frac{d^2y}{dt^2},$$

where y is the displacement of the cylinder. More interesting is the part due to the wave motion which will now be calculated. The velocity potential ϕ is easily derived from the stream function. It is given by

$$\frac{\pi\sigma\phi}{gb} = \Phi_c(Kr;\theta)\cos\sigma t + \Phi_s(Kr;\theta)\sin\sigma t +$$

$$+\cos\sigma t\sum_1^\infty p_{2m}(Ka)a^{2m}\left[\frac{\cos 2m\theta}{r^{2m}} + \frac{K}{2m-1}\,\frac{\cos(2m-1)\theta}{r^{2m-1}}\right] +$$

$$+\sin\sigma t\sum_1^\infty q_{2m}(Ka)a^{2m}\left[\frac{\cos 2m\theta}{r^{2m}} + \frac{K}{2m-1}\,\frac{\cos(2m-1)\theta}{r^{2m-1}}\right]$$

from which the pressure $-\rho\,\partial\phi/\partial t$ can be derived.

Here $\Phi_c(Kr;\theta)$, $\Phi_s(Kr;\theta)$ are the harmonic conjugates of $\Psi_c(Kr;\theta)$, $\Psi_s(Kr;\theta)$:

$$\Phi_c(Kr;\theta) = \pi e^{-Kr\cos\theta}\cos(Kr\sin\theta),$$

$$\Phi_s(Kr;\theta) = -\int_0^\infty \frac{e^{-kr\sin\theta}}{K^2+k^2}\{k\cos(kr\cos\theta) - K\sin(kr\cos\theta)\}\,dk +$$

$$+\pi e^{-Kr\cos\theta}\sin(Kr\sin\theta).$$

It is seen that the pressure on the cylinder is of the form

$$M\cos\sigma t + N\sin\sigma t,$$

while the displacement of the cylinder is of the form

$$P\cos\sigma t+Q\sin\sigma t.$$

The component of the pressure in phase with the displacement is therefore

$$\frac{MP+NQ}{P^2+Q^2}(P\cos\sigma t+Q\sin\sigma t).$$

The force per unit length acting on the cylinder is

$$-\int\limits_{-\frac{1}{2}\pi}^{\frac{1}{2}\pi}\rho a\frac{\partial\phi}{\partial t}\cos\theta\,d\theta\quad(r=a),\qquad\text{i.e.}\qquad\frac{2\rho abg}{\pi}(M_0\cos\sigma t-N_0\sin\sigma t),$$

where

$$M_0=\int\limits_0^{\frac{1}{2}\pi}\Phi_s(Ka;\theta)\cos\theta\,d\theta+\sum_1^\infty\frac{(-1)^{m-1}q_{2m}(Ka)}{4m^2-1}+\tfrac{1}{4}\pi Kaq_2(Ka),$$

$$N_0=\int\limits_0^{\frac{1}{2}\pi}\Phi_c(Ka;\theta)\cos\theta\,d\theta+\sum_1^\infty\frac{(-1)^{m-1}p_{2m}(Ka)}{4m^2-1}+\tfrac{1}{4}\pi Kap_2(Ka).$$

The displacement is

$$\frac{b}{\pi Ka}(A\sin\sigma t-B\cos\sigma t),$$

where $A(Ka)$, $B(Ka)$ are the functions shown in Table 1.

It follows that the force component in phase with the acceleration is

$$-\frac{2\rho abg}{\pi}\frac{M_0B+N_0A}{A^2+B^2}(A\sin\sigma t-B\cos\sigma t),$$

while the acceleration is

$$-\frac{b\sigma^2}{\pi Ka}(A\sin\sigma t-B\cos\sigma t).$$

The virtual mass is their ratio

$$2\rho a^2\frac{M_0B+N_0A}{A^2+B^2}.$$

The values of the non-dimensional quantity

$$m(Ka)=\frac{M_0B+N_0A}{A^2+B^2},$$

which may be described as an inertia coefficient, are given in the last column of Table 1.

It can be shown that as $Ka \to 0$,

$$m(Ka) - \log \frac{1}{Ka} \to \tfrac{3}{2} - 2\log 2 - \gamma = -0{\cdot}46,$$

where γ is Euler's constant. Hence the hydrodynamic inertia coefficient tends to infinity like $\log\{1/(Ka)\}$, while the hydrostatic coefficient tends to infinity like $\pi/(2Ka)$.

The work done by the cylinder in a cycle must be equal to the energy transmitted by the waves at a distance from the cylinder in the same time. In terms of the various parameters, $M_0 A - N_0 B = \tfrac{1}{2}\pi^2$. This relation may be used to check the computations.

Discussion of results

The computations show that the amplitude ratio

$$\frac{\pi Ka}{\sqrt{(A^2+B^2)}}$$

is small for small values of Ka/π and increases as Ka/π increases, until Ka/π is approximately $0{\cdot}6$. As Ka/π increases beyond this value, the amplitude ratio decreases steadily throughout the range of computation. This effect may be ascribed to interference between waves originating from different parts of the cylinder surface. Qualitatively similar behaviour is exhibited by cylinders of various other sections. As Ka/π tends to zero, the amplitude ratio tends to $2Ka$. It may be shown that this result, which is in agreement with Holstein's approximate theory (ref. **4**), is still valid for cylinders of section other than circular, provided that $2a$ denotes the horizontal diameter in the surface (beam).

The inertia coefficient is of order 1 through the greater part of the range, except near $Ka = 0$, where it tends to infinity. On the other hand, the hydrostatic inertia coefficient tends to infinity even more rapidly, whence it may be concluded that in very slow heaving the deformation of the surface does not cause a significant change in the force on the cylinder. These results may be compared with the measurements made by Holstein (ref. **5**) on a cylinder of rectangular section. Holstein measured the amplitude of the waves for various mean depths of immersion of the lower edge. When the depth is equal to about half the beam the amplitude should be comparable to that due to a circular cylinder. It is found that theory and experiment are consistent in the range of measurement ($0{\cdot}5 < Ka/\pi < 0{\cdot}8$). Holstein's experiments on virtual mass (ref. **6**) are too rough for comparison with theory.

Note on the magnitude of $p_{2m}(Ka)$, $q_{2m}(Ka)$

It has been shown that the calculation of the wave-motion requires the expansion of a function $G(\theta)$, where

$$0 \leqslant \theta \leqslant \tfrac{1}{2}\pi, \qquad G(0) = G(\tfrac{1}{2}\pi) = 0,$$

in a series of non-orthogonal polynomials

$$f_{2m}(x;\theta) = -\left[\sin 2m\theta + \frac{x}{2m-1}\{\sin(2m-1)\theta - \sin\theta \sin\tfrac{1}{2}(2m-1)\pi\}\right] \quad (m = 1,2,3,\ldots),$$

where x is a numerical parameter which is usually less than 5.

Let the coefficients be denoted by $p_{2m}(x)$ so that

$$G(\theta) = \sum_{m=1}^{\infty} p_{2m}(x) f_{2m}(x;\theta).$$

This expansion must converge uniformly throughout the range $0 \leqslant \theta \leqslant \frac{1}{2}\pi$; it has been assumed in the text that functions $p_{2m}(x)$ exist such that

$$p_{2m}(x) = O(1/m^2) \text{ for fixed } x.$$

A proof that, in fact,

$$p_{2m}(x) = O(1/m^3) \tag{1}$$

will now be given when x is assumed small ($|x| < 1{\cdot}5$).

THEOREM. *Let $G(\theta)$ be defined in the range $0 \leqslant \theta \leqslant \frac{1}{2}\pi$ and let its second differential coefficient be of bounded variation. Then if $|x| < 1{\cdot}5$ there exists an expansion*

$$G(\theta) = \sum_{m=1}^{\infty} p_{2m}(x) f_{2m}(x;\theta), \tag{2}$$

where

$$|p_{2m}(x)| < \frac{A(x)}{(2m-1)^3}. \tag{3}$$

We first prove the following

LEMMA 1. (*Limiting case $x = 0$.*)

Consider the expansion of $G(\theta)$ in terms of the orthogonal polynomials

$$f_{2m}(0;\theta) = -\sin 2m\theta.$$

Then

$$|p_{2m}(0)| < \frac{A(0)}{(2m-1)^3}.$$

Proof. By Fourier's theorem,

$$p_{2m}(0) = -\frac{4}{\pi}\int_0^{\frac{1}{2}\pi} G(\theta)\sin 2m\theta\, d\theta$$

$$= \frac{1}{\pi m^2}\int_0^{\frac{1}{2}\pi} G''(\theta)\sin 2m\theta\, d\theta, \text{ by integration by parts.}$$

Since $G''(\theta)$ is of bounded variation, the last integral is of order $1/m$ (ref. **6**, § 9.41), whence the lemma follows.

Suppose now that each coefficient $p_{2m}(x)$ can be expanded in a power-series in x

$$p_{2m}(x) = \sum_{n=0}^{\infty} a_{2m}^{(n)} x^n \quad (m = 1, 2, 3,...). \tag{4}$$

Substitute in equation (2) and equate coefficients of x^n; then

$$\sum_{m=1}^{\infty} a_{2m}^{(0)} \sin 2m\theta = -G(\theta) \tag{5}$$

$$\sum_{m=1}^{\infty} a_{2m}^{(n)} \sin 2m\theta + \sum_{m=2}^{\infty} \frac{a_{2m}^{(n-1)}}{2m-1}\{\sin(2m-1)\theta - \sin\theta \sin \tfrac{1}{2}(2m-1)\pi\} = 0 \quad (n \geqslant 1). \tag{6}$$

Suppose further that the infinite series in equations (5) and (6) converge uniformly throughout the range. It is then permissible to multiply each equation by $\sin 2r\theta$ and to integrate term by term.

From equation (5),

$$\tfrac{1}{4}\pi a_{2r}^{(0)} = -\int_0^{\frac{1}{2}\pi} G(\theta) \sin 2r\theta \, d\theta. \tag{7}$$

From equation (6),

$$\tfrac{1}{4}\pi a_{2r}^{(n)} = \frac{2r}{4r^2-1} \sum_{m=2}^{\infty} \frac{a_{2m}^{(n-1)}}{2m-1} (-1)^{m+r} \frac{(2m-1)^2-1}{(2m-1)^2-(2r)^2}. \tag{8}$$

It must now be shown that equation (8) defines a double array $a_{2r}^{(n)}$; that the corresponding power-series defined by equation (4) are convergent for small x; that these power-series satisfy (3), and that

$$\sum_{m=1}^{\infty} f_{2m}(x;\theta) \sum_{n=0}^{\infty} a_{2m}^{(n)} x^n = G(\theta).$$

LEMMA 2. *To show that*

$$|a_{2r}^{(0)}| < \frac{A(0)}{(2r-1)^3}. \tag{9}$$

Proof. From equation (7) $a_{2r}^{(0)} = p_{2r}(0)$, so that the result follows from Lemma 1. It also follows that equation (5) holds.

LEMMA 3. *To show that*

$$|a_{2r}^{(n)}| < \frac{A_n}{(2r-1)^3}, \quad \text{where} \quad A_n = (\tfrac{2}{3})^n A(0). \tag{10}$$

Proof by induction on n

From Lemma 2, equation (10) holds when n is zero. Suppose that equation (10) holds for $n = 0, 1, 2,..., N-1$. From equation (8),

$$|\tfrac{1}{4}\pi a_{2r}^{(N)}| = \frac{2r}{4r^2-1}\left|\sum_{m=2}^{\infty}\frac{a_{2m}^{(N-1)}}{2m-1}(-1)^{m+r}\frac{(2m-1)^2-1}{(2m-1)^2-(2r)^2}\right|$$

$$< \frac{2r}{4r^2-1}\sum_{m=2}^{\infty}\frac{|a_{2m}^{(N-1)}|(2m-1)^2}{(2m-1)|(2m-1)^2-(2r)^2|}$$

$$< \frac{2rA_{N-1}}{4r^2-1}\sum_{m=2}^{\infty}\frac{1}{(2m-1)^2|(2m-1)^2-(2r)^2|}$$

$$= \frac{2rA_{N-1}}{4r^2-1}\left[\sum_{m=2}^{\infty}\frac{1}{(2m-1)^2\{(2r)^2-(2m-1)^2\}}+\right.$$

$$\left.+2\sum_{m=r+1}^{\infty}\frac{1}{(2m-1)^2\{(2m-1)^2-(2r)^2\}}\right].$$

Now

$$\sum_{m=2}^{\infty}\frac{1}{(2m-1)^2\{(2r)^2-(2m-1)^2\}}$$

$$< \frac{1}{4r^2}\left[\sum_{2}^{\infty}\frac{1}{(2m-1)^2}+\sum_{m=1}^{\infty}\frac{1}{(2r)^2-(2m-1)^2}\right]$$

$$< \frac{1}{4r^2}(\tfrac{1}{4}+0) = \frac{1}{16r^2}.$$

The second series may be written

$$\sum_{m=r+1}^{\infty}\frac{1}{(2m-1)^2\{(2m-1)^2-(2r)^2\}} = \frac{1}{(2r+1)^2(4r+1)}+\frac{1}{(2r+3)^2(12r+9)}+$$

$$+\frac{1}{(2r+5)^2(20r+25)}+\sum_{m=r+4}^{\infty}\frac{1}{(2m-1)^2\{(2m-1)^2-(2r)^2\}}.$$

Now

$$\frac{r^2}{(2r+1)^2(4r+1)} \leqslant \frac{1}{45} \qquad (r = 1, 2, 3,...),$$

$$\frac{r^2}{(2r+3)^2(12r+9)} < \frac{1}{400} \qquad (r = 1, 2, 3,...),$$

$$\frac{r^2}{(2r+5)^2(20r+5)} < \frac{1}{1000} \qquad (r = 1, 2, 3,...),$$

$$\sum_{m=r+4}^{\infty} \frac{1}{(2m-1)^2\{(2m-1)^2-(2r)^2\}} < \int_{r+3}^{\infty} \frac{du}{(2u-1)^3\{(2u-1)^2-(2r)^2\}}$$

$$< \frac{1}{2(20r+25)} \int_{r+3}^{\infty} \frac{du}{(2u-1)^3}$$

$$= \frac{1}{4(20r+25)(2r+5)} < \frac{1}{160r^2},$$

$$\sum_{m=r+1}^{\infty} \frac{1}{(2m-1)^2\{(2m-1)^2-(2r)^2\}} < \frac{1}{r^2}\left[\frac{1}{45}+\frac{1}{400}+\frac{1}{1000}+\frac{1}{160}\right] < \frac{1}{31r^2}.$$

Hence

$$|\tfrac{1}{4}\pi a_{2r}^{(N)}| < \frac{2rA_{N-1}}{(4r^2-1)r^2}\left(\frac{1}{16}+\frac{2}{31}\right),$$

$$|a_{2r}^{(N)}| < \frac{\frac{2}{3}A_{N-1}}{(2r-1)^3} = \frac{A_N}{(2r-1)^3}.$$

This proves Lemma 3.

It follows immediately that

$$\sum_{m=2}^{\infty} \frac{a_{2m}^{(n-1)}}{2m-1}\{\sin(2m-1)\theta-\sin\theta\sin\tfrac{1}{2}(2m-1)\pi\} \tag{11}$$

is uniformly convergent. Its associated Fourier sine series is

$$-\sum_{m=1}^{\infty} a_{2m}^{(n)} \sin 2m\theta \quad (n \geqslant 1),$$

where $a_{2m}^{(n)}$ is defined by (8). It follows from Lemma 3 that the last series converges throughout the range, and so its sum is equal to (11); that is, equation (6) holds.

It also follows from Lemma 3 that

$$p_{2m}(x) = \sum_{n=0}^{\infty} a_{2m}^{(n)} x^n$$

is defined for $|x| < 1{\cdot}5$; again

$$|p_{2m}(x)| < \frac{A(0)}{(2m-1)^3}[1+\tfrac{2}{3}|x|+(\tfrac{2}{3})^2|x|^2+\ldots]$$

$$= \frac{A(x)}{(2m-1)^3} \quad (|x| < 1{\cdot}5), \tag{12}$$

and since $|f_{2m}(x;\theta)| < 1+2|x|$, $\sum_{m=1}^{\infty} p_{2m}(x) f_{2m}(x;\theta)$ converges.

It only remains to be shown that

$$\sum_{m=1}^{\infty} p_{2m}(x) f_{2m}(x;\theta) = G(\theta).$$

LEMMA 4. *To show that*

$$\lim_{N\to\infty}\sum_{m=1}^{\infty} f_{2m}(x;\theta)\Big(\sum_{n=0}^{N} a_{2m}^{(n)}x^n\Big) = \sum_{m=1}^{\infty} p_{2m}(x)f_{2m}(x;\theta). \tag{13}$$

For
$$\Big|f_{2m}(x;\theta)\sum_{n=0}^{N} a_{2m}^{(n)}x^n\Big| < \frac{A(x)}{(2m-1)^3}(1+2|x|);$$

since $\sum_{m=1}^{\infty}\frac{A(x)(1+2|x|)}{(2m-1)^3}$ converges, the series converges uniformly with respect to N, by Weierstrass's M-test (ref. **2**, § 3.34); hence equation (13) holds.

Proof of the theorem. Consider the expression

$$\sum_{m=1}^{\infty} f_{2m}(x;\theta)\sum_{n=0}^{N} a_{2m}^{(n)}x^n.$$

From (5) and (6)

$$\sum_{m=1}^{\infty} f_{2m}(x;\theta)\Big(\sum_{n=0}^{N} a_{2m}^{(n)}x^n\Big) - G(\theta)$$

$$= -x^{N+1}\sum_{m=2}^{\infty}\frac{a_{2m}^{(N)}}{2m-1}\{\sin(2m-1)\theta - \sin\tfrac{1}{2}(2m-1)\pi\sin\theta\},$$

but

$$\Big|x^{N+1}\sum_{m=2}^{\infty} a_{2m}^{(N)}\{\sin(2m-1)\theta - \sin\tfrac{1}{2}(2m-1)\pi\sin\theta\}\Big|$$

$$< 2|x|^{N+1}(\tfrac{2}{3})^N A(0)\sum_{m=1}^{\infty}\frac{1}{(2m-1)^4} \quad \text{(from Lemma 3)},$$

which tends to zero, as N tends to infinity provided that $|x| < 1{\cdot}5$; so that

$$\lim_{N\to\infty}\sum_{m=1}^{\infty} f_{2m}(x;\theta)\sum_{n=0}^{N} a_{2m}^{(n)}x^n = G(\theta).$$

From Lemma 4, the left-hand side is $\sum_{m=1}^{\infty} p_{2m}(x)f_{2m}(x;\theta)$; also from (12),

$$|p_{2m}(x)| < \frac{A(x)}{(2m-1)^3},$$

which proves the theorem.

Note. The foregoing proof applies only when $|x| < 1{\cdot}5$, but it has been assumed that the theorem is valid in a larger range including $|x| < 1{\cdot}5$.

I am indebted to the Mathematics Division of the National Physical Laboratory for the computations in this paper, and to the Admiralty for permission to publish.

REFERENCES

1. H. Lamb, *Hydrodynamics*, 6th ed. (Cambridge, 1932).
2. E. T. Whittaker and G. N. Watson, *Modern Analysis*, 4th ed. (Cambridge, 1927).
3. T. H. Havelock, *Proc. Roy. Soc.* A **113** (1917), 522.
4. M. Schuler, *Z.A.M.M.* **16** (1936), 65.
5. H. Holstein, *Ingenieur-Archiv*, **8** (1937), 103.
6. ——, *Werft, Reederei, Hafen*, **23** (1936), 385.

THE BALLISTIC EFFECTS OF BORE RESISTANCE

By J. CORNER (*Armament Research Establishment, Fort Halstead, Sevenoaks*)

[Received 7 July 1948]

SUMMARY

Resistance to motion of a projectile down the bore of a gun alters the pressure and velocity attained, but is usually neglected in ballistic theory. It is shown that weighting factors can be calculated for each point in the shot travel, such that the effect of a bore resistance with any desired dependence on travel can be quickly found by integration of the product of weighting factor and resistance. The method fails if the resistance is sufficient to stop the shot for a time, and initial engraving resistance is therefore not a special case of this solution.

1. Introduction

THE classical central problem of internal ballistics is the calculation of the pressure, travel, and time relations in a gun, given the characteristics of the charge. The number of solutions advanced is already very large, and when assembled, as in the compendium of Cranz (**3**), they tend to produce the feeling that little remains to be done. This is not correct. The initial resistance to motion, due to the engraving resistance of the driving-band of the projectile, is commonly taken into account, often as a 'shot-start pressure'. On the other hand, it usually happens that resistance which occurs while the shot is moving down the bore is included, if at all, by assuming that this resistance depends on time in the same way as the accelerating pressure, so that the effect is exactly equivalent to an increase of shot mass. This is a very special form of resistance, a poor approximation to the types found in practice,† and while it does not enable the shape of the resistance–travel curve to be varied in studying a given firing, yet the form changes against one's wishes when the charge is altered. Among published work the only solutions of greater value are those of Proudman (**4**), Voituriez (**6**), and Clemmow (**2**). The two former writers assumed a constant resistance, which is a special form but has the virtue that it does not change its shape with the ballistic parameters in the solution, and is often approached in practice. These authors found the essential parameters which specify the solution, though they did not give any explicit results, which would apparently have to be found by numerical integration. Clemmow studied the effect of bore resistance with the approximations of a covolume equal to the volume of the solid propellant, and γ, the ratio of specific heats of the propelling gas, equal to unity until the charge

† Except that it is often a fairly good approximation in small-arms firing jacketed shot.

is completely burnt (the 'isothermal approximation'). Clemmow found the most general law of resistance which allowed a solution in finite terms; he studied also the case of a constant resistance, finding a form for the solution which reduced the labour of computation of any particular example, and an approximation for small resistance. The Clemmow resistance law covers a fairly wide range of types of behaviour and shows in an elegant way the nature of the effects produced by such kinds of resistance. This solution is, however, not easily applied in practice when one is given the details of the gun and an actual resistance–travel curve; the determination of a Clemmow curve is laborious and it is not always possible to come reasonably close to the assigned resistance law. There is, of course, also the restriction that $\gamma = 1$, which has been superseded in most modern ballistic systems.

In the unpublished literature ballistic results taking bore resistance into account have been computed by numerical integration for a number of special forms of resistance. For resistance depending on travel in any other way it would be necessary to repeat the entire computation.

Thus there has been no simple rapid way to find the effect of a bore resistance depending in any desired manner on the travel of the projectile. Such a method is given in the present paper. As an introduction it may be helpful to state, in a general way, the experimental results which led to this work and some of the technical problems to which it can be applied.

Evidence for a resistance persisting for a substantial part of the travel of the shot has accumulated from many directions; much of this evidence is only qualitative, though its bulk and its general consistency are impressive. It is found that the fitting of theoretical ballistics to observed results often leaves a discrepancy which could be attributed to a mean resistance equivalent to a pressure of order 1 ton/sq. in. It is true that in many cases one might reduce the discrepancy by altering the details of the theory or by postulating small errors in some of the data assumed; however, such *ad hoc* manipulations are, in bulk, less plausible than the idea of a bore resistance. From the experimental side, the strains recorded in the barrel are sufficient to indicate an appreciable axial resistance even when the coefficient of friction has fallen as low as 0·01. A resistance is also usually indicated when attempts are made to correlate measured space–time curves with pressure–time curves recorded at gauges spaced along the barrel. Considerable progress was made in this field during the war, though the only published work is that of Rossmann (**5**). Pre-war work was summarized by Bodlien (**1**), and was mostly on small-arms. Here the whole body of the projectile is engraved, being kept pressed against the rifling by the deformation under the high acceleration in the gun; a substantial

resistance to motion is therefore to be expected in small-arms. Unfortunately the time-scale of the phenomena is shortest in these guns, and it has not been until recent years that the natural frequency of the recording system has been raised sufficiently to give significant results for the resistance.

It can be taken, then, that in many cases a resistance does persist over much of the travel of a projectile, and it is desirable to investigate its ballistic consequences. It is clear, too, that knowledge of the resistance is not yet in a final form, and that, therefore, it is better not to restrict attention to any particular form for the dependence on travel. For many purposes it is sufficient to be able to 'touch-up' some ballistic solution (which neglects bore resistance) by adding a correction to be computed for the particular resistance in use.

In this paper a method is given by which the changes in muzzle velocity, peak pressure, and position of 'burnt' can be computed quickly for a bore resistance of any desired form, provided only that the resistance is nowhere sufficient to halt the shot for a time. The change in the complete pressure-space curve, which is of interest in gun design, could be found from the same formulae, but it is quicker to make an accurate numerical integration after the desired peak pressure or muzzle velocity has been obtained by using the results of this paper. The condition that the velocity of the shot must not fall to zero during the application prevents initial resistance to motion being included as a special case of our bore resistance.

The line of approach is the choice of a standard form of resistance, the determination of its ballistic effects, and the construction of more realistic resistance laws by superposition of standard forms suitably spaced along the travel. Analogous methods are common in applied mathematics. In external ballistics, for example, the change in range due to perturbations such as head wind, which occur with varying strength at different heights, are obtained by integration over the actual distribution of wind, weighted by a factor which represents the effect of unit wind concentrated along unit length of the trajectory. This 'weighting factor' for the effect of head wind on range is a function of position along the trajectory, and is one of a series of analogous weighting factors which are computed from a set of equations adjoint to the primary ballistic equations.

A similar practice is found in operational methods for sets of linear differential equations. The behaviour of the system is investigated for a standard impressed force, the Heaviside unit function. The response to a force varying in any way with time is obtained by splitting this force into a sum or integral of unit functions suitably spaced in time. The response to the complex force is, by the linearity of the system, equal to

the sum of the responses to the individual unit functions. Since the equations of internal ballistics are not linear, it cannot be taken for granted that the ballistic effects of a set of 'unit bore resistances' can be superposed; that the error is small has to be verified. There is one similarity between the Heaviside unit function and the unit bore resistance which will be chosen in this paper: the usefulness of the former is in no way impaired by its artificial character (for it is an idealization which can be approached but not attained in practice); likewise it is possible to use a standard bore resistance which is an idealized form, so long as by superposition one can construct any bore resistance likely in practice.

The method given in this paper has been applied to some technical problems and abnormal behaviour of guns, thought to be due to bore resistance. One may mention certain effects produced by chromium plating of machine-gun barrels, or by using tapered bores, the effect of grease in a gun on the ballistics of the first round of a series, and the variations of muzzle velocity during repeated firing.

It is to be expected that when the bore resistance is better understood it will be found desirable to choose simple forms and to compute ballistic tables with such resistances taken into account in an accurate way. This would be a task of some magnitude, particularly if a wide variety of shapes had been found to be necessary, and though the results of the present paper form only an interim stage, it is possible that for a long time this may be all that is justified by our knowledge of bore resistance.

2. Equations of unresisted motion

Let A be the area of cross-section of the bore. The standard bore resistance will be taken as a constant, AP_0, over a short travel Δx near the point x_0, and zero at all other shot positions. The effect on the ballistics can be calculated, to the first order in $P_0\Delta x$, by subtracting an energy $AP_0\Delta x$ from the kinetic energy of the projectile as it passes through the point x_0. The ballistic equations from the point x_0 onwards are exactly the same as before except for a perturbing term linear in $P_0\Delta x$. If the ballistic system is a simple one this perturbation can be integrated exactly. If not, numerical integration would be necessary, in which case it would probably be quicker to abandon weighting factors altogether.

One is thus led to consider the choice of a suitable ballistic system to which to apply this method. As has just been seen, it must give an analytical solution, the simpler the better. A second point can be revealed by letting the resistance of length Δx occur at shot-start. Then, if P_0 is finite, there is a finite change of muzzle velocity even if Δx tends to zero. The weighting factor which multiplies $P_0\,\Delta x$ must therefore tend to infinity

as x_0 moves towards shot-start. Hence the weighting-factor method fails to represent initial resistance at all, and must become increasingly inaccurate as the position of the resistance approaches shot-start. It is therefore immaterial whether the basic system, before the addition of bore-resistance terms, be a good or bad representation of initial resistance.

In this paper there is used a simple ballistic system, well known in the open literature. It is assumed that η, the covolume of the propellant gas, and δ, the density of the solid propellant, are related by $\eta = 1/\delta$. This 'neglect of covolume terms' simplifies the equations considerably, but at the same time it is possible to make partial correction for the error by changing the 'force' of the propellant.

Conventional assumptions are made about the Lagrange pressure-gradient in the propellant gas.

The burning law assumed is

$$\phi = (1-f)(1+\theta f), \tag{1}$$

$$D\frac{df}{dt} = -\beta P, \tag{2}$$

where ϕ is the fraction of the charge burnt up to time t, D is a length characteristic of the effective size of the propellant grains, β and θ are parameters, constant during any one firing, and P is the pressure at the breech. The variable f could be eliminated from (1) and (2), and, indeed, this is often done in continental treatments of internal ballistics; f is, however, a useful auxiliary variable in the process of solution. From (1), it follows that $f = 1$ at the start of the firing, where $\phi = 0$.

An unsophisticated interpretation of (1) and (2) is that $\frac{1}{2}\beta P$ is the rate of recession of a cordite surface at pressure P, and that the grains are long compared with their cross-section, which is a simple shape with fD as the least distance between exposed surfaces; θ is then obtainable from the geometry of the grains. For example, long cords would have $\theta = 1$, D as the initial diameter, and fD as the remaining diameter at time t. Long tubes would have $\theta = 0$, D as the initial annulus, and fD as the remaining annulus. In practice there are many factors which alter the interpretation of (1) and (2) while not removing their empirical value. The rate of burning of a cordite surface often increases less slowly than P and is also influenced by transverse gas velocities, which may be important in shapes with perforations. Initial resistance to motion is often counterfeited by increasing β. The heterogeneity of any practical charge increases θ, as also does non-uniformity of any kind within the single grain.† Short chopped grains

† For the effect of an eccentric perforation in tubular propellant, cf. Kleider, *Zeit. ges. Schiess- und Sprengstoffwesen*, **38** (1943), 131.

or cubical or spherical grains do not satisfy (1) exactly, even on the geometrical interpretation, but these propellant shapes are of little importance. It remains true that (1) and (2) lead to simple formulae and most of the difficulties can be circumvented, at least to practical accuracy, by suitable choice of β and θ.

Let $V(t)$ be the velocity of the shot, x its travel, U the chamber capacity, A the bore area, C and W the weights of charge and shot, RT_0 the 'force' of the propellant, γ its ratio of specific heats, suitably increased to allow for heat loss, and let $T_0\,T'(t)$ be the gas temperature, averaged throughout the volume behind the shot at time t. A correction for the rotational inertia of the projectile can, if desired, be included in W. The temperature of the propellant gases when formed without performance of external work is T_0, and R has the meaning conventional in ballistics, namely, (gas constant per mole)/(mean molecular weight of the propellant gases).

The equations of unresisted motion are

$$\phi = (1-f)(1+\theta f), \tag{1}$$

$$D\frac{df}{dt} = -\beta P, \tag{2}$$

$$(W+\tfrac{1}{2}C)\frac{dV}{dt} = AP, \tag{3}$$

$$AP(x+l) = CRT_0\phi T'(1+\tfrac{1}{2}C/W)/(1+\tfrac{1}{3}C/W), \tag{4}$$

$$\phi(1-T') = (\gamma-1)(W+\tfrac{1}{3}C)V^2/2CRT_0, \tag{5}$$

where the length l is defined by

$$Al = U-C/\delta. \tag{6}$$

These equations are orthodox and do not need any commentary.

3. Solution with standard bore-resistance

For the standard bore-resistance one may take a thrust AP_0 acting through a small distance Δx at a point x_0, where $f=f_0$, $V=V_0$, and so on.† The factor A is included for ease of visualization of the resistance as an effective pressure. It is supposed, to begin with, that Δx is infinitesimal and $P_0\,\Delta x$ finite.

This bore resistance acts for a time $\Delta x/V_0$, which is assumed to be infinitesimal. The only immediate result is therefore a decrease of the kinetic energy of the shot by $AP_0\,\Delta x$. Take first the case where the resistance occurs before 'burnt'. For travel less than x_0, the solution is the normal solution of equations (1)–(5). For travel greater than x_0 only the energy equation (5) needs alteration, though there has also been an instantaneous drop in the velocity V.

† No confusion need be feared with the 'force' RT_0.

One should note two limitations of this method. Firstly, if V_0 is zero $\Delta x/V_0$ is not infinitesimal; hence initial resistance cannot be represented by this model. Secondly, if the kinetic energy of the shot when it meets the resistance is less than $AP_0\Delta x$ the method breaks down, for it gives the projectile an imaginary velocity after crossing the resistance. In practice the projectile would come to rest and would restart after the pressure had built up behind the shot, that is, after a finite time. This is again a matter of $\Delta x/V_0$ not being infinitesimal.

Just before meeting the resistance the kinetic energy of the charge and projectile is $\frac{1}{2}(W+\frac{1}{3}C)V^2$; immediately afterwards the kinetic energy is $\frac{1}{2}(W+\frac{1}{3}C)V^2-AP_0\Delta x$. The instantaneous drop of velocity of the projectile is transmitted through the gas with a finite velocity, namely a_0, the velocity of sound in the propellant gases, and the time taken for the waves to settle down is of order $2(U+Ax_0)/Aa_0$, which is comparable with the time taken for the shot to reach the muzzle. The problem of the pressure-distribution in the column of propellant gas is therefore more difficult than in a conventional solution. If the velocity of the projectile immediately after the resistance is written as V_1, then it is assumed here that the kinetic energy of the system at that moment is $\frac{1}{2}(W+\frac{1}{3}C)V_1^2$. In reality it should be $\frac{1}{2}WV_1^2+\frac{1}{6}Cv^2$, where $v(t)$ drops from V_0 towards the $V(t)$ curve. The approximation here adopted replaces this gradual approach by an immediate transition of v from V_0 to V_1. The extent of the error which could arise is small except for guns with C of order W, and velocities therefore around 4,000 ft./sec., but then the conventional Lagrange corrections also fail for such guns.

With this approximation, then

$$(W+\tfrac{1}{3}C)V_1^2 = (W+\tfrac{1}{3}C)V_0^2-2AP_0\Delta x. \tag{7}$$

Equations (1)–(4) remain true after the resistance, and (5) is replaced by

$$2CRT_0\phi(1-T') = (\gamma-1)[(W+\tfrac{1}{3}C)V^2+2AP_0\Delta x]. \tag{8}$$

From (3),
$$V = V_1+AD(f_0-f)/\beta(W+\tfrac{1}{2}C), \tag{9}$$

so that (8) becomes

$$2CRT_0\phi(1-T') = (\gamma-1)(W+\tfrac{1}{3}C)[V_0^2+\{AD(f_0-f)/\beta(W+\tfrac{1}{2}C)\}^2+ \\ +2ADV_1(f_0-f)/\beta(W+\tfrac{1}{2}C)]. \tag{10}$$

Combining (4) and (10),

$$2CRT_0\phi = (\gamma-1)(W+\tfrac{1}{3}C)[V_0^2+\{AD(f_0-f)/\beta(W+\tfrac{1}{2}C)\}^2+ \\ +2ADV_1(f_0-f)/\beta(W+\tfrac{1}{2}C)]+2AP(x+l)(W+\tfrac{1}{3}C)/(W+\tfrac{1}{2}C), \tag{11}$$

which may be written as

$$CRT_0\phi = (\gamma-1)(W+\tfrac{1}{3}C)A^2D^2\frac{(1-f)^2-2(1-V_1/V_0)(1-f_0)(f_0-f)}{2\beta^2(W+\frac{1}{2}C)^2}+$$
$$+AP(x+l)(W+\tfrac{1}{3}C)/(W+\tfrac{1}{2}C).$$

Up to this point the equations have been exact. Now, keeping only first-order terms in (7), (9), and (11):

$$V_1 = V_0-AP_0\Delta x/(W+\tfrac{1}{3}C)V_0, \tag{7a}$$

$$V = AD(1-f)/\beta(W+\tfrac{1}{2}C)-AP_0\Delta x/(W+\tfrac{1}{3}C)V_0, \tag{9a}$$

$$2CRT_0\phi = (\gamma-1)(W+\tfrac{1}{3}C)[\{AD(1-f)/\beta(W+\tfrac{1}{2}C)\}^2-$$
$$-2AP_0\Delta x(f_0-f)/(1-f_0)(W+\tfrac{1}{3}C)]+2AP(x+l)(W+\tfrac{1}{3}C)/(W+\tfrac{1}{2}C). \tag{11a}$$

It is convenient to introduce the 'central ballistic parameter'

$$M = A^2D^2(W+\tfrac{1}{3}C)/\beta^2CRT_0(W+\tfrac{1}{2}C)^2 \tag{12}$$

so that (11 a) can be written as

$$(1-f)(1+\theta f) = (\gamma-1)M(1-f)^2/2-(\gamma-1)AP_0\Delta x(f_0-f)/(1-f_0)CRT_0+$$
$$+(x+l)\frac{df}{dx}[AP_0\Delta x/(1-f_0)CRT_0-M(1-f)],$$

leading to

$$Z+M(x+l)\frac{df}{dx} = AP_0\Delta x\left[(x+l)\frac{df}{dx}-(\gamma-1)(f_0-f)\right]\bigg/(1-f)(1-f_0)CRT_0, \tag{13}$$

where
$$Z = 1-\tfrac{1}{2}(\gamma-1)M+\theta_1 f \tag{14}$$
and
$$\theta_1 = \theta+\tfrac{1}{2}(\gamma-1)M. \tag{15}$$

Equation (13) shows the first-order effects of the resistance on the equation of unresisted motion

$$Z+M(x+l)\frac{df}{dx} = 0, \tag{16}$$

and one can obtain a solution correct to terms of order $P_0\Delta x$ by using (16) on the right of (13). This gives

$$Z+M(x+l)\frac{df}{dx} = -AP_0\Delta x[Z/M+(\gamma-1)(f_0-f)]/(1-f)(1-f_0)CRT_0,$$

and so

$$\int\frac{dx}{(x+l)} = -M\int\frac{df}{Z}+\frac{AP_0\Delta x}{CRT_0(1-f_0)}\left[\int\frac{df}{Z(1-f)}+(\gamma-1)M\int\frac{(f_0-f)\,df}{Z^2(1-f)}\right]. \tag{17}$$

The lower limit in these integrals corresponds to the point, suffix zero, at which the resistance occurred. The integrals are easily evaluated:

$$\theta_1 \int\limits_0 df/Z = \ln(Z/Z_0), \qquad \theta_1 \int\limits_0 df/Z^2 = 1/Z_0 - 1/Z,$$

$$(1+\theta) \int\limits_0 df/Z(1-f) = \ln\{Z(1-f_0)/Z_0(1-f)\},$$

$$(1+\theta)^2 \int\limits_0 df/Z^2(1-f) = \ln\{Z(1-f_0)/Z_0(1-f)\} + (1+\theta)\{1/Z_0 - 1/Z\}.$$

Substitution in (17) gives

$$\ln(1+x/l) = \frac{M}{\theta_1}\ln\{(1+\theta)/Z\} +$$
$$+ \frac{AP_0\,\Delta x}{CRT_0(1-f_0)}\left[\frac{\{1+\theta-(\gamma-1)M(1-f_0)\}}{(1+\theta)^2}\ln\left\{\frac{Z(1-f_0)}{Z_0(1-f)}\right\} +\right.$$
$$\left. +(\gamma-1)M\{1+\theta-\theta_1(1-f_0)\}\{1/Z_0-1/Z\}/\theta_1(1+\theta)\right]. \tag{18}$$

Solution with 'unburnt' at 'muzzle'. In this case the value of f at the muzzle is computed from (18) and the muzzle velocity follows by (7) and (9). This case is not of practical importance and one need not test the accuracy of superposition and higher-order terms, which may be expected to be of the same order as when 'all-burnt' occurs inside the gun.

Solution for 'all-burnt' inside gun. This is the important problem. It will be remembered that one is dealing here with a resistance during the burning period. Resistance during the adiabatic expansion will be discussed later.

One needs the change in $\ln(x_B+l)$, where suffix B refers to conditions at 'all-burnt'. This change is

$$\Delta\ln(x_B+l) = \frac{AP_0\,\Delta x}{CRT_0(1-f_0)}\left[\frac{\{1+\theta-(\gamma-1)M(1-f_0)\}}{(1+\theta)^2}\ln\{Z_B(1-f_0)/Z_0\} +\right.$$
$$\left. +(\gamma-1)M\{1+\theta-\theta_1(1-f_0)\}\{1/Z_0-1/Z_B\}/\theta_1(1+\theta)\right]. \tag{19}$$

Let suffix E refer to values at shot-ejection. Then integration along the adiabatic from 'all-burnt' to the ejection of the shot gives

$$V_E^2 = V_B^2 + AP_B(x_B+l)\Phi/(W+\tfrac{1}{2}C), \tag{20}$$

where
$$\Phi = 2\{1-r^{1-\gamma}\}/(\gamma-1) \tag{21}$$

and
$$r = (x_E+l)/(x_B+l). \tag{22}$$

In (20), V_B, $P_B(x_B+l)$, and Φ are all altered by the resistance.

From (11*a*),

$$AP_B(x_B+l)/(W+\tfrac{1}{2}C) = CRT_0\{1-\tfrac{1}{2}(\gamma-1)M\}/(W+\tfrac{1}{3}C) +$$
$$+(\gamma-1)AP_0\,\Delta x f_0/(1-f_0)(W+\tfrac{1}{3}C). \tag{23}$$

Also $$\Delta\Phi = 2r^{-\gamma}\Delta r = -2r^{1-\gamma}\Delta\ln(x_B+l), \tag{24}$$

and from (9 *a*) $$\Delta(V_B^2) = -2AP_0\Delta x/(1-f_0)(W+\tfrac{1}{3}C), \tag{25}$$

so that

$$\Delta(V_E^2) = -2AP_0\Delta x\{1-f_0+f_0r^{1-\gamma}\}/(1-f_0)(W+\tfrac{1}{3}C)-$$
$$-\frac{2r^{1-\gamma}\{1-\frac{1}{2}(\gamma-1)M\}AP_0\Delta x}{(W+\frac{1}{3}C)(1-f_0)}\left[\frac{\{1+\theta-(\gamma-1)M(1-f_0)\}}{(1+\theta)^2}\ln\{Z_B(1-f_0)/Z_0\}+\right.$$
$$\left.+(\gamma-1)M\{1+\theta-\theta_1(1-f_0)\}(1/Z_0-1/Z_B)/\theta_1(1+\theta)\right],$$

and finally

$$(W+\tfrac{1}{3}C)V_E(1-f_0)\Delta V_E/AP_0\Delta x$$
$$= -1+f_0-f_0r^{1-\gamma}-r^{1-\gamma}Z_B\left[\frac{\{1+\theta-(\gamma-1)M(1-f_0)\}}{(1+\theta)^2}\ln\{Z_B(1-f_0)/Z_0\}+\right.$$
$$\left.+(\gamma-1)M\{1+\theta-\theta_1(1-f_0)\}(1/Z_0-1/Z_B)/\theta_1(1+\theta)\right]. \tag{26}$$

This gives the change of muzzle velocity ΔV_E, due to a bore-resistance $AP_0\Delta x$ occurring at the point (f_0, Z_0), in terms of the characteristics of the solution without resistance.

For resistance very early in the travel, f_0 is nearly unity, and

$$(W+\tfrac{1}{3}C)V_E\Delta V_E/AP_0\Delta x \sim \frac{r^{1-\gamma}Z_B}{(1+\theta)(1-f_0)}\ln\left\{\frac{(1+\theta)}{Z_B(1-f_0)}\right\},$$

showing that for resistance occurring sufficiently early in the travel the muzzle velocity rises. For resistance at 'burnt', $f_0 = 0$ and

$$(W+\tfrac{1}{3}C)V_E\Delta V_E/AP_0\Delta x = -1,$$

and the muzzle velocity falls. When resistance occurs during the adiabatic expansion the kinetic energy of the shot and gases at the muzzle are reduced by the work done on the resistance, without other effect on the ballistics (except on the time to traverse the bore). Hence

$$(W+\tfrac{1}{3}C)V_E\Delta V_E/AP_0\Delta x = -1$$

if the resistance occurs after 'all-burnt'.

4. Accuracy of first-order theory

The results of the preceding section were obtained by expansion in powers of $AP_0\Delta x$, keeping only the first term. To find the importance of higher-order terms it is easiest to take a specific example. A heavy A.A. gun was considered, and a charge of 8 lb. 5 oz. of cordite, giving 20 tons/sq. in. peak pressure, was assumed. With $\theta = 0{\cdot}3$, $\gamma = 1{\cdot}34$, and no covolume term, the velocity from the basic method is 2,642 ft./sec. Peak pressure occurs at a travel of about 4 calibres and 'burnt' about 10 calibres farther on. A series of exact solutions, with exact allowance for the

assumed resistance, was computed on a National accounting machine. To get sufficient accuracy in the differences ΔV_E, these solutions were computed to an accuracy of 0·1 ft./sec.

Table 1 shows the effect of increasing $P_0\Delta x$ at a given point early in the travel. At this point, where $x_0 = 0{\cdot}58$ calibres, the shot would be brought to rest by an instantaneous $P_0\Delta x$ of 7·99 ton/in., so that one would not expect this theory to be more than extremely rough at such values of $P_0\Delta x$. The agreement shown in Table 1 is therefore very satisfying. The deviation of $\Delta V_E/P_0\Delta x$ from first-order theory is only 7 per cent. when $P_0\Delta x$ reaches half the value needed to stop the shot.

TABLE 1

$P_0\Delta x/7{\cdot}99$	$\dfrac{(W+\frac{1}{3}C)(1-f_0)V_E\Delta V_E}{AP_0\Delta x}$	*Method*
0	0·624	First-order theory
0·25	0·65½	Exact integration
0·5	0·67	,, ,,
1	0·85	,, ,,

Accuracy of first-order theory at 0·58 calibres travel ($f_0 = 0{\cdot}9$). $P_0\Delta x = 7{\cdot}99$ *ton/in. stops the shot.*

Another way to show the agreement is to calculate the effect of $P_0\Delta x = 7{\cdot}99$ ton/in. at various positions along the bore. Table 2 shows the comparison to be extremely satisfactory except when the resistance stops the shot.

TABLE 2

f_0	$(W+\frac{1}{3}C)(1-f_0)V_E\Delta V_E/AP_0\Delta x$		*Error*
	Exact integration	*First-order theory*	
0·9	0·85	0·624	0·23
0·8	0·25	0·231	0·02
0·7	−0·02	−0·026	0·01
0·6	−0·22	−0·226	0·01
0·4	−0·53	−0·540	0·01
0·2	−0·78	−0·789	0·01
0	−1	−1	0

Standard bore resistance, $P_0\Delta x = 7{\cdot}99$ *ton/in. at various positions along the bore.*

One may conclude that first-order theory is adequate to represent the effect of a *concentrated* bore resistance except when this is sufficient to halt the projectile.

5. Calculation of the effect of long stretches of bore resistance

One often wishes to find the effect of bore resistance extending over a large part of the travel. Such a resistance, no matter how it varies, can

be represented as an integral over suitably chosen resistances of our standard type. To see the errors likely in this process it is sufficient to consider the special case of constant resistance, and since the exact solution is known from 'all-burnt' to 'muzzle', one need consider only the part up to 'all-burnt'. The weighting-factor theory makes

$$\begin{aligned}\Delta V_E &= \int \frac{\Delta V_E}{\Delta x}\frac{dx}{df}\,df \\ &= -\int \frac{\Delta V_E}{\Delta x}\frac{M(x+l)}{Z}\,df \\ &= -\frac{MA}{V_E(W+\frac{1}{3}C)}\int \frac{(x+l)P_0}{(1-f)Z}\left[\frac{(1-f)V_E\,\Delta V_E(W+\frac{1}{3}C)}{AP_0\,\Delta X}\right]df. \qquad (27)\end{aligned}$$

This integral is easily evaluated. P_0 is a known function of x, which is itself a simple function of f. So is Z, and the 'weighting-factor' in brackets comes from (26). Thus (27) is easily computed by a numerical integration, whatever the variation of the bore resistance.

The examples solved exactly on a National accounting machine had a constant resistance equivalent to $P_0 = 1$ ton/sq. in. of bore area, extending from 'burnt' to $f_0 = 0{\cdot}5$, $0{\cdot}7$, and $0{\cdot}9$. Table 3 shows that the agreement with (27) is very satisfactory.

TABLE 3

Position in bore	Position in unperturbed solution	ΔV_E (ft./sec.) Exact	ΔV_E (ft./sec.) (27)	Error
$x = 0{\cdot}58$ to $13{\cdot}43$ calibres	$f_0 = 0{\cdot}9$ to 0	$-23{\cdot}3$	$-23{\cdot}5$	$0{\cdot}2$
$2{\cdot}02$ to $13{\cdot}43$,,	$0{\cdot}7$ to 0	$-29{\cdot}8$	$-30{\cdot}7$	$0{\cdot}9$
$4{\cdot}96$ to $13{\cdot}43$,,	$0{\cdot}5$ to 0	$-26{\cdot}9$	$-27{\cdot}5$	$0{\cdot}6$

The effect of a constant bore resistance for a considerable part of the travel. $P_0 = 1$ *ton/sq. in.*

Another simple test is the effect of $P_0 = 1$ ton/sq. in. from $0{\cdot}58$ calibres travel to the muzzle. This is $-115{\cdot}9$ ft./sec. by exact calculation, and $-116{\cdot}1$ ft./sec. by using (27) up to 'burnt' and thereafter the exact solution

$$(W+\tfrac{1}{3}C)\Delta(V_E^2) = -2AP_0(x_E-x_B). \qquad (28)$$

6. The effect of bore resistance on peak pressure

This can be treated by a weighting factor in the same way as muzzle velocity. The peak pressure is, however, much the less important of the two, being needed only if one is 'touching-up' a ballistic system which omits bore resistance. Furthermore, the peak pressure is affected only by resistance in the first few calibres of travel.

From (11*a*) and (18),

$$\ln P = \ln[CRT_0(W+\tfrac{1}{2}C)(1-f)/(U-C/\delta)(W+\tfrac{1}{3}C)] - \frac{M}{\theta_1}\ln(1+\theta) +$$
$$+(1+M/\theta_1)\ln Z +$$
$$+\frac{AP_0\,\Delta x}{CRT_0(1-f_0)}\Big[(\gamma-1)\frac{(f_0-f)}{(1-f)Z} + \frac{1+\theta-(\gamma-1)M(1-f_0)}{(1+\theta)^2}\ln\Big\{\frac{Z_0(1-f)}{Z(1-f_0)}\Big\} -$$
$$-(\gamma-1)M\{1+\theta-\theta_1(1-f_0)\}(1/Z_0-1/Z)/\theta_1(1+\theta)\Big]. \tag{29}$$

The maximum pressure P_m occurs when

$$\frac{dP}{df} = 0,$$

and the solution is

$$f = \frac{\gamma M+\theta-1}{\gamma M+2\theta} + \text{a term proportional to } AP_0\,\Delta x/CRT_0(1-f_0).$$

The change in $\ln P_m$ is obtained, to the first order in $AP_0\,\Delta x/CRT_0(1-f_0)$, by writing $f = (\gamma M+\theta-1)/(\gamma M+2\theta)$ throughout (29). Hence

$$CRT_0(1-f_0)\Delta P_m/P_m\,AP_0\,\Delta x$$
$$= (\gamma-1)(\gamma M+2\theta)\{(\gamma M+2\theta)f_0+1-\theta-\gamma M\}/(1+\theta)^2\{\theta+\tfrac{1}{2}(\gamma+1)M\}+$$
$$+\frac{\{1+\theta-(\gamma-1)M(1-f_0)\}}{(1+\theta)^2}\ln[Z_0/(1-f_0)\{\theta+\tfrac{1}{2}(\gamma+1)M\}]+$$
$$+(\gamma-1)M\{1+\theta-\theta_1(1-f_0)\}\times$$
$$\times[\gamma M+2\theta-(1+\theta)\{\theta+\tfrac{1}{2}(\gamma+1)M\}Z_0]/\theta_1(1+\theta)^2\{\theta+\tfrac{1}{2}(\gamma+1)M\}. \tag{30}$$

This holds if $f_0 \geqslant (\gamma M+\theta-1)/(\gamma M+2\theta) \geqslant 0$. If

$$f_0 < (\gamma M+\theta-1)/(\gamma M+2\theta) \geqslant 0,$$

then there is no change in the maximum pressure. The only other possible case is

$$f_0 \geqslant 0 > (\gamma M+\theta-1)/(\gamma M+2\theta)$$

in which the peak pressure always occurs at 'burnt'. The change in peak pressure is obtained from (29) by writing $f = 0$, giving

$$CRT_0(1-f_0)\Delta P_m/P_m\,AP_0\,\Delta x$$
$$= (\gamma-1)f_0/\{1-\tfrac{1}{2}(\gamma-1)M\}+$$
$$+\{1+\theta-(\gamma-1)M(1-f_0)\}(1+\theta)^{-2}\ln\Big[\frac{Z_0}{(1-f_0)\{1-\tfrac{1}{2}(\gamma-1)M\}}\Big]+$$
$$+(\gamma-1)M\{1+\theta-\theta_1(1-f_0)\}[\{1-\tfrac{1}{2}(\gamma-1)M\}^{-1}-Z_0^{-1}]/\theta_1(1+\theta). \tag{31}$$

It is sufficient to test this against exact solutions for concentrated

resistances. The agreement is shown in Tables 4 and 5, and is as good as the corresponding results for the muzzle velocity (Tables 1 and 2). One need not test the accuracy of superposition, which will obviously run parallel to the accuracy obtained for the velocity.

TABLE 4

$P_0 \Delta x/7\cdot99$	$\dfrac{CRT_0(1-f_0)\Delta P_m}{P_m A P_0 \Delta x}$	*Method*
0	1·89	First-order theory
0·25	1·93	Exact integration
0·5	2·18	,, ,,
1	3·85	,, ,,

Accuracy of first-order theory at 0·58 *calibres travel.*
$f_0 = 0\cdot9$; $P_0\,\Delta x = 7\cdot99$ *ton/in. stops the shot.*

TABLE 5

f_0	ΔP_m, *exact integration*	*First-order theory*	*Error*
0·9	4·78	2·35	2·43
0·8	0·79	0·76	0·03
0·7	0·31	0·33	−0·02
0·6	0·11	0·14	−0·03

Standard bore resistance, $P_0\,\Delta x = 7\cdot99$ *ton/in., at various positions along the bore.*

I am indebted to the Chief Scientist, Ministry of Supply, for permission to publish this paper, to Professor N. F. Mott, F.R.S., for his encouragement of the work, and to Mr. Tadman for arranging the solution of test examples on a National machine.

REFERENCES

1. K. H. BODLIEN, *Zeit. ges. Schiess- und Sprengstoffwesen*, **34** (1939), 33, 65, 97.
2. C. A. CLEMMOW, *Phil. Trans. Roy. Soc.* **231** A (1933), 263.
3. C. CRANZ, *Innere Ballistik* (Berlin, 1926).
4. J. PROUDMAN, *Proc. Roy. Soc.* A **100** (1921), 289.
5. T. ROSSMANN, *Jahrb. der Deut. Akad. d. L.F.F.* (1940).
6. M. VOITURIEZ, *Mém. Artill. Franç.* **4** (1925), 131.

FLOW PATTERNS AND THE METHOD OF CHARACTERISTICS NEAR A SONIC LINE

By M. HOLT

(*Department of Mathematics, The University, Manchester*)

[Received 11 May 1948]

SUMMARY

The work described has two aims: (i) to investigate the geometry of the flow pattern near a sonic line, and (ii) to develop a method for the numerical integration of the equations of motion near a sonic line, where the usual method based on characteristics (ref. **1**) breaks down. Only isentropic irrotational steady flow with two independent variables is considered, and attention is mainly confined to plane flow.

(i) The directions of the Mach lines coincide at a sonic line, and, in general, their curvatures are infinite; the Mach lines are approximately semi-cubical parabolas (eqn. (21)), the isoclines approximately parabolas (eqn. (15)), and the equipotential lines approximately cubical parabolas (eqn. (14)). The state of affairs is different if the curvature of the streamline vanishes on the sonic line; the curvatures of the Mach lines at the sonic point are then discontinuous but bounded; other results for this special case are set out in § 6.

(ii) Two methods are described for extending computations near a sonic line. In one method double Taylor series for the velocity components are used; in the other method expansions in the neighbourhood of a sonic point are used for the coordinates of a Mach line through the sonic point in powers of the complement of the Mach angle. The methods are developed for plane flow; the necessary modifications are indicated for flows with axial symmetry.

1. Taylor expansions of the velocity components near a sonic point

TAKE some sonic point as origin of rectangular Cartesian axes with the x-axis in the flow direction. We assume that the velocity components are analytic functions of x and y; then, denoting the values of quantities at the origin by the suffix s and partial derivatives by suffixes x and y, we may write

$$\left.\begin{aligned} u &= u_s+xu_x+yu_y+\frac{1}{2!}(x^2u_{xx}+2xyu_{xy}+y^2u_{yy})+\dots \\ v &= v_s+xv_x+yv_y+\frac{1}{2!}(x^2v_{xx}+2xyv_{xy}+y^2v_{yy})+\dots \end{aligned}\right\}, \tag{1}$$

(For clarity the suffices s are omitted from the velocity derivatives. A derivative at a general point is distinguished by its full symbol, $\partial u/\partial x$ for instance.) The equations satisfied by u and v are

$$\frac{\partial v}{\partial x}-\frac{\partial u}{\partial y} = 0, \tag{2}$$

$$(u^2-a^2)\frac{\partial u}{\partial x}+2uv\frac{\partial u}{\partial y}+(v^2-a^2)\frac{\partial v}{\partial y} = 0, \tag{3}$$

where $$2a^2+(\gamma-1)q^2 = (\gamma+1)a_s^2. \tag{4}$$

With our choice of axes $v_s = 0$, and hence $u_s = q_s = a_s$, the critical velocity. Expressing each term in equations (2) and (3) as power series in x and y by use of the equations (1) and (4) and comparing coefficients of corresponding powers, we find

$$v_x = u_y, \qquad v_y = 0,$$

$$v_{xx} = u_{xy}, \qquad v_{xy} = u_{yy} = \frac{2}{a_s}\left\{\frac{\gamma+1}{2}u_x^2+u_y^2\right\}. \tag{5}$$

$$v_{yy} = (\gamma+1)\frac{u_x u_y}{a_s}, \quad \text{etc.} \tag{6}$$

We note that the flow can be determined at any point near the origin provided only the x derivatives of u and v at the origin are given.

If $h_\sigma d\sigma$ is the element of length in the stream direction, κ_σ the curvature of the streamline, then

$$\frac{u_y}{a_s} = \left(\frac{\partial\theta}{h_\sigma \partial\sigma}\right)_s = (\kappa_\sigma)_s \tag{7}$$

and $$u_x = \left(\frac{\partial q}{h_\sigma \partial\sigma}\right)_s. \tag{8}$$

A point on the sonic line at which $(\kappa_\sigma)_s = 0$ will be called a *singular sonic point*.

2. The slope and curvature of the sonic line

To avoid ambiguity in the sign of the curvature of the sonic line we first define the positive direction of the sonic line as that obtained from the local stream direction by counterclockwise rotation through an angle η, with

$$0 < \eta < \pi \quad \text{when} \quad \frac{\partial q}{h_\sigma \partial\sigma} > 0,$$

$$-\pi < \eta < 0 \quad \text{when} \quad \frac{\partial q}{h_\sigma \partial\sigma} < 0,$$

and, when $\dfrac{\partial q}{h_\sigma \partial\sigma} = 0$, $\eta = 0$ or π according as $\kappa_\sigma < 0$ or $\kappa_\sigma > 0$.

From the equation of the sonic line, $q^2 = a_s^2$, with q^2 expressed in terms of x and y by equation (1), we obtain the slope of the sonic line at the origin

$$\frac{dy}{dx} = -\frac{u_x}{u_y} = \tan\eta_s. \tag{9}$$

If $h_s ds$ denotes the element of length in the positive direction of the sonic line, the curvature of the sonic line at the origin is

$$\kappa_s = \left(\frac{\partial(\theta+\eta)}{h_s \partial s}\right)_s$$

$$= \frac{1}{a_s(u_x^2+u_y^2)^{\frac{3}{2}}}\{u_y^4+a_s u_y^2 u_{xx}+a_s u_x^2 u_{yy}-2a_s u_x u_y u_{xy}\}. \tag{10}$$

This can also be written, without reference to any particular system of coordinates, in the form

$$\kappa_s = \frac{\cos^3\eta_s}{a_s(\kappa_\sigma)_s}\{2\tau_\sigma a \tan\eta+2\kappa_\sigma^2 a \tan^2\eta-(\gamma+1)\kappa_\sigma^2 a \tan^2\eta-q_{\sigma\sigma}\}_s, \tag{11}$$

where $$\tau_\sigma = \frac{\partial \kappa_\sigma}{h_\sigma \partial\sigma}, \qquad q_{\sigma\sigma} = \frac{\partial}{h_\sigma \partial\sigma}\left(\frac{\partial q}{h_\sigma \partial\sigma}\right).$$

3. The curvature of Mach lines at the sonic line

The angle between the positive direction of the $\pm$ Mach line through the point (x,y) and the positive x-axis is $\epsilon = \theta\mp\mu$ (ref. **1**), and at the origin the positive direction of the $\pm$ Mach line is along the $\mp$ y-axis. Let $h_\alpha d\alpha$, $h_\beta d\beta$ be the elements of length along a Mach line and along the normal to a Mach line, respectively. The curvature of a Mach line, $\kappa_\alpha = \partial\epsilon/h_\alpha \partial\alpha$ is given by the second characteristic equation (**1**)

$$v_\beta\left\{v_\beta \frac{\partial v_\alpha}{h_\alpha \partial\alpha}-v_\alpha \frac{\partial v_\beta}{h_\alpha \partial\alpha}-(v_\alpha^2+v_\beta^2)\kappa_\alpha\right\}+\frac{v_\alpha}{\rho}\frac{\partial p}{h_\alpha \partial\alpha} = 0.$$

With the help of Bernoulli's equation this may be written

$$\kappa_\alpha = \pm\frac{\gamma-1+2\cos 2\nu}{2q^2\sin\nu\cos\nu}\, q\frac{\partial q}{h_\alpha \partial\alpha}, \tag{12}$$

where $$\nu = \tfrac{1}{2}\pi-\mu.$$

Hence, near the origin, on a Mach line through the origin,

$$\kappa_\alpha = -\frac{\gamma+1}{2}\frac{(\kappa_\sigma)_s}{\nu}+O(1). \tag{13}$$

At any sonic point the two Mach lines have a common tangent. At all non-singular sonic points $(\kappa_\alpha)_s$ is infinite; near such points, on both Mach lines, κ_α and $(\kappa_\sigma)_s$ have opposite signs.

4. The behaviour of the equipotential and isocline near an ordinary sonic point

By expanding the velocity potential as a Taylor series and using equations (5) and (6) we can show that the equipotential through the origin has the form

$$y^3 = -\frac{6a_s^2 x}{(\gamma+1)u_x u_y} \tag{14}$$

near the origin.

The equation of the isocline (i.e. the line along which the velocity has constant direction), through the origin, is $v = 0$. Hence, from (1), (5), (6), the isocline approaches the parabola

$$y^2 = -\frac{2a_s x}{(\gamma+1)u_x}. \tag{15}$$

The relative positions of each Mach line, streamline, isocline, and equipotential through a non-singular sonic point depend on the signs of $(q_\sigma)_s$

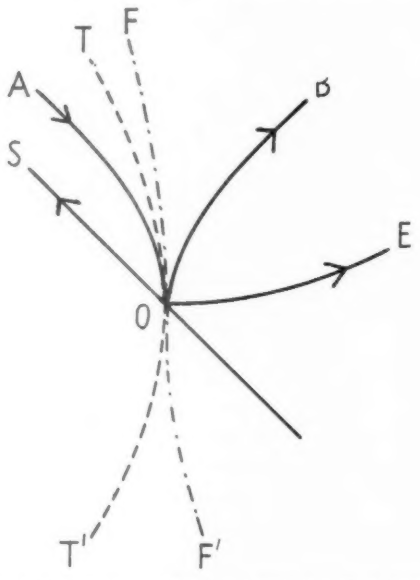

FIG. 1. $(q_\sigma)_s > 0$, $(\kappa_\sigma)_s > 0$. OA and OB are respectively + and − Mach lines, OS is the sonic line, OE, TOT' and FOF' are the streamline, isocline, and equipotential respectively.

and $(\kappa_\sigma)_s$ and are easily found with the aid of equations (9), (13), (14), and (15). As an example, they are shown in Fig. 1 with $(q_\sigma)_s$ and $(\kappa_\sigma)_s$ both positive.

5. Determination of the flow in the characteristic triangle based on a sonic initial line

When initial data are given on the sonic line the usual method of characteristics cannot be used to find the continuation of the flow in the supersonic region. Of the two methods here designed for this purpose the first employs the double Taylor series (1) to find the flow at chosen points in the supersonic region on normals to the sonic line, and the

second determines the coordinates of points on both Mach lines through each sonic point corresponding to chosen values of ν. Each method enables us to construct a new initial line beyond which the continuation of the flow can be found by the usual characteristics method.

5.1. *First method of continuation*

At a point in the supersonic region at a given distance, ξ, along a variable curve through an origin on the sonic line, the value of μ, and hence the value of the Mach line curvature, is least if the curve is the line of steepest pressure gradient through the origin. If we replace it, for simplicity, by the straight normal to the sonic line through the origin, we can determine the velocity components at a point on a new initial line by taking a given sonic point as origin and evaluating the series (1) at the point (x, y) where

$$\frac{x}{\sin\eta_s} = -\frac{y}{\cos\eta_s} = \xi.$$

The value of ξ corresponding to a chosen value of ν on the new initial line can be found approximately from the equation

$$\frac{q^2}{a^2} = \sec^2\nu,$$

which gives

$$\xi = -\frac{1}{\gamma+1}\frac{\cos\eta_s}{(\kappa_\sigma)_s}\nu^2+O(\nu^4). \tag{16}$$

5.2. *Second method of continuation*

Referred to Cartesian rectangular axes through a given sonic point with the x-axis in the flow direction, the coordinates of any point in the supersonic region are functions of θ and μ. At each point on a given Mach line of either family a fixed relation exists between θ and μ, given by the second characteristic equation; the coordinates of a point and the values of flow quantities on a Mach line can therefore be expressed as functions of μ only. Provided these functions are analytic we may represent the coordinates near the origin of either Mach line through the origin by the power series

$$x = a_1\nu+a_2\nu^2+\dots,$$
$$y = b_1\nu+b_2\nu^2+\dots. \tag{17}$$

When the origin is an ordinary sonic point the slope and curvature of each Mach line are infinite at the origin. Hence $a_1 = b_1 = a_2 = 0$.

The coefficients $a_3, a_4, \dots, b_2, b_3, \dots$ are found in terms of physical constants and the boundary conditions at the origin from two identities in ν. In the first characteristic equation,

$$\frac{dx}{dy} = -\tan(\theta\pm\nu), \tag{18}$$

dx/dy is expressed in terms of ν by means of (17) and θ is related to ν by combining the second characteristic equation with Bernoulli's equation, whence

$$\theta = \mp\frac{2\nu^3}{\gamma+1}\left\{\frac{1}{3}+\frac{5-\gamma}{15(\gamma+1)}\nu^2+\frac{2(\gamma^2-28\gamma+61)}{315(\gamma+1)^2}\nu^4+\dots\right\}. \tag{19}$$

The second identity is provided by the strip condition satisfied on a Mach line, i.e. the condition that q, x, y are all functions of ν only,

$$q\frac{dq}{d\nu} = q\frac{\partial q}{\partial x}\frac{dx}{d\nu}+q\frac{\partial q}{\partial y}\frac{dy}{d\nu}. \tag{20}$$

All the terms of equation (20) can be expanded in powers of ν: $q\dfrac{dq}{d\nu}$ by Bernoulli's equation, $q\dfrac{\partial q}{\partial x}\dfrac{dx}{d\nu}$ and $q\dfrac{\partial q}{\partial y}\dfrac{dy}{d\nu}$ by means of (1) and (17).

Equating coefficients of corresponding powers of ν in equations (18) and (20), and solving the resulting equations for $a_3, a_4,\dots, b_2, b_3,\dots$, we obtain the following expansions in powers of ν for the coordinates of the $\pm$ Mach line through an ordinary sonic point

$$x = \mp\frac{2a_s}{(\gamma+1)u_y}\left\{\frac{\nu^3}{3}\pm\frac{u_x}{u_y}\frac{\nu^4}{4}-\frac{\gamma}{3(\gamma+1)}\frac{\nu^5}{5}\mp\right.$$
$$\left.\mp\left[\frac{11}{3(\gamma+1)}\frac{u_x}{u_y}+\frac{5}{3}\frac{u_x^3}{u_y^3}-\frac{5}{3(\gamma+1)}\frac{a_s u_{xy}}{u_y^2}\right]\frac{\nu^6}{6}\dots\right\},$$

$$y = \frac{2a_s}{(\gamma+1)u_y}\left\{\frac{\nu^2}{2}\pm\frac{u_x}{u_y}\frac{\nu^3}{3}-\frac{(2\gamma-1)}{3(\gamma+1)}\frac{\nu^4}{4}\mp\right.$$
$$\left.\mp\left[\frac{\gamma+10}{3(\gamma+1)}\frac{u_x}{u_y}+\frac{5}{3}\frac{u_x^3}{u_y^3}-\frac{5}{3(\gamma+1)}\frac{a_s u_{xy}}{u_y^2}\right]\frac{\nu^5}{5}\dots\right\}. \tag{21}$$

Equation (21) shows that near the origin each Mach line behaves like one branch of the semi-cubical parabola

$$y^3 = \frac{9a_s}{2(\gamma+1)u_y}x^2 = \frac{9}{2(\gamma+1)(\kappa_\sigma)_s}x^2.$$

The series (21) diverge when u_x/u_y is sufficiently large. The first method must therefore be used to construct the new initial line when the origin lies close to a singular sonic point. When the origin is itself singular the Mach lines through it can be represented by the special power series described below. The second method is particularly useful for finding the continuation of flow in a local supersonic region of potential flow; $(\kappa_\sigma)_s$ and u_y are everywhere different from zero on the sonic line bounding such a region, and singular points are absent.

6. The Mach lines, the equipotential, and the isocline at a singular sonic point

We have seen that when $(\kappa_\sigma)_s = u_y/a_s = 0$ the curvature of either Mach line through the origin may be finite at the origin. In finding the expansions for the coordinates of such a Mach line we therefore retain the coefficients a_2 and b_1. Equating coefficients of corresponding powers of ν in equations (18) and (20) we obtain two sets of equations for $a_2,\ldots,$ $b_1,\ldots,$ which now begin with

$$2a_2 = \mp b_1$$

and

$$2a_s u_x a_2 + a_s u_{yy} b_1^2 = \frac{2}{\gamma+1}a_s^2,$$

respectively. Solving these with the aid of (5) we find

$$\mp b_1 = 2a_2 = \frac{a_s}{(\gamma+1)u_x} \quad \text{or} \quad -\frac{2a_s}{(\gamma+1)u_x}.$$

Hence from equation (12)

$$(\kappa_\alpha)_s = \pm\frac{(\gamma+1)u_x}{a_s} \quad \text{or} \quad \mp\frac{(\gamma+1)u_x}{2a_s}. \tag{22}$$

Thus each Mach line has a discontinuity of curvature at the singular sonic point and has two branches. From equation (10) the curvature of the sonic line itself at the singular sonic point is $\kappa_s = (\gamma+1)u_x/a_s$. The first branch of each Mach line is convex to the subsonic flow with $(\kappa_\alpha)_s = \pm\kappa_s$: the second branch is concave to the subsonic flow with $(\kappa_\alpha)_s = \mp\frac{1}{2}\kappa_s$. The equipotential through a singular sonic point can be shown to behave, near the origin, like

$$y^4 = -\frac{24a_s^3 x}{(\gamma+1)^2u_x^3}.$$

The corresponding isocline has a double point at the singular origin. One branch touches the y-axis with curvature $\frac{1}{3}(\gamma+1)u_x/a_s$; the slope of the other branch at the origin is $-\frac{1}{2}u_{xy}/u_{yy}$. The locus $\kappa_\sigma = 0$ lies between these two isocline branches, with slope at the origin equal to $-u_{xy}/u_{yy}$.

The complete flow pattern near a singular sonic point at which $(\tau_\sigma)_s$ and $(q_\sigma)_s$ are positive is shown in Fig. 2; it agrees with that found by Lighthill (**2**) in symmetrical channel flow. The + Mach lines represented by PQR do not originate on the sonic line; they are the reflections of − Mach lines starting from OS.

It is of interest to determine the point at which the curvature of the Mach line PQR changes sign. Craggs (**3**) has shown that the branches OA', OB' of the singular Mach lines in Fig. 2 are branch lines. It can be shown further that a point where the Mach line curvature vanishes must lie on the isobar where the Mach number $M = 2/\sqrt{(3-\gamma)}$ or on a branch

line or a higher singularity of the same type. Since we are considering fields of flow where the velocity derivatives are bounded and continuous, the Mach line curvature can change sign only where it vanishes (except

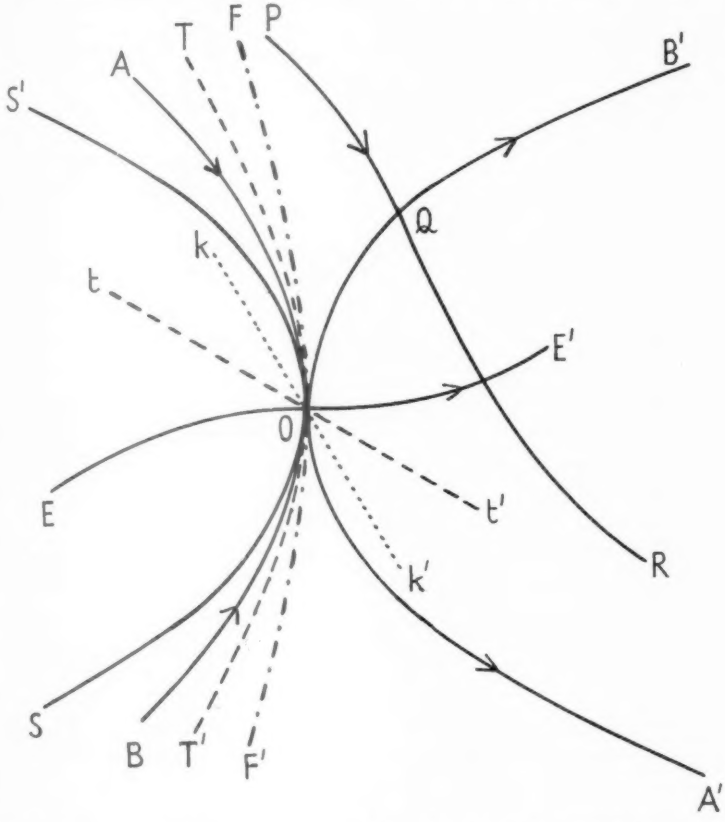

FIG. 2. $(\kappa_\sigma)_s = 0$, $(\tau_\sigma)_s > 0$, $(q_\sigma)_s > 0$. O is the singular sonic point, SOS' is the sonic line, AOA' and BOB' are singular Mach lines of the $+$ and $-$ family respectively, TOT' and tOt' are the two isocline branches; EOE' and FOF' are respectively the streamline and equipotential through O; kOk' is the locus $\kappa_\sigma = 0$.

at the singular point itself), and it follows that the curvature of each Mach line PQR changes sign at Q, the point where it crosses $A'OB'$.

7. Completion of a known supersonic field up to its sonic boundary

Consider a field of supersonic flow which is determined from given conditions on an initial line inside the field. As we integrate along Mach lines towards the sonic line a stage will be reached at which the Mach

line curvature is too large for further application of the usual methods of integration by characteristics to be possible. We now give two methods of finding the continuation of the flow beyond this stage up to the sonic boundary.

7.1. *First method*

Suppose O is a point in the known flow field, beyond which the usual method based on characteristics becomes inaccurate. With O as origin we take rectangular Cartesian axes with the x-axis towards the sonic line and the y-axis in the direction of the isobar at O. If the velocity components are analytic functions of x and y, their values at a point near O on the x-axis are given by

$$\left.\begin{aligned} u &= u_0+u_x x+\frac{1}{2!}u_{xx}x^2+\ldots \\ v &= v_0+v_x x+\frac{1}{2!}v_{xx}x^2+\ldots \end{aligned}\right\}, \tag{23}$$

where $u_x = (\partial u/\partial x)_0$, etc.

The coefficients u_x, u_{xx},... are easily found if the supersonic field behind O has been integrated from isobar to isobar.

The sonic point on the x-axis is then found by solving the equation

$$u^2+v^2 = a_s^2$$

for x by successive approximation.

7.2. *Second method*

Using rectangular axes through O, with the x-axis now in the stream direction at O, we represent either Mach line near O by expansions

$$\left.\begin{aligned} x &= a_1\phi+a_2\phi^2+\ldots \\ y &= b_1\phi+b_2\phi^2+\ldots \end{aligned}\right\}, \quad \text{where } \phi = \nu_0-\nu,\ \nu_0 = (\nu)_{x=0}.$$

We express θ and $q\,dq/d\phi$ as power series in ϕ using the relations

$$q = q_{\max}\left\{1+\frac{2}{\gamma-1}\cos^2(\phi-\nu_0)\right\}^{-\frac{1}{2}},$$

$$\frac{dq}{q}\tan(\nu_0-\phi)\pm d\theta = 0.$$

We may then express the first characteristic equation and the strip condition as power series in ϕ and by equating coefficients of corresponding powers obtain two sets of equations giving a_1, a_2,..., b_1, b_2,... in terms of boundary conditions at O. The sonic point on each Mach line through O is then given by

$$\left.\begin{aligned} x &= a_1\nu_0+a_2\nu_0^2+\ldots \\ y &= b_1\nu_0+b_2\nu_0^2+\ldots \end{aligned}\right\}.$$

8. Application of the methods to flow with axial symmetry

All the methods developed for plane flow can in principle be extended to apply to flow with axial symmetry. Relations between the coefficients in the Taylor expansions for u and v have to be revised; to the expression on the left of the governing equation (3) must be added the term

$$\frac{u\sin\theta_0+v\cos\theta_0}{r_0+x\sin\theta_0+y\cos\theta_0},$$

where r_0 is the distance of the origin from the axis of symmetry and θ_0 is the angle between the x-axis and the axis of symmetry; otherwise the first method of continuation is unaltered. The second method of continuation suffers an additional change. The relation obtained from the second characteristic equation now involves x and y in addition to θ and μ so that, while the coordinates and values of flow quantities on a Mach line can still be expressed as functions of μ only, the relation between θ and μ is no longer universal but varies with the boundary conditions at the origin. In the development of the second method we have therefore to find a third set of coefficients, arising in the expansion of θ in powers of ν. The three sets of equations now required are found from the first and second characteristic equations and the strip condition, all expressed as identities in ν. Corresponding changes are made in the methods of completing a known supersonic field up to its sonic boundary.

When the origin is taken at the singular sonic point on the axis of symmetry the relations between coefficients in the Taylor expansions take a particularly simple form and the expansions in powers of ν for the coordinates on the Mach lines through the sonic point can easily be found. The following results are obtained:

The curvature of the sonic line at the origin $= \frac{1}{2}u_x(\gamma+1)/a_s$.

The curvature of the $\pm$ Mach line at the origin is

$$\pm\tfrac{1}{4}(\surd 5+1)(\gamma+1)u_x/a_s \quad \text{or} \quad \mp\tfrac{1}{4}(\surd 5-1)(\gamma+1)u_x/a_s.$$

The results should be compared with those found in plane flow. It is seen that the flow pattern is qualitatively the same as that in Fig. 2. One difference may be noted; the curvature of the Mach line PQR no longer changes sign on crossing the line OB', unless the flow at Q is parallel to the axis.

The author wishes to thank Professor Goldstein and Dr. R. E. Meyer for their criticism of this paper.

REFERENCES

1. R. E. MEYER, 'The method of characteristics for problems of compressible flow involving two independent variables', *Quart. J. Mech. and Applied Math.* **1** (1948), 196.
2. M. J. LIGHTHILL, 'The hodograph transformation in trans-sonic flow. I. Symmetrical channels', *Proc. Roy. Soc.* A, **191** (1947), 327.
3. J. W. CRAGGS, 'The breakdown of the hodograph transformation for irrotational compressible fluid flow in two dimensions', *Proc. Camb. Phil. Soc.* **44** (1948), 374.

ble flow
Math.
. Sym-
ational
8), 374.